Impact of Tumor Necrosis Factor Receptor-1 signalling to *Listeria monocytogenes*-containing phagosomes and its role for bacterial eradication

DISSERTATION ZUR ERLANGUNG

DES DOKTORGRADES DER NATURWISSENSCHAFTEN (DR. RER. NAT.)

DER NATURWISSENSCHAFTLICHEN FAKULTÄT III –

BIOLOGIE UND VORKLINISCHE MEDIZIN

DER UNIVERSITÄT REGENSBURG

vorgelegt von

Ulrike Heigl

aus Prien am Chiemsee

im Jahr 2011

Promotionsgesuch eingereicht am: 08.08.2011

Die Arbeit wurde angeleitet von: PD Dr. Wulf Schneider

_____

Ulrike Heigl

Prüfungsausschuss:

Prüfungsvorsitz:	Prof. Dr. Wolf Hayo Castrop
Prüfer:	Prof. Dr. Richard Warth
	PD Dr. Wulf Schneider
	Prof. Dr. Thomas Langmann

Meiner Familie

Contents

Symbols

α-	anti
Δ	deletion
µ	micro (10^{-6})
A	
A	Ampere
ASMase	acid sphingomyelinase
ActA	actin assembly protein A
ATP	adenosine triphosphate
APC	antigen presenting cells
Apaf	apoptotic protease activating factor 1
AP-1	activator protein-1
B	
Bax	Bcl-2 asociated x protein
BCG	Bacillus Calmette-Guerin
Bcl-2	B-cell lymphoma 2
BHI	brain heart infusion
BID	BH3 interacting domain death agonist
BMDM	bone marrow derived macrophages
BSA	bovine serum albumin
C	
CARP2	caspase-associated ring protein-2
CCL2	CC-chemokine ligand-2
CCR2	CC-chemokine-receptor 2
CDC	cholesterol dependent cytolysin
c.f.u	colony forming units
c-IAP1/2	cellular inhibitor of apoptosis 1/2
CRD	cysteine rich domain
CSF-1	colony stimulating factor-1
CTSD	Cathepsin D
CTL	cytotoxic T-lymphocyte
D	
DD	death domain
DED	death effector domain
DISC	death inducing signalling complex

DNA	deoxyribonucleic acid
DMEM	DULBECCO'S minimal essential medium
E	
ECL	enhanced chemiluminescence
EDTA	Ethylendiamin-N-N,N',N'-tetraacetat
EEA1	Early endosomal antigen - 1
ELISA	Enzyme-linked immunosorbent assay
ERK	extracellular signal regulated kinase
et al.	*et alii, et aliae*
F	
FADD	fas associated death domain protein
FAN	factor associated with neutral sphingomyelinase
FCS	Fetal calf serum
FITC	Fluorescein-isothiocyanat
G	
g	Gramm
GAPDH	Glyceraldehyde-3-phosphate dehydrogenase
GEF	Guanine nucleotide exchange factor
GDP	guanosine diphosphat
GFP	green fluorescent protein
GILT	gamma-Interferon inducible lysosomal reductase
GSK3β	Glycogen synthase kinase-3β
GTP	guanosine triphosphat
H	
h	human
HGF	hepatocyte growth factor
HRP	horseradish peroxidase
Hpt	hexose-6-phosphat-translocase
I	
ICAM-1	Inter-Cellular Adhesion Molecule 1
IgG	Immunglobulin G
IF	Immunofluorescence
IFN	Interferon
interm.	intermediate
iNOS	inducible nictric oxide synthase
IL	Interleukin

InlA/B	Internalin A/B
IκB	inhibitor of nuclear factor κB
IKK	IκB kinase
IRF9	IFN-regulatory factor-9
ISG	IFN-stimulated genes
ISGF3	IFN-stimulated gene factor 3
ISRE	IFN-stimulated response elements

J

JAK	Janus activated kinase
JNK	c-Jun amino-terminal kinase

K

kDa	kilo Dalton

L

LB	Lipobiotin
LAMP1	lysosomal associated membrane protein 1
L.m.	*Listeria monocytogenes*
LLO	Listerolysin O
LPS	Lipopolysaccharides
LRG-47	Immunity related GTPase 47

M

m	mouse
M	magnetic fraction
MAPK	mitogen activated kinase
MCP-1	monocyte chemotactic protein-1
MCSF	macrophage colony stimulating factor
MHC	major histocompatibility complex
min	minutes
MK2	mitogen-activated protein kinase-activated protein kinase2
MOI	multiplicity of infection
Mtb	*mycobacterium tuberculosis*
MW	molecular weight
MVB	multivesicular body
MyD88	myeloid differentiation primary-response protein 88

N

NADPH	Nicotinamide adenine dinucleotide phosphate
NEMO	NF-κB essential modulator
NF-κB	nuclear factor κB
nm, ng	nanometer, nanogramm (10^{-9})
NK cells	natural killer cells
NM	non magnetic fraction
NO	Nitric oxide
NOX 1	NADPH oxidase 1
NSD	Neutral sphingomyelinase domain
N-terminal	amino-terminal end of a protein
Nu p62	Nucleoporin p62

O

OD_{600}	optical density, wavelength λ = 600 nm
ON	overnight

P

PAGE	Polyacrylamide Gel-electrophoresis
PBS	Phosphate buffered saline
PI-PLC	Phosphatidylinositol-specific phospholipase
p.i.	*post infectionem*
PLAD	preligand assembly domain
PNS	post nuclear supernatant

R

r	recombinant
Rab	ras associated in brain
RER	rough endoplasmic reticulum
RILP	Rab7-interacting lysosomal protein
RIP-1	receptor interacting protein-1
rpm	Rounds per minute
RT	Room temperature
ROS	Reactive Oxygen Species
RNI	Reactive nitrogen intermediates

S

SA	Streptavidin
SE	standard error

SD	Standard deviation
SDS	Sodium dodecyl sulfate
STAT	signal transducer and activator of transcription

T

TACE	TNF alpha converting enzyme
TBS	Tris Buffered Saline
TBS-T	Tris Buffered Saline-Tween
TEM	Transmission electron microscopy
TGFβ	Transforming growth factor β
TGN	*Trans*-Golgi network
TLR	Toll-like receptor
TNFα	Tumor necrosis factor α
TNF-R1	Tumor necrosis factor Receptor 1
TNF-R2	Tumor necrosis factor Receptor 2
TRADD	TNF receptor associated death domain
TRID	TNF receptor internalisation domain
TRAF	TNF receptor associated factor
TRAIL	TNF-related apoptosis-inducing ligand
TRAIL-R	TNF-related apoptosis-inducing ligand receptor
TipDCs	TNF and iNOS producing dendritic cells
Tyk	Tyrosine kinase

V

V	Volt
V-ATPase	vacuolar ATPase

W

WT	wild type

Summary

The contribution of tumor necrosis factor α (TNFα) and tumor necrosis factor receptor-1 (TNF-R1) to the eradication process of intracellular bacteria is well-known and undisputed. Mice deficient in TNF-R1 or components of TNF-R1 signalling (acid sphingomyelinase or ASMase) were strongly impaired in their capacity to kill *Listeria monocytogenes* (*L.m.)* and died upon infection with low doses of this pathogen (Pfeffer *et al.*, 1993; Utermöhlen *et al.*, 2003). Upon TNFα stimulation, TNF-R1 internalises and throughout the endocytic trafficking pathway fuses with *trans*-golgi-vesicles and forms multivesicular structures known as late receptosomes. These compartments were shown to contain activated cathepsin D (CTSD) within their lumen (Schneider-Brachert *et al.*, 2004). Over the last decades, reactive oxygen species (ROS), generated by NADPH oxidase complex and generation of reactive nitrogen intermediates (RNI) by the inducible nitric oxide synthase (iNOS) have been assumed to be the major effector components in the bacterial eradication process (Aktan, 2004; Nauseef, 2004; Segal, 2005). In the recent years, however, it has been established that lysosomal proteases contribute to the effective control of infectious pathogens with similar importance (Segal, 2005; Cerro-Vadillo *et al.*, 2006; Utermöhlen *et al.*, 2008; Carrasco-Marin *et al.* 2009). In particular, the aspartyl-protease CTSD was shown to be an important effector molecule in listerial killing. Mice expressing a truncated form of this protease are highly susceptible to infection with the intracellular bacterium *L.m*. (Cerro-Vadillo *et al.*, 2006). In addition, CTSD was shown to target in particular one specific virulence factor of the pathogen *L.m.*, the cytolysin Listeriolysin O (LLO). This virulence factor is one of the major determents of listerial infection because it enables the pathogen to escape into the cytoplasm and therefore to evade the degradative environment of the phagolysosomal compartment. CTSD was suggested to cleave this protein, resulting in the inactivation of its pore-forming activity and preventing the escape of the pathogen out of the phagosome (Carrasco-Marin *et al.*, 2009).

Based on these earlier findings, in the present study it was hypothesised that the biological function of TNF-R1 internalisation might be a key mechanism for routing bactericidal products such as protease CTSD towards the bacteria-containing phagosome. Proving that internalised TNF-R1 receptosomes fuse with the *L.m.*-containing phagosome was considered to be a fundamental step, as it had not been contemplated in previous studies. For the first time, this finding was confirmed by several methods including confocal microscopy, transmission electron microscopy and Western blot analysis of isolated *L.m*.-containing phagosomes and isolated TNF-R1-receptosomes. The cytokine driven molecular mechanisms in bacterial killing were examined in further experiments. In bacterial growth assays, the microbicidal properties of the cytokines TNFα and IFNγ were tested in different macrophage populations infected with *L.m.* TNFα stimulation alone was insufficient to control

bacterial growth in all tested macrophages. Stimulation of macrophages with IFNγ, however, resulted in restriction of bacterial propagation. TNF-R1$^{-/-}$ macrophages, in turn failed to control listerial growth even upon IFNγ stimulation, suggesting a relevant contribution of TNF-R1 signalling to IFNγ mediated infection control. A general synergism of IFNγ and TNFα during the bacterial eradication process seems to be the only plausible explanation, and was confirmed with the results of this work. The precise underlining molecular mechanism of bacterial eradication mediated by TNF-R1 was further investigated. In order to analyse specific alteration of the protein composition on bacteria-containing phagosomes influenced by TNF-R1 signalling, a new immunomagnetic approach for the isolation of these compartments was applied and adapted for the use of *L.m.* and J774 macrophages.

Monitoring the cytokine specific effects on isolated bacteria-containing phagosomes could show that TNFα stimulation alone was sufficient to activate CTSD on the phagosome in J774 macrophages, although bacterial growth restriction failed upon TNFα stimulation. Concomitantly, irrespective of TNF-R1 or IFNγR knockout condition and of any given cytokine stimulation, primary cells showed activation of CTSD on bacteria-containing phagosomes. This was observed in cells where no bacterial growth restriction occurred. These results suggest that CTSD might not be the bactericidal molecule assumed to mediate TNF-R1 dependent bacterial killing and questions its essential role in the eradication process in general.

Other proteins known to be involved in the bacterial infection control such as Rab5, LRG-47 and iNOS were analysed in order to find molecules that might be involved TNF-R1-mediated signals for the bactericidal mechanisms. The small GTPase Rab5 seems to be an interesting candidate as it failed to appear on phagosomes of TNFα and non stimulated TNF-R1 deficient macrophages and in addition, on phagosomes of IFNγR deficient macrophages.

In conclusion, this work demonstrated for the first time that TNF-R1 becomes a part of *L.m*.-containing phagosomes and that TNF-R1-receptosomes fuse with this compartment after internalisation. At this stage several components known to be involved in bacterial eradication process, were monitored in order to find a component that is associated to TNF-R1 signalling. CTSD does not seem to fulfil the promising molecular role it was previously assumed to have. It may however be involved in bacterial killing, but it seems to be insufficient for mediating eradication of *L.m.,* which stays in contrast to previously published work. The GTPase Rab5 might be an interesting component in the context of TNFα mediated killing but it needs further investigations. In addition, a new method for the isolation of bacteria-containing phagosomes was applied and validated for the use of the pathogen *L.m.* and J774 macrophages.

Zusammenfassung in deutscher Sprache

Die Abwehr intrazellulärer Erreger wie *Listeria monocytogenes* (*L.m.*) erfolgt unter Beteiligung des Zytokins TNFα und seines Rezeptors TNF-R1. Dies konnte an Mäusen gezeigt werden, die entweder defizient für den TNF-R1 sind, oder Defekte in der TNFα-vermittelten Aktivierung von Proteasen, z.B. der sauren Sphingomyelinase (ASMase), aufweisen und deshalb die Infektion nicht mehr kontrollieren können (Pfeffer *et al.*, 1993; Utermöhlen *et al.*, 2003). Während ursprünglich ROS (*reactive oxygen species*) und RNI (*reactive nitrogen intermediates*) für lange Zeit als die entscheidenden Komponenten der Eradikation intrazellulärer Erreger gehalten wurden (Aktan *et al.*, 2004; Nauseef *et al.*,2004; Segal *et al.*, 2005), gewannen in den letzten Jahren auch lysosomale Proteasen wie Cathepsin D (CTSD) in diesem Zusammenhang immer mehr an Bedeutung (Segal, 2005; Cerro-Vadillo *et al.*, 2006; Utermöhlen *et al.*, 2008; Carrasco-Marin *et al.*, 2009). CTSD bewirkt die Spaltung und Inaktivierung von Listeriolysin O (LLO), das eines der wichtigsten Virulenzfaktoren von *L.m.* ist, und verhindert die Lyse der Phagosomenmembran und damit Translokation der Bakterien ins Zytoplasma (Carrasco-Marin *et al.*, 2009). Die Bakterien werden im Phagosom festgehalten, können sich nicht vermehren und werden schließlich im sauren Milieu des Phagolysosoms abgetötet. Schneider *et al.* konnten vor wenigen Jahren zeigen, dass die Stimulation von Zellen mit TNFα zur Internalisierung des TNF-R1 führt, wobei sich das sog. Rezeptosom, das sind frühe endosomale Kompartimente, und nach Fusionen mit trans-Golgi Vesikeln multivesikuläre Strukturen entwickeln, die aktiviertes CTSD enthalten (Schneider-Brachert *et al.*, 2004). Basierend auf diesen Erkenntnissen entstand die Hypothese, die Internalisierung des TNF-R1 und die Bildung spezifischer endosomaler Vesikel als bakteriziden Mechanismus der Zelle zu begreifen, bei dem die aktive Protease CTSD zum Listerien-haltigen Phagosom gebracht werden könnte, um die Infektion sowohl zu kontrollieren als auch zu terminieren. Die Fusion von TNF-R1-Rezeptosomen und Phagosomen stellt hier das Schlüsselereignis der Hypothese dar. In der vorliegenden Arbeit konnte zum ersten Mal, unter Verwendung verschiedener experimenteller Ansätze, die Verschmelzung von TNF-R1-haltigen Vesikeln und Listerien-haltigen Phagosomen gezeigt werden. Durch die Etablierung einer neuen Methode zur Aufreinigung magnetisch markierter Listerien gelang es, Phagosomen aus infizierten Makrophagen zu isolieren und ihre Proteinzusammensetzung im Western Blot zu analysieren. Dabei konnte der TNF-R1 spezifisch in diesem phagosomalen Kompartiment gemeinsam mit Listerien nachgewiesen werden. Im Elektronenmikroskop wurde dies mit Hilfe von Goldpartikel-markierter TNF-Rezeptoren auch visuell bestätigt.

Da ein synergistischer Effekt von IFNγ und TNFα bei der Infektionsbekämpfung in Makrophagen bereits bekannt war, wurde zunächst die bakterizide Wirkung von TNFα und IFNγ auf verschiedene Makrophagenpopulationen (J774 Makrophagen und Knochenmarksmarkrophagen aus Wildtyp, TNF-

R1$^{-/-}$ und IFNγR$^{-/-}$ Mäusen) untersucht. Die Experimente zur bakteriziden Eigenschaft dieser Zytokine zeigten, dass allein die Stimulation mit TNFα die Vermehrung der Bakterien nicht verhindern konnte, eine Co-Stimulation mit IFNγ jedoch zu einer Stagnation des bakteriellen Wachstums resultierte. In Infektionsversuchen mit den TNF-R1-defizienten Makrophagen konnte gezeigt werden, dass trotz IFNγ-Stimulation die Translokation der Listerien ins Zytoplasma nicht verhindert werden kann. Diese Ergebnisse bestätigen auf Grundlage der Phagosomenanalyse, dass zur Infektionskontrolle ein generelles synergistisches Zusammenspiel beider Zytokine zur Bakterieneradiaktion notwendig ist.

Um die spezifische Rolle des TNF-R1 bzw. der TNFα-mediierten Signalwege besser zu verstehen und die molekularen Veränderungen bedingt durch den TNFα/TNF-R1-Komplex am Phagosom zu untersuchen, wurden Phagosomen zu verschiedenen Zeitpunkten aus Listerien-infizierten Makrophagen isoliert. Zur Trennung der TNFα - und IFNγ - spezifischen Effekte wurden nicht nur WT-Makrophagen, sondern auch TNF-R1$^{-/-}$, sowie IFNγR$^{-/-}$ Makrophagen verwendet. Die Analyse der Phagosomen im Western Blot ergab, dass die Stimulation mit TNFα in diesen Zellen die Aktivierung von CTSD im Phagosom zur Folge hatte, jedoch TNF-R1- und IFNγR-defiziente Makrophagen nach der Infektion ebenfalls eine Aktivierung von CTSD am Phagosom zeigten. Die Freisetzung und Vermehrung der Bakterien wurde durch die Aktivierung der Protease aber nicht verhindert. Somit war feststellbar, dass die Stimulation mit TNFα zwar die Aktivierung von CTSD in J774 Makrophagen induzieren kann, dies aber für eine erfolgreiche Infektionskontrolle nicht ausreichend ist. Nur die alleinige Aktivierung von CTSD am Phagosom scheint somit für die Eradikation der Bakterien nicht hinreichend zu sein, was im Widerspruch zu bereits publizierten Daten steht. Daher wurde zusätzlich die Rekrutierung weiterer Proteine, wie Rab5, iNOS und LRG-47, die für ihre Beteiligung an der Infektionskontrolle bekannt sind, an das Phagosom untersucht. Interessanterweise konnte dabei festgestellt werden, dass die GTPase Rab5 unabhängig von einer TNFα-Stimulation sowohl in TNF-R1- als auch in IFNγR-defizienten Makrophagen am Phagosom nur schwach bis gar nicht nachweisbar war.

Zusammenfassend konnte in der vorliegenden Arbeit erstmals eine neue Methode zur Isolierung Listerien-haltiger Phagosomen etabliert werden. Die ursprüngliche Arbeitshypothese, dass es zu einer Fusion von TNF-R1-Rezeptosomen und Listerien-haltigen Phagosomen kommt, konnte mit mehreren unabhängigen Methoden erfolgreich verifiziert werden. Durch die Analyse magnetisch isolierter Phagosomen konnte zwar eine teilweise Beteiligung des TNFα-Stimulus zur Aktivierung der Protease CTSD (in J774 Makrophagen) nachgewiesen werden, die aber zur Eradikation der intraphagosomalen Bakterien nicht ausreichend war. Die Beobachtung, dass in Listerien-haltigen Phagosomen von IFNγR-defizienten Zellen die CTSD-Aktivierung am stärksten war, deutet darauf hin, dass auch die Rolle von CTSD für die Kontrolle der Listerieninfektion generell in Frage gestellt werden muss. Interessanterweise konnte für die GTPase Rab5 eine mögliche Beteiligung im TNFα-mediierten

Infektionsabwehrprozess aufgezeigt werden, da sie in TNF-R1-defizienten Zellen nicht mehr ans Phagosom rekrutiert wird.

1. Introduction

1.1. The pathogen *Listeria monocytogenes*

***L**isteria **m**onocytogenes* (*L.m.*) is a Gram-positive, facultative intracellular pathogen, which belongs to the pathogenic species of the *Listeria* genus. *Listeria spp.* can be isolated from diverse environmental sources including soil and water. Its appearance in meat, dairy products and ready to eat food is potentially life-threatening for humans. *L.m*. survives in high concentrations of salt, relatively low pH values (up to 5.0) and can replicate at refrigeration temperatures, which makes it a serious concern in the food industry. It causes diseases in humans and animals, with clinical appearance ranging from gastroenteritis to meningitis, encephalitis, abortions and perinatal infections. This diversity of clinical features derives from the capability of *L.m.* to cross the three important barriers in humans and animals: the intestinal, the blood-brain and the placental barrier (Lecuit, 2005). Driven by different virulence factors, the pathogen is able to enter, survive and multiply in both phagocytic and non-phagocytic cells (Bonazzi *et al.*, 2009), (see 1.2). The pathogenesis of *L.m.* starts with ingestion of the pathogen, followed by passing through the acid environment of the stomach and finally reaching the gastrointestinal tract. There it enters intestinal epithelial cells and macrophages (Karunasagar *et al.*, 1994) to begin translocation via the bloodstream to organs like the liver and spleen. *L.m.* enters hepatocytes for replication mediated by the virulence factor **I**nter**n**a**l**in **B** (InlB) (Gaillard *et al.*, 1996). Normally, the clearance of bacteria mediated by both innate and adaptive immune response is very efficient, so bacteria start to disappear in mouse organs between five to seven days post infection (Gregory and Wing, 1998).

1.2. The life cycle of *Listeria monocytogenes* in host cells

L.m. developed specific mechanisms to enter different cell types. For the infection of intestinal epithelial cells the expression of **I**nter**n**a**l**in **A** (InlA) on the bacterial surface is required. This protein interacts with the **e**pithelial surface protein **cadherin** (E-cadherin), a member of cell adhesion molecules. Thus, *L.m.* exploits cell-proteins that are usually involved in formation of adherens junctions to induce its entry (Sousa *et al.*, 2005). InlB is another protein which *L.m*. utilizes to invade hepatocytes. This surface protein of *L.m.* interacts with the **h**epatocyte **g**rowth **f**actor (HGF) receptor Met, induces phagocytosis of the entire bacterium and promotes the invasion of the pathogen into the cell (Shen *et al.*, 2000). In both cases bacteria are initially trapped in a phagocytic vacuole, where the escape process takes its initial steps (figure 1.1). This is also found after phagocytosis in macrophages resulting in the bacteria-containing phagosome.

The intracellular life cycle of *L.m.* begins with the escape from the vacuole or phagosome, which is mainly mediated by the pore-forming cytolysin **L**isterio**l**ysin **O** (LLO), also known as hemolysin. More details on this protein and its function are described in 1.2.1. In the acidic environment of the phagosome or vacuole, the cytolysin LLO is activated, starts destroying the vesicle membrane and results in releasing the pathogen into the cytoplasm. Translocated into the cytosol, *L.m.* uses hexose phosphate from the host cell as an energy source for rapid intracellular growth. The uptake is mediated by the **h**exose-6-**p**hosphat **t**ranslocase (Hpt), which is also a virulence factor required for intracellular life of the bacterium. *L.m.* strains which lack Hpt have been shown to be less virulent in mice (Chico-Calero *et al.*, 2002). In the cytoplasm, *L.m.* starts replication and undergoes direct cell-to-cell spread via polarised actin polymerisation, which generates a force to propel them through the cytoplasm of the infected cell and into uninfected neighbouring cells. The molecular mechanism that drives actin polymerisation is mediated by the **act**in-**a**ssembly-inducing protein (ActA), required for creation of the so-called "actin-comet tails". Entering the newly infected cell this way, requires an escape strategy from a double membrane vacuole, which is supported by secretion of two proteins, additional to LLO. These are the **p**hosphat**i**dylinositol-specific **p**hospho**l**ipase **C** (PI-PLC) and a broad range **p**hospho**l**ipase **C** (PLC). Both contribute to the pathogen's vacuolar escape and virulence (Smith *et al.*, 1995). In the newly infected cell, *L.m.* can start replication and spreading to other cells once again. The whole life cycle of virulent *L.m.* is summarized in figure 1.1. based on Tilney and Portnoy (Tilney and Portnoy, 1989). Molecular mechanisms of entry and replication have been elucidated by a series of detailed and intricate experiments, which are reviewed in Vazquez-Boland *et al.* and others (Hamon *et al.*, 2006; Vazquez-Boland *et al.*, 2001)

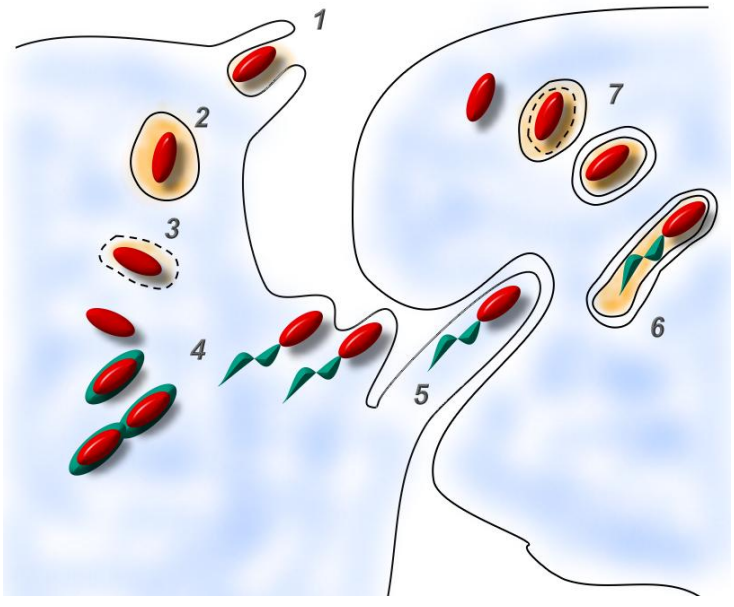

Figure 1.1: intracellular life cycle of Listeria monocytogenes
*L.m. induces its uptake into cells by the expression of InlA and InlB or is engulfed by macrophages (**1**).Bacteria are trapped within a phagocytic vacuole (**2**), which is disrupted by the activity of LLO, releasing L.m. into the cytosol (**3**). In the cytoplasm free bacteria can replicate and start to polymerise cellular actin (**4**). L.m. enters adjacent cells by actin based motility (**5**) and is surrounded by a double membrane structure (**6**). These membranes are lysed again by the activity of LLO and the support of PI-PLC and PLC (**7**). L.m. is now able to start another round of replication in the newly entered cell (based on Tilney and Portnoy, 1989).*

1.2.1. The cytolysin listeriolysin O

The cytolysin LLO is the major determinant of *L.m.* pathogenesis, as mutants lacking LLO (∆hly mutant) lose their virulence in mice (Cossart *et al.*, 1989). The coding gene for listeriolysin, *hlyA,* was identified in 1987 (Mengaud *et al.*, 1987) and Gillard *et al.* confirmed that hly mutants were unable to escape from the vacuole anymore (Gaillard *et al.*, 1987). LLO belongs to the cholesterol dependent cytolysins (CDC´s) that are also expressed by many other Gram-positive bacteria (Gilbert, 2010). The unique feature of LLO is its low pH stability, with an optimal activity at pH 5.5. The pH optimum is well-adapted to the intraphagosomal environment, but activation of LLO is not only mediated by a low pH value, as recent studies have shown. The γ-interferon **i**nducible **l**ysosomal **t**hiol reductase (GILT) is a critical host factor for *L.m.* and is responsible for activation of LLO *in vivo* (Singh *et al.*, 2008). On the other hand, rapid denaturation of LLO occurs in neutral pH values (Schuerch *et al.*, 2005), which might avoid further damage to the cell after release of the bacteria. Other regulation mechanisms also contribute to degradation of the protein, like the PEST-like sequence (sequences rich in proline/**P**, glutamic acid/**E**, serine/**S** and threonine/**T**) in the N-terminal region of the toxin. In this region LLO is ubiquinated and phosphorylated targeting it for degradation by proteasomes in the cytosol (Schnupf *et al.*, 2006). This demonstrates the well adapted structure of this protein to its host. LLO also plays a critical role in host mediated resistance to *L.m.* Recent studies revealed that LLO is a target for the aspartyl-protease cathepsin D which specifically cleaves the protein (Carrasco-Marin *et al.*, 2009). LLO also seems to be important for the protective immune response to *L.m.* given that this antigen is recognised by Listeria-specific $CD8^+$ T-cells (Sirard *et al.*, 1997) and also stimulates Listeria-specific $CD4^+$ T-cells (Safley *et al.*, 1995).

1.3. Immune response to *Listeria monocytogenes* - components and mechanisms

For over 50 years, *L.m.* has been used for studies to examine immune response and the molecular mechanisms of intracellular pathogens. In the 1960s, Mackaness showed for the first time that macrophages are the cells predominantly implicated in *L.m* replication and survival (Mackaness, 1962). Macrophages were also shown to be invaded by a large number of other pathogens. Normally, invasive microbial diseases are prevented by effective defense mechanisms of the infected host. However, considering the fact that pathogens have coevolved with their host, these microbes developed different strategies to overcome the protective host barriers and take advantage of the host's immune responses. The general immune response of the host consists of two distinct systems, the innate and the adaptive immune system which will be introduced in the following. A summary of the most important components of both systems are shown in figure 1.2.

1.3.1. Innate immune response

Innate immunity is the host's first response to bacterial invasion and is essential for controlling infections. This system comprises cells and mechanisms for non-specific defense against pathogens. The recruitment of immune cells to the infection site, release of various cytokines, activation of the complement cascade and identification of foreign structures are the major steps in the processes of innate immune response. The involved cells are **N**atural **K**iller (NK) cells, mast cells, eosinophils, basophils and the phagocytic cells including macrophages, neutrophils and dendritic cells. All these cells function within the immune system by identifying and eliminating pathogens that might cause infection. The complement system is the humoral component of the innate immune system. This system comprises small molecules which help phagocytic cells to clear pathogens from the organism by tagging pathogens with these complement molecules, a process also known as opsonisation.

Activation of the adaptive immune system through the process of antigen presentation by **A**ntigen **P**resenting **C**ells (APCs) finally leads to the induction of long-lasting protective immunity. The innate immune system recognises characteristic pathogen structures. These structures are generally called pathogen associated molecular patterns (PAMPs) and their binding receptors are known as pattern recognition receptors, including **T**oll-**l**ike-**r**eceptors (TLR). This particular type of pattern recognition receptor plays a pivotal role in the defense against microbes. TLRs are expressed on neutrophils, macrophages, dendritic cells and epithelial cells. Different TLRs show affinity for specific microbial products. LPS expressed on Gram negative bacteria is a well-known example among the potent TLR stimuli. In terms of *L.m.*, a representative Gram positive bacterium, components such as lipoteichoic acid, flagellin, peptidoglycan and bacterial DNA stimulate TLR-signalling. For example, TLR2 and TLR5 have been shown to be involved in recognition of *L.m.* (Hayashi *et al.*, 2001; Seki *et al.*, 2002). The major downstream effect of TLR-signalling is the activation of the transcription factor **n**uclear **f**actor **κB** (NF-κB) resulting in gene expression of inflammatory cytokines (tumor necrosis factorα/TNFα, **I**nter**l**eukin-1/IL-1), antiviral cytokines (IFNα, IFNβ) and chemokines (**m**onocyte **c**hemotactic **p**rotein-1/MCP-1, **C**C-**c**hemokine **l**igand-2/CCL2). Some of these TLRs use an adapter protein **my**eloid **d**ifferentiation primary-response protein **88** (MyD88) as an alternate way for signalling. TLR-signalling in association with this protein is probably important for *L.m.* resistance because mice lacking this MyD88 are highly susceptible to *L.m*. infection (Seki *et al.*, 2002).

In general, the effector cells of the innate immune system are neutrophils, mononuclear phagocytes and NK cells. During bacterial infection macrophages and neutrophils establish the first line of defense, which engulf and degrade invading microorganisms. During *L.m.* infection macrophages release CCL2, recognized by monocytes which express CCR2 (**C**C-**c**hemokine-**r**eceptor **2**). The interaction of CCL2 and its receptor facilitates the recruitment and arrival of an increasing number of monocytes to the infection site (Pamer, 2004). Consequently, these monocytes differentiate into

TipDCs (**T**NF and **i**NOS **p**roducing **d**endritic **c**ells). Neutrophils are simultaneously mobilised by IL-8 secreted by macrophages, epithelial cells or endothelial cells for initial infection control. With the aim of attracting more macrophages, they release the chemokine MCP-1 and the monocyte proliferation factor **c**olony-**s**timulating **f**actor-1 (CSF-1). In response to infection, macrophages in turn release TNFα and IL-12, driving NK cells to produce IFNγ, resulting in further activation of macrophages (Havell, 1987; Tripp *et al.*, 1993). IFNγ is one of the most important cytokines for the process of bacterial killing and induces expression of proteins essential for clearance of bacteria. Mice deficient in IFNγ-Receptor showed increased susceptibility to *L.m*. infection (Huang *et al.*, 1993). One defense mechanism of IFNγ-activated macrophages is RNI (**r**eactive **n**itrogen **i**ntermediates) production, described in chapter 1.3.4. Release of **n**itric **o**xide (NO) is mediated by the enzyme iNOS (**i**nducible **n**itric **o**xide **s**ynthase), catalysing the conversion of arginine to citrullin and NO, which is toxic to bacteria by causing damage to the microbial DNA. RNI formation and the "respiratory burst" are essential mechanisms in bacterial killing via macrophages.

In the recent years, other molecules like special GTPases have shown to be involved in the immune response to infected macrophages. The IFNγ and **L**PS-**r**esponsive **G**TPase LRG-47 belongs to a unique class of **I**FNγ-inducible **47**-kilodalton immunity **r**elated **G**TPases (p47 IRGs) which are thought to drive their antimicrobicidal effects in particular by remodeling the pathogen-containing niche or by interfering in vesicular memrane trafficking. LRG-47 was suggested to promote maturation and acidification of mycobacterial phagosomes as a mechanism to combat ***m**ycobacterium **t**u**b**erculosis* (*Mtb*) infection. This was shown by macrophages deficient in this protein which fail to control *Mtb* infection properly (Collazo *et al.*, 2001; Tiwari *et al.*, 2009).

Another interesting mechanism was observed during *L.m.* infection. Microbial products of this pathogen were shown to induce Type I interferon response, comprising IFN α and β (Nakane and Minagawa, 1984). These cytokines are usually associated with anti-viral immune response, resulting in the transcription of pro-apoptotic and antigen presentation genes. Induction of type I interferons is essential for clearance of many viral pathogens. The bacterium *L.m.,* on the contrary, induces type I interferon release for its own benefit in order to dampen inflammation. IFN α and β were shown to induce T-cell apoptosis early during *L.m.* infection, resulting in IL-10 secretion by regulatory macrophages (See 1.3.3). This seems to be in favour of *L.m.* and is probably induced by the pathogen itself as a potential survival mechanism (Carrero *et al.*, 2004).

1.3.2. Adaptive immune response

Both innate and adaptive immune responses are essential for the infection control of intracellular bacteria (Unanue, 1997). The adaptive immune system allows a strong immune response and

immunological memory. Recognition of specific antigens during the process of antigen presentation by infected macrophages is the initial step in control of intracellular bacteria such as *L.m*. **T**hymus (**T**)-lymphocytes are the main players for cell mediated immunity. One member of this type of lymphocytes are T helper cells (T_H Cells), also known as $CD4^+$ T-cells, which assist in immunologic processes by secreting cytokines such as IFNγ. They stimulate the bactericidal activity of macrophages against phagocytosed pathogens and are activated by **M**ajor **H**istocompatibility **C**omplex (MHC) class II presented peptide antigens expressed on the surface of APCs. $CD4^+$ T-cells also bring B-lymphocytes to differentiate and proliferate for antigen specific immunity. Another member of T-lymphocytes are **c**ytotoxic **T c**ells (CTLs), also known as $CD8^+$ T-cells, which recognise antigens associated with MHC class I presented on the surface of nearly all cells of the organism. These T-cells mediate the destruction of pathogen infected and dysfunctional cells by releasing cytotoxins such as perforin and granzymes. During *L.m*. infection antigens are presented in different ways, depending on which cells are infected. *L.m.* secretes LLO for disruption of the phagosomal membrane (see 1.2) and other proteins, culminating in their degradation by proteasomes. After transport through the endoplasmatic reticulum, peptides derived from cytosol proteins are loaded on MHC class I molecules and are then presented to $CD8^+$ T-cells. By APCs exposed *L.m.* antigens derive from bacterial secreted, non-secreted or surface-proteins. Among these, LLO is the most potent inductor of specific $CD8^+$ T-cells. APCs also present proteins derived from lysosomal compartments to $CD4^+$ T-cells via MHC class II. However, $CD8^+$ T-cells seem to be more relevant for anti-listerial immunity. These lymphocytes destroy infected cells by releasing perforin, creating pores in the membrane. Apoptosis inducing granzymes penetrate through these pores, leading to exposition of intracellular *L.m.* to IFNγ activated macrophages. In the context of secondary infection, a crucial role lies in perforin action during $CD8^+$ T-cell mediated bacterial eradication, as $CD8^+$ T-cells of perforin deficient mice were impaired in their ability to transfer antilisterial immunity to naive hosts (Kagi *et al.*, 1994). However, there was evidence of a perforin-independent pathway of $CD8^+$ T-cells mediated protective immunity which was shown to be a TNF-dependent mechanism (White and Harty, 1998).

Following an effective bacterial eradication, long-lasting protective immunity against intracellular bacteria is provided by memory T-cells. They specifically destroy infected cells and secrete IFNγ leading to activation of macrophages in order to control a secondary infection more rapidly. Intracellular bacteria induce the production of very specific memory T-cells demonstrating the importance of adaptive immunity in infection control of *L.m.* (Jiang *et al.*, 2003).

Humoral immunity against *L.m.* is theoretically less essential because intracellular bacteria are seldom found in the extracellular milieu. In certain experimental conditions however, LLO produces

high titers of antibody and may play a role in protection against *L.m.* infection (Edelson and Unanue, 2001).

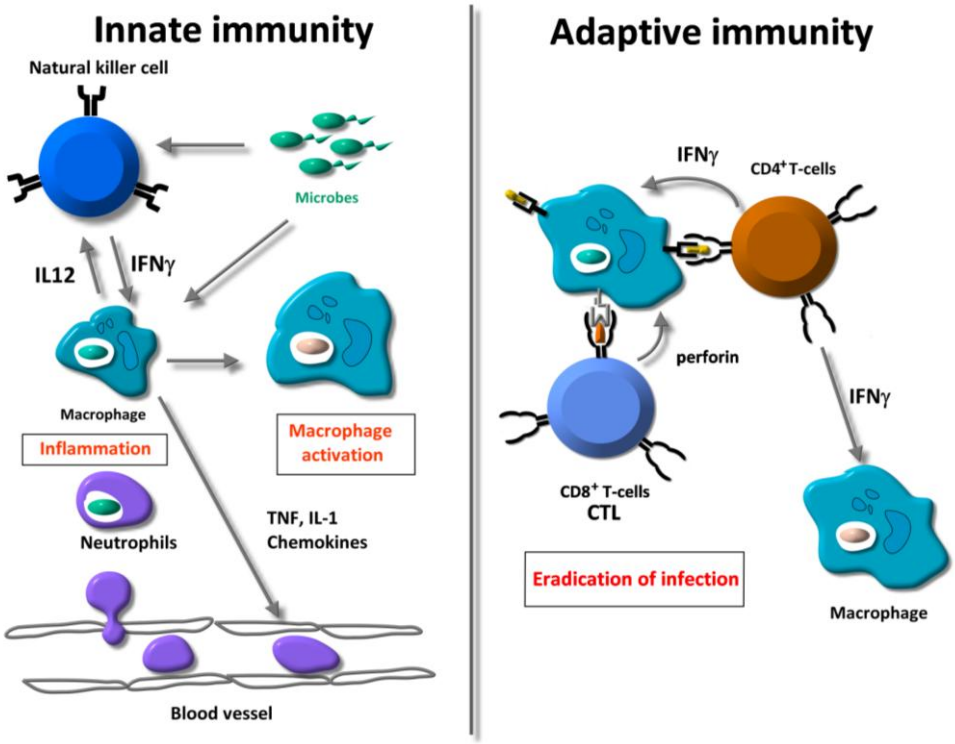

Figure 1.2: Innate and adaptive immune response to intracellular bacteria
Left: *Innate immune response to intracellular bacteria is mediated by macrophages, which engulf bacteria and release cytokines. IL-12 activates NK cells to release IFNγ, which in turn enhances the ability of macrophages to kill bacteria. Other cytokines like TNFα and IL-1 are also released to mediate local inflammation. Chemokines attract other effector cells like neutrophils.*
Right: *In adaptive immunity, cytokines stimulate proliferation and differentiation of antigen-stimulated lymphocytes and activate effector cells. CD4$^+$T cells respond to class II MHC-assiociated peptide antigens. These T cells pruduce IFNγ which activates the infected macrophage to destroy the microbes. CD8$^+$T cells respond to class I-associated peptides and kill the infected cell. This finally terminates the infection. (based on Abbas, cellular and molecular immunology, 6th edition); CTL= cytotoxic T-cell*

1.3.3. Macrophages

Almost 100 years ago, macrophages were described to be the effector cells in systems that are now known as the innate and adaptive immune system. In 1908, Ilya Mechnikov (also known as Elie Metchnikoff) and Paul Ehrlich were awarded with the Nobel Prize in physiology and medicine for discovering the function of macrophages. Mechnikov described phagocytes as the functional cells for ensuring homeostasis and protecting the host from infection through a process he called “innate immunity”. Paul Ehrlich held the opinion that host defense depended on soluble host macromolecules with high specificity to factors needed by pathogens and he believed immunity was rather a molecular than a cellular process. At that time both views were regarded as competing

alternatives. Today we know that these are complementary systems and Ehrlich's discovered soluble components belong to the system called "adaptive immune system" (Nathan, 2008).

Macrophages are bone marrow derived cells and part of the mononuclear phagocyte system. They are released from the bone marrow into the bloodstream and are called monocytes until they enter various tissues, mature and become macrophages. During monocyte development, myeloid progenitor cells (termed granulocyte/macrophage-colony forming units) undergo several differentiation steps in the bone marrow. In response to **m**acrophage **c**olony-**s**timulating **f**actor (MCSF) they differentiate into monoblasts, then pro-monocytes before becoming monocytes and entering the bloodstream (Mosser and Edwards, 2008). Some publications suggest that two different populations of monocytes exist in the bloodstream of mice before reaching their parenchymal destination. Based on different phenotypes and biochemical signatures, they are divided into inflammatory and resident monocytes. Inflammatory monocytes exit the blood rapidly and differentiate into macrophages in the infiltrated tissue, in contrast to resident monocytes, which probably stay longer in the blood system and mature in non-inflamed tissues (Geissmann *et al.*, 2003). Macrophages, however, depending on the localisation site and different stimuli, acquire different morphological forms, branching them out into various subpopulations. For instance, macrophages are known as microglia in the central nervous system, Kupffer cells in the liver, alveolar macrophages in pulmonary airways and osteoclasts in the bones.

Generally, macrophages have three major functions: phagocytosis, antigen presentation and the modulation of immune responses through production of various cytokines and growth factors. They play a critical role in defense against a wide variety of microorganisms including, bacteria, viruses, fungi and protozoa. They are involved in the initiation, maintenance and resolution of inflammation and respond to a variety of microbial products and cytokines. Such cytokines are produced by cells of the innate immune in the case of injury or infection, or by antigen-specific immune cells. Additionally, macrophages produce several factors themselves for autocrine stimulation. The response of macrophages to different activator and inhibitory ligands results in a complex modulation in phenotype and tremendous heterogeneity in their activities. Based in this heterogeneity a classification of macrophages into two major groups was suggested, namely the classical activated also known as M1 macrophages, and the alternatively activated, known as M2 macrophages. This classification arose in analogy with their activation by cytokines released from **T**-**h**elper-**1** (Th1) and **T**-**h**elper **2** (Th2) lymphocytes (IFNγ and IL-4 or IL-13, respectively) (Gordon and Martinez, 2010; Pluddemann *et al.*, 2011).

According to their diversity of functions, Mosser and Edwards suggested a subdividing of macrophages into three groups, namely the classically activated, the wound healing (or alternatively activated) and the regulatory macrophages (Mosser and Edwards, 2008). Classically activated

macrophages arise in response to the priming stimulus of **I**nter**f**ero**n**-γ (IFNγ) and a second signal, TNFα. These two cytokines enhance macrophages' microbicidal activity and activate them to release pro-inflammatory cytokines (Nathan, 1991). The second signal TNFα is in general released by macrophages themselves as a result of TLR-signalling due to contact with microbial products such as **l**ipo**p**oly**s**accharide (LPS) and induced by IL-1 also released from macrophages or is produced by a variety of other cells including mast cells, endothelial cells and fibroblasts. The main task of these types of macrophages is to migrate to the site of inflammation and engulf pathogens for degradation (Mosser, 2003). A second feature of classically activated macrophages is their enhanced capacity to kill intracellular bacteria which is in part due to their ability to produce oxidative burst products such as **n**itric **o**xide (NO) (Hibbs, Jr., 2002; MacMicking *et al.*, 1997). Furthermore, they express IL-1, IL-6 and IL-23 also important components of host defense.

Wound healing macrophages show different functions. For instance, these macrophages fail to produce NO and therefore are less efficient in eradicating intracellular microbes. This is mediated by IL-4, which induces the activation of Arginase1 (Arg1). Arginase competes with iNOS for the substrate arginine resulting in less NO (Rutschman *et al.*, 2001). Arginase 1 is also involved in polyamine and proline biosynthesis, which is important for collagen formation and tissue repair. This contributes to the wound healing activity of these macrophages (Hesse *et al.*, 2001; Kreider *et al.*, 2007).

Regulatory macrophages have various functions but their primary role is to suppress immune response and limit inflammation, mainly by production of high levels of the anti-inflammatory cytokine IL-10. Regulatory macrophages arise in response to stimuli such as glucocorticoids released during stress response, the cytokine TGFβ released by macrophages after phagocytosis of apoptotic cells (Fadok *et al.*, 1998) and prostaglandins (Strassmann *et al.*, 1994).

An additional, general task of macrophages is the removal of cellular debris that is generated during tissue remodelling and they rapidly clear cells that have undergone apoptosis. Phagocytosis of such cellular debris and clearance of the interstitial environment from cellular material are principal functions of macrophages besides their activity in immune response.

1.3.4. Phagocytosis and phagosome maturation

Phagocytosis is a type of endocytosis which generally describes the uptake of extracellular material. The ability of phagocytosis is limited to only a few cells such as macrophages, monocytes and neutrophils, usually in order to eliminate pathogens and clear the organism from apoptotic cell debris. The phagocytic process is complex and hard to describe with a single model. The first step in phagocytosis is the recognition of microbes and apoptotic cells by specific receptors, which are functionally linked to the mechanism of phagocytosis. These receptors are very important because

macrophages are constantly exposed to the body's own structures and need to differentiate between them and exogenous structures. Some of these receptors are pattern recognition receptors, TLR´s and receptors that in particular recognise microbes coated with antibodies, complement proteins or lectins, a process known as opsonisation. The final purpose of phagocytosis is to kill the ingested microbe by means of microbicidal molecules in the phagolysosome. The particle or bacteria uptake which occurs throughout phagocytosis involves many different proteins and signalling molecules. The phagocytosed particle or pathogen is first surrounded by the cell membrane, forming the phagosome. The initial phagosome is not able to kill pathogens, it must previously interact with a series of endosomes and lysosomes, resulting in a process called phagosome maturation (Haas, 2007; Vieira *et al.*, 2002).

This maturation process requires fission and fusion events, termed 'kiss and run' by M. Desjardin (Duclos *et al.*, 2000), resulting in a degradative environment in the vacuole. 'Kiss and run' means these organelles do not completely fuse, but rather more partially fuse ('kiss') to mix their cargo and membrane proteins with the phagosome. Subsequent fission events separate them again ('run'), preventing complete intermixing of these organelles. However, final membrane fusion with lysosomes has been observed by Luzio *et al*. (Luzio *et al.*, 2005).

Small GTPases of the Rab-family ("**Ra**s-related in **b**rain") play an essential role in this maturation process. These molecules have functions in vesicle transport and vesicle fusion which also includes fusion with phagosomes (Jordens *et al.*, 2005). One of the first GTPases appearing on the phagosomal compartment is Rab5. This protein drives early endosome fusion events to the extent that overexpression of a constitutive active form of Rab5 stimulated endocytosis and vesicle fusion resulting in giant endosomal vesicles. On the contrary, overexpression of a dominant negative mutant with a higher affinity to GDP resulted in blockade of endocytosis and endosome fusion (Stenmark *et al.*, 1994). Rab5 appears in three isoform Rab5a, Rab5b and Rab5c, which are all involved in vesicular trafficking. Rab5-GTP, the active form of Rab5 on the phagosomal membrane, recruits the **e**arly **e**ndosome **a**ssociated protein **1** (EEA1), a protein for vesicular transport (Mu *et al.*, 1995). Regarding motility of phagosomes in the cell, current data suggests actin is involved in transport of large phagosomes, whereas smaller ones probably travel along microtubules. Nevertheless, both microtubules and microfilaments seemed to be involved in phagosomal transport (Moller *et al.*, 2000; Toyohara and Inaba, 1989).

The lumens of these early phagosomes show mildly acid pH of 6.3 which changes to about 5.5 when these compartments mature and enter the late phagosomal stage. This stage is characterized by a multivesicular structure and the appearance of other proteins like Rab7 and **l**ysosomal **a**ssociated **m**embrane **p**roteins (LAMP´s). The transition of late phagosome to phagolysosme is also suggested to be driven by Rab proteins (Funato *et al.*, 1997). Rab7 and its interacting protein RILP (**R**ab7-

interacting **l**ysosomal **p**rotein) seemed to be essential for phagolysosomal formation, additionally linking the microtubule/dynein machinery to this process (Harrison *et al.*, 2003). Acidification of the lysosomal compartment is an essential step in phagosome maturation, as a low pH value is a prerequisite for sufficient activation of cathepsin familiy proteases and optimal for hydrolytic enzyme function. Phagosome acidification is regulated by vacuolar ATPase complex (V-ATPase) which translocates protons from the cytoplasm into the intraphagosomal lumen resulting in pH values lower than 4.5 towards the end of this process (Lukacs *et al.*, 1990). Acidic vesicles are the optimal environment for degradation of proteins and pathogens. An important protease in this acidic lumen is the aspartyl-protease CTSD. Together with LAMPs, processed CTSD is among the major characteristics of a lysosomal compartment.

In addition, activated macrophages respond to bacterial infection by producing **r**eactive **o**xygen **s**pecies (ROS) where molecular oxygen is reduced to superoxide radicals and hydrogen peroxide. Known as “respiratory burst”, this rapid release of ROS is mediated by phagocyte oxidase, a multisubunit enzyme which assembles on the phagolysosomal membrane and is activated by IFNγ and TLR´s signals. Another IFNγ driven process is the production of RNI, generated by the action of iNOS. This enzyme catalyzes the formation of NO from L-arginine and molecular oxygen. The emerged NO is an unspecific toxic radical which can lead to tissue injury in the host or be cytoprotective by destroying pathogenic microorganisms. The free radical NO can react with superoxide resulting in formation of peroxynitrite, one of the most powerful oxidants known to be generated in organisms. It can change protein structures by nitrosylation and nitration of amino acids and cause DNA damage, including base modification or DNA strand breakage. Together ROS and RNI contribute to the eradication of microbes within the phagolysosomal compartment. Sequential steps of the phagosomal maturation process is shown in figure 1.3

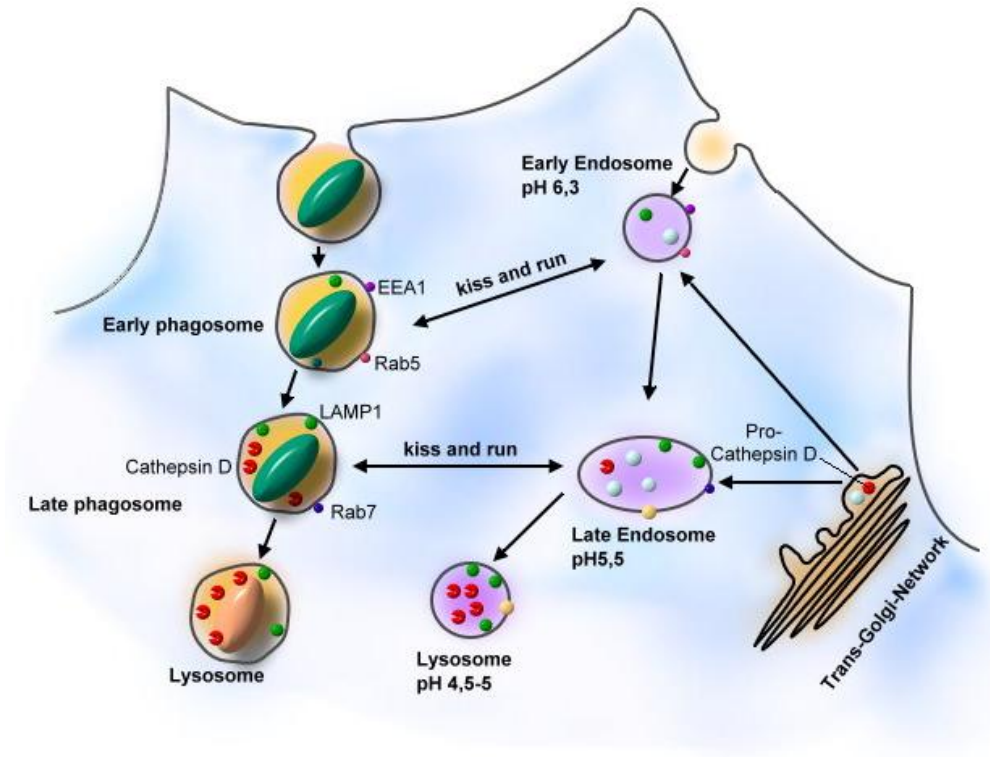

Figure 1.3: Sequential steps of phagsome maturation
0-5 min: *the early phagosome appears with markers like EEA1 and Rab5.* ***5-30 min:*** *' kiss and run' events drive the maturation process into a late phagosome, where markers like LAMP1 and Rab7 are recruited from the trans-Golgi network to the endosomal-phagosomal compartment.* ***30-60 min:*** *Rab7 promotes fusion with lysosomes and recruitment of procathepsin D. Decreasing pH promotes maturation of cathepsin D (based on Russell, 2001).*

1.3.5. Cathepsin D

As described above, CTSD is found in lysosomal organelles. However, before CTSD reaches the phagosome in its mature active form it must undergo several maturation steps in the endosomal compartment. CTSD is an aspartatic protease of the pepsin superfamily with several physiological functions such as protein degradation, apoptosis and autophagy. In humans, CTSD is synthesized as a single polypeptide on the **r**ough **e**ndoplasmatic **r**eticulum (RER). This Pre-pro-CTSD contains a secretion signal peptide, which is removed during co-translational translocation across the ER membrane resulting in the inactive form of pro-CTSD (52 kDa). On two N-linked glycosylation sites CTSD is glycosylated and transported to the Golgi stacks. In order to finally reach its destination, the lysosomal compartment, glycosylated CTSD is phophorylated at mannose residues of the N-linked oligosaccharides. These are recognised by the mannose-6-phophat receptor (MPR300) in the *trans*-Golgi network, where lysosomal hydrolases are packed in budding transport vesicles before routing them into endosomes and lysosomes. Pro-CTSD is proteolytically processed in these compartments, initially through the dissociation of MPR300 and its phosphate groups, along with the removal of the propeptide. This propeptide, also known as the activation peptide, is reported to be essential for

correct folding, activation and delivery of the protein to lysosomes (Laurent-Matha *et al.*, 2006; Takeshima *et al.*, 1995). Its removal generates the resulting active intermediate molecule of CTSD (48 kDa) (Zaidi *et al.*, 2008). This 48 kDa CTSD intermediate is further processed into the mature form consisting of an aminoterminal light chain (14 kDa) and a carboxyl-terminal heavy chain (34 kDa). Both forms represent the active form of CTSD. The molecular mechanism of CTSD processing is controversially discussed. An activation-process mediated by cystein proteases such as cathepsin L and cathepsin B have been reported (Laurent-Matha *et al.*, 2006). On the other hand, *in vitro* studies claimed an autocatalytical generation of active CTSD as a consequence of the low pH values resulting in an enzyme form that retains 18 residues of the propeptide (Hasilik *et al.*, 1982; James and Sielecki, 1986). However, this CTSD form was shown to be not a required intermediate for CTSD-processing, therefore it rather seemed to be an *in vitro* artefact (Laurent-Matha *et al.*, 2006).
Another way of CTSD activation was reported via ceramide generated by the hydrolase acid sphingomyelinase (ASMase), which links TNF-R1 signalling to CTSD activation (Heinrich *et al.*, 2004). Earlier studies showed that CTSD is a target of the second messenger lipid ceramide and is activated by this molecule (Heinrich *et al.*, 1999). TNF-R1 was shown to internalise upon TNFα stimulation and to undergo a vesicle maturation process. Interestingly, the mature form of CTSD was found to be localised within these isolated TNF-R1 containing compartments (see 1.5.1).

1.4. Structural and functional features of TNFRs and ligands

1.4.1. TNFR superfamily

TNFα and TNF-R1 belong to the TNF/TNFR (TNF-receptor) superfamily, a system which consists of more than 40 identified ligand and receptor proteins, to date. The binding of TNF family members to their receptors induces a variety of different responses. These responses are either anti- or pro-apoptotic leading to activation of the transcription factors NF-κB and **A**ctivator **P**rotein-1 (AP-1) or to activation of initiator and effector caspases, respectively. The selected pathway depends on the particular receptor which is used and the cell type on which the receptor is expressed. The TNFR superfamily members share equal structures in the ligand-binding region, but vary greatly in their intracellular cytoplasmatic domains. TNFRs are transmembrane proteins typ I and are expressed on almost all cell types except erythrocytes and unstimulated T-lymphocytes. At present, 19 superfamily ligands have been identified, binding to 32 different TNFRs. These receptors are characterized by several copies of **c**ystein **r**ich **d**omains (CRD) connected by disulfide bonds, creating the scaffold of the extracellular part (Locksley *et al.*, 2001; Smith *et al.*, 1994). The intracellular part consists of several functional domains. The TNFR superfamily can further be divided into roughly three groups, depending on their binding domain functionality in the intracellular part. The first group possesses a

so-called **d**eath **d**omain (DD), a region of about 80 amino acid residues in the cytoplasmatic domain. The second group is characterised by a motif in its intracellular domain binding accessory molecules, called **T**NF **r**eceptor **a**ssociated **f**actors (TRAFs). The last group apparently does not transmit any signal, belonging to what is known as decoy receptors (Grivennikov *et al.*, 2006). DD receptors can induce apoptosis by binding various cytoplasmic adapter molecules. These death receptors are CD95, TNF-R1, DR3 (death receptor 3), TRAIL-R1 (**T**NF-**r**elated **a**poptosis-**i**nducing **l**igand **r**eceptor 1), TRAIL-R2, DR6, p75-NGFR (p75-**n**erve **g**rowth **f**actor **r**eceptor) and EDAR (**e**ctodermal **d**ysplasia **r**eceptor) (Wajant , 2003). The extrinsic signalling pathway of apoptosis is mediated by these death receptors. The DD of these receptors serves as a platform for the recruitment of different adapter molecules which lead to the apoptotic signal. In the case of TNF-R1, FADD (**F**as **a**ssociated **d**eath **d**omain), TRADD (**T**NF-**r**eceptor **a**ssociated **d**eath **d**omain) and the initiator caspase-8 are indispensible components for the generation of the **d**eath **i**nducing **s**ignalling **c**omplex or DISC (Scaffidi *et al.*, 1999). The TNF-R1 signalling pathway is discussed in detail in 1.5.1.

Prior to ligand-binding, TNFRs preassemble into trimer complexes on the cell surface. This formation requires a region at the amino terminal end of the receptors and is termed PLAD for **p**re **l**igand **a**ssembly **d**omain (Chan *et al.*, 2000; Siegel *et al.*, 2000). TNFRs usually form homotrimers and this is essential for ligand-binding and signal transmission.

1.4.2. Tumor Necrosis Factor α

TNFα is a key mediator in immunity and inflammation and has a plethora of functions. Its biological role ranges from protective effects in inflammation to host defense and important cytokine action in organogenesis. It plays a part in cell proliferation, survival, differentiation and apoptosis, addressing different signal transduction pathways (Hehlgans and Pfeffer, 2005). Furthermore, a role of TNFα in the pathogenesis of many human diseases, including sepsis, cerebral malaria, diabetes, cancer, osteoporosis, allograft rejection, and autoimmune diseases such as multiple sclerosis, rheumatoid arthritis, and inflammatory bowel diseases has been implicated (Chen and Goeddel, 2002).

The action TNFα first surfaced in the 19th century surgical ward of Paul von Bruns (Bruns, 1888), based on the anti-tumoural response observed in patient upon a bacterial infection. These findings were further examined by the American physician W.B Coley, who developed an anti-tumoural therapy with bacterial extracts known as the Coley's toxin (Coley, 1893). Studies of mice infected with Bacillus Calmette-Guerin (BCG) and treated with endotoxin showed that the endotoxin is doubtfully the substance responsible for tumour regression, but rather a factor released from the host cell itself. This factor was named **t**umor **n**ecrosis **f**actor (TNF) because of its necrotic action with tumours (Carswell *et al.*, 1975). In 1985, Bruce A. Beutler and Anthony Cerami discovered that a

hormone that induces cachexia and previously-named cachectin was actually TNF (Beutler *et al.*, 1985).

TNF is also termed TNFα to distinguish it from the closely related cytokine lymphotoxin/TNF β, which binds the same receptors. There are two existing molecules of TNFα, the 27 kDa type II transmembrane protein and the 17 kDa soluble cytokine. The membrane associated protein is cleaved by the metalloproteinase TACE (**T**NF **a**lpha **c**onverting **e**nzyme*)*, giving way to the 17 kDa soluble TNF (Black *et al.*, 1997; Gearing *et al.*, 1994). These smaller resulting molecules arrange into a homotrimeric structure, forming the 51 kDa TNF cytokine (Eck *et al.*, 1989; Jones *et al.*, 1989). Both membrane bound and soluble TNF are biologically active.

TNFα is released in very high amounts by macrophages after LPS stimulation, and to a certain extent by antigen stimulated T-Cells, NK cells and mast cells (see 1.3.3). One of the primary biological functions of TNFα is to bring inflammatory cells towards the infection site and activate their microbicidal capacity. With this aim, TNFα induces the expression of adhesion molecules on the surface of vascular endothelial cells, grasping circulating leucocytes as they pass through the site of infection. This process is mediated by the expression of proteins such as E-selectin and **i**ntercellular **a**dhesion **m**olecule-**1** (ICAM-1) (Munro *et al.*, 1989). TNFα also induces the release of chemokines for the attraction of immune cells like MCP-1 during inflammation (Rollins *et al.*, 1990). Low concentrations of TNFα induce inflammation, but high amounts cause acute damage to the organism. Metabolic disturbances, rapid decrease in blood pressure and intravascular thrombosis are among these potentially fatal consequences. LPS induced TNFα is also the principal factor leading to septic shock, characterised by the aforementioned pathological conditions.

Apart from its function in the immune response, TNFα also induces apoptosis in some cell types, which plays a role in the elimination of virus infected cells. This apoptotic activity is mediated by TNF-Receptor-1 signalling described in detail in 1.5.1.

1.4.3. Tumor Necrosis Factor Receptor-1

The diverse cellular functions of TNFα are mediated by two distinct receptors of the TNFR superfamily, TNF-R1 (55 kDa) and TNF-R2 (75 kDa). Both receptors show similarities in their extracellular domains, but diverge in their intracellular part. In contrast to TNF-R1, the intracellular part of TNF-R2 lacks the death domain (DD). Therefore, the main function of TNF-R2 is the activation of the NF-κB-signalling pathway via TRAF binding. This results in cytokine production or transcription of anti-apoptotic factors like c-IAP1 and c-IAP2 (cellular inhibitor of apoptosis 1 and 2) (Wang *et al.*, 1998). Nevertheless, TNF-R2 also seems to be engaged in TNF-R1 signalling. The “ligand passing” model describes the rapid binding of TNFα to TNF-R2, increasing the local level of TNFα on the cell

surface in order to pass it over to TNF-R1, thus resulting in signalling enhancement (Tartaglia *et al.*, 1993).

Another difference between those two receptors is their affinity to different TNF-molecules. TNF-R2 is mainly activated by the transmembrane form, whereas TNF-R1 shows higher affinity to soluble TNFα (Grell *et al.*, 1995; Grell *et al.*, 1998). Due to its widespread appearance and high expression levels, TNFα induced signalling is mainly transmitted by TNF-R1. In order to mediate its diverse actions, it contains several functional domains such as intracellular DD and the **N**eutral **S**phingomyelinase **D**omain (NSD). The DD platform is used for binding various proteins, either to start apoptotic signalling or to promote cell survival with the activation of NF-κB signalling. This dichotomy of TNF-R1 signalling is regulated by receptor internalisation. TNF binding and receptor internalisation leads to activation of the apoptotic signalling pathway. The deletion of a functional sequence in the intracellular domain called **T**NF-**r**eceptor **i**nternalisation **d**omain (TRID) prevents apoptotic signalling but allows NF-κB signalling (Schneider-Brachert *et al.*, 2004). These findings suggested that receptor internalisation is a prerequisite event to start apoptosis but not necessary for NF-κB signalling. However, apoptotic signalling is not only induced after TNF-R1 internalisation. Other ways exist to induce apoptosis alternatively via TNF-R1 (see 1.5.2).

Ligand binding induces critical steps for downstream signalling events: first receptor trimerisation, followed by receptor internalisation and resulting DISC formation (see 1.5.1). Another functional domain for transmission of apoptotic signals is previously mentioned NSD (Adam *et al.*, 1996). The factor FAN (**f**actor **a**ssociated with **n**eutral sphingomyelinase) interacts with NSD and activates the enzyme neutral sphingomyelinase on the plasma membrane, facilitating the hydrolysis of sphingomyelin to ceramide and phosphocholine. This signalling molecule ceramide induces cell death, independent of DISC formation (Adam-Klages *et al.*, 1996).

1.5. The diversity of TNF-R1 signalling

1.5.1. Apoptotic signalling via DISC formation

The initial step for TNF-R1 induced apoptotic signalling is the DISC-formation. The DISC consists of the adapter-proteins TRADD, FADD and the initiator caspase-8. Schneider-Brachert *et al*. were able to demonstrate that TNF-R1 associated DISC-formation is one of several possible ways of inducing apoptotic signalling which comprises receptor internalisation as the primordial event (Schneider-Brachert *et al.*, 2004). The above mentioned intracellular TRID sequence contains a distinct motif (YQRW), also known for receptor endocytosis by clathrin coated vesicles (Bonifacino and Traub, 2003). Deletion of this domain or mutations in this motif lead to complete loss of internalisation, DISC formation and TNFα induced apoptotic signalling. This is in contrast to the work of Micheau and

Tschopp who suggested two sequential signalling complexes for TNF-R1 mediated signalling. In this model on plasma membrane bound Complex I triggers NF-κB signalling and is composed of TNF-R1, TRADD, RIP, TRAF2 and c-IAP. Apoptosis signalling is induced by Complex II, which lacks TNF-R1 but includes FADD and procaspases-8 and -10 (Micheau and Tschopp, 2003). These controversial findings regarding TNF-R1 associated DISC formation can be explained by the different experimental approaches used. Schneider-Brachert *et al.* worked with a new isolation technique based on magnetically labelling of TNF-R1. This method allowed the purification of specific receptor containing vesicles. In this particular model ligand binding induces TNF-R1 internalisation and initiates the recruitment of TRADD to the cytoplasmatic DD (Hsu *et al.*, 1996b). From this point on, both pro- and anti-apoptotic signalling pathways can begin. In case of apoptosis, TRADD binds FADD and procaspase-8 binds to the death effector domain (DED) of FADD. Procaspase-8 is autocatalytically processed and activated. Caspase-8 induces subsequent activation of caspase-3, an effector-caspase which initiates successive mechanisms of apoptosis. In some cell types, activation of caspase-8 is insufficient for caspase-3 activation and a second mitochondria-associated pathway is deemed necessary to amplify the apoptotic signal. In this case, the cytosolic protein and pro-apoptotic Bcl-2 (**B**-**c**ell **l**ymphoma **2**) family member Bid (**b**orane **i**nteracting **d**omain death agonist) is cleaved by caspase-8. Translocation of **t**Bid (truncated Bid) from the cytoplasm into the mitochondria-membrane induces cytochrom C release, initiating apoptosome assembly and caspase-3 activation (Li *et al.*, 1998; Luo *et al.*, 1998) (see 1.5.2)

Throughout the TNF-R1 internalisation process, receptor-containing vesicles called "TNF-R1-receptosomes" undergo endocytic maturation. These receptosomes follow the endocytic pathway and fuse with *trans*-Golgi-vesicles. These maturational steps can be traced by the appearance of early endosomal markers such as GTPases (Rab4, Rab5), *trans*-Golgi membrane proteins (p47A, Vti1b) and lysosomal proteins (LAMP1, mature cathepsin D) on receptosomes. Other components such as the activated acid sphingomyelinase (ASMase) can also be found in TNF-R1 compartments (Schneider-Brachert *et al.*, 2004). Concomitantly, activation of ASMase seems to be tightly linked to internalisation because TNF-R1-mutants with deletion of TRID (TNF-R1ΔTRID) fail to activate this enzyme.

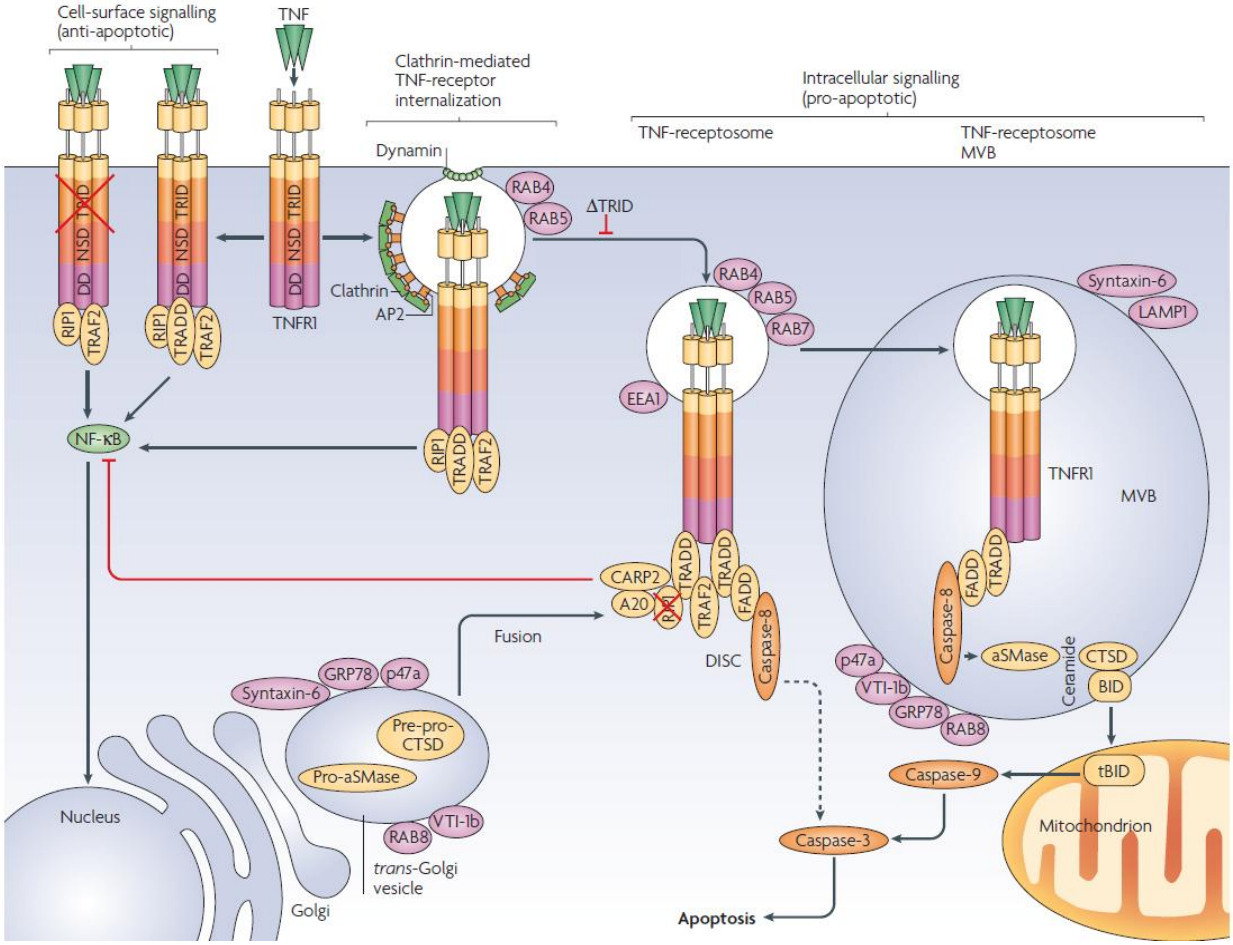

Figure 1.4: Model of TNFα induced TNF-R1 signalling pathways
Ligand binding of TNFα to TNF-R1 leads to several signalling cascades. Activation of NF-κB is mediated via recruitment of TRADD, TRAF2 and RIP1 at the cell surface. Blockade of internalisation by deletion of TRID gives way to NF-κB signalling via recruitment of TRAF2 and RIP1. TNF-R1 internalizes via clathrin mediated endocytosis to terminate NF-κB signalling via CARP-2 and A20. In order to induce apoptotic signalling, the recruitment of the DISC (TRADD, FADD, caspase-8) is essential. Caspase-8 activation is internalisation dependent and can induce caspase-3 activation. Throughout the endocytic pathway, TNF-R1 fuses with trans-Golgi-vesicles which contain pro-ASMase and pre-pro-Cathepsin D. Activated caspase-8 induces the mitochondrial apoptotic pathway via ASMase activation, cathepsin D activation, cleavage of BID and caspase-9 activation (Schütze and Schneider-Brachert, 2008)

1.5.2. Apoptotic signalling via acid and neutral sphingomyelinase activation

As mentioned earlier, an alternate apoptotic signalling pathway has been identified which occurs in association with mitochondria. Usually this pathway, also known as intrinsic pathway of apoptosis, is induced by viral infections and in response to DNA damage. Processes in this pathway are strictly under control of Bcl-2 family proteins which can either inhibit or promote apoptosis. Proapoptotic members of this familiy, Bid and Bax (**B**cl-2-**a**ssociated **X** protein) localise to the mitochondria and induce pore formation and permeabilisation of the outer mitochondrial membrane in order to release several proteins (Youle and Strasser, 2008). In particular, the cytosolic protein Bid is cleaved by caspases or proapoptotic proteases generating tBid which translocates into mitochondria,

interacts with proapoptotic Bcl-2 members (Bax and/or Bak for **B**cl-2 homologous **a**ntagonist/**k**iller) and initiates release of proteins from the inner mitochondrial membrane into the cytosol. Among these proteins is cytochrome C, a key component of the mitochondrial electron transfer chain. Cytochrome C adheres to the cytosolic factor Apaf-1 (**a**poptotic **p**rotease **a**ctivating **f**actor **1**) leading to the assembly of a heptameric protein ring called apoptosome (Shi, 2006; Wang, 2001). In order to facilitate apoptosome formation, Apaf-1 is equipped with an N-terminal caspase recruitment domain (CARD), a nucleotide-binding oligomerization domain (NOD) and cytochrome C binding region. The generated Apaf-1/cytochrome C-complex requires nucleotides (dATP or ATP) for procaspase-9 recruitment and activation (Zou *et al.*, 1999). After its association, procaspase-9 induces its autoactivation and active caspase-9 dissociates from the apoptosome-complex in order activate further downstream caspases such as caspase-3, caspase-6 and caspase-7 (Rodriguez and Lazebnik, 1999). These caspases in turn, cleave many intracellular substrates finally leading into the morphological changes characteristic for apoptosis.

In particular, TNF-R1 and the protease CTSD have been linked to this alternative pathway of apoptosis via acid and neutral sphingomyelinase. Upon TNF stimulation, TNF-R1 internalisation induces ASMase activation and ceramide generation (Heinrich *et al.*, 2004). The newly synthesised ceramide binds to CTSD, inciting the protease's autocatalytical activation. Activated CTSD subsequently cleaves the Bcl2-member protein Bid resulting again in tBid and starts the above described intrinsic pathway of apoptosis (Heinrich *et al.*, 1999).

Furthermore, missing TNF-R1 internalisation due to TRID motif deletion (TNF-R1ΔTRID) does not impede a residual activation of caspase-3 upon TNFα stimulation, irrespective of absent caspase-9 activation (Neumeyer *et al.*, 2006). These cells lack DISC formation and active caspase-9 but nevertheless enter apoptotic cell death. In this case, capsase-3 is activated by another enzyme, the neutral sphingomyelinase (N-SMase). Although TNF-R1ΔTRID is retained on the cell surface, TNF-R1 is still able to interact with the protein FAN using its NSD motif. Prolonged interaction with FAN results in overactivation of NSMase, which also hydrolyses sphingomyelin for ceramide generation. An overview of the precise process of apoptosome formation and the components for mitochondrial apoptotic signalling gives Figure 1.5.

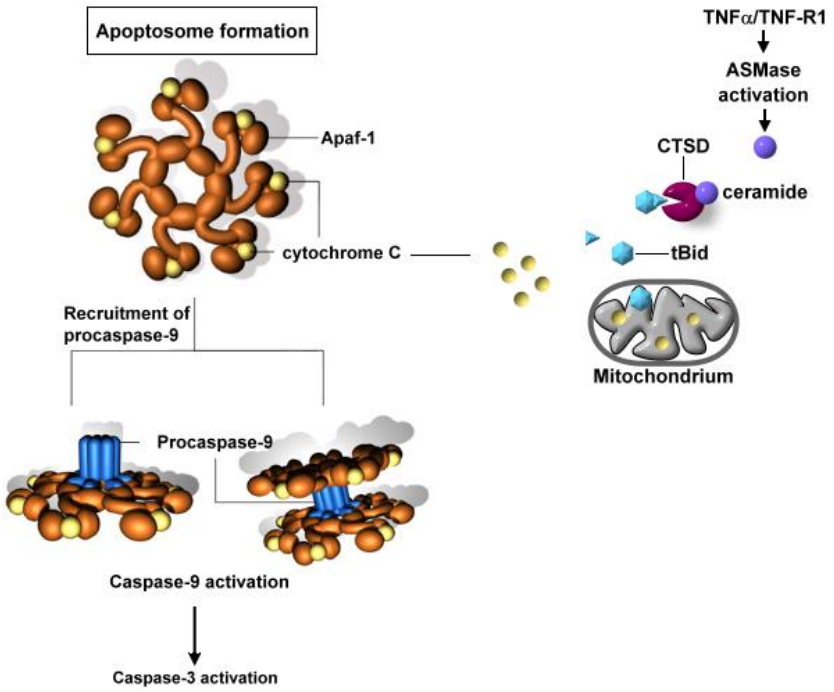

Figure 1.5: Apoptotic signalling via mitochondria: Apoptosome formation
TNF-R1-signalling results in activation of SMase which processes sphingomyelin resulting in ceramide. Ceramide activates CTSD which cleaves Bid. The resulting tBid translocates to mitochondria inducing cytochrome C release. In the cytosol, binding of cytochrome C to Apaf-1 and dATP/ATP leads to the formation of the apoptosome. After assembly of caspase-9 with the apoptosome, caspase-3 is cleaved by activated caspase-9, initiating apoptosis (Apaf-1: Dash Phil. "Caspases and apoptosis", Caspase activation. http://www.sgul.ac.uk/depts/immunology/~dash/apoptosis/caspases.htm 23. July 2011)

1.5.3. Anti-apoptotic signalling via NF-κB

As previously mentioned TNF-R1 can induce anti-apoptotic signalling also, resulting in NF-κB activation. NF-κB is a transcription factor known for promoting expression of a enormous variety of genes involved in cell survival, inflammation, immunity and cell proliferation (Karin and Lin, 2002). Many bacterial products and stimulation of a variety of cell-surface receptors lead to NF-κB activation. TLRs as specific pattern recognition receptors are the most prominent ones. Mammals express five Rel (NF-κB) proteins, which share an N-terminal Rel homology domain (RHD) responsible for DNA binding and homo- and heterodimerization. These proteins can be categorised into two groups. The first group consists of proteins which are synthesized as mature forms: RelA/p65, c-Rel and RelB. The NF-κB proteins p50/NF-κB1 and p52/NF-κB2 constitute the second group, which first appear as large precursor proteins (p105 and p100, respectively) and reach their mature form only after proteolytic processing. Dimerisation of these numerous aforementioned subunits results in the generation of functional transcription factors with diverse DNA-binding specificities and transactivation potentials (Li and Verma, 2002). These homo/heterodimer-complexes translocate

into the nucleus and induce gene transcription. NF-κB in general is responsible for regulating rapid cellular responses. Because of its constantly presence in the cytoplasm of the cell and no need of new protein synthesis for its activation, signalling through this factor allows a rapid response to diverse stimuli.

In the case of TNF-R1 signalling, NF-κB consists of the p50/p65 heterodimer and induces transcription of genes which generate anti-apoptotic proteins responsible for cell survival. Inactive NF-κB is located in the cytoplasm attached to its inhibitors IκBs (**i**nhibitor **κ**B) (Baeuerle and Baltimore, 1996; Siebenlist *et al.*, 1994). These inhibitors need to be removed to generate the active NF-κB protein which is mediated by the activated IKK (IκB Kinase) complex.

NF-κB signalling via TNF-R1 starts with the binding of TRADD to the DD, serving as an assembly platform for the proteins TRAF-2 (**T**NF **r**eceptor-**a**ssociated **f**actor-**2**) and RIP1 (**r**eceptor **i**nteracting **p**rotein-**1**) (Devin *et al.*, 2000; Hsu *et al.*, 1996a). Binding of TRAF-2 however is controversially discussed as there is evidence of an additional binding phenomenon, independent of TRADD. Here, RIP-1 and TRAF-2 bind directly to TNF-R1 DD (Jin and El Deiry, 2006; Zheng *et al.*, 2006). From this point, activation of the IKK-complex starts. The IKK-complex consists of the catalytic subunits IKKα, IKKβ and the regulatory subunit IKKγ (=NEMO for **N**F-kB **e**ssential **mo**dulator) (DiDonato *et al.*, 1997; Hu *et al.*, 1999; Li *et al.*, 1999). This complex is specifically activated by the DD kinase RIP (Li *et al.*, 1999; DiDonato *et al., 1997;* Hsu *et al.,* 1996a; Hsu, 1995; Stanger, 1995). RIP is a serine/threonin kinase, which is heavily ubiquitinated after recruitment to the TNF-R1. The IKK subunit NEMO specifically recognises these polyubiquitinated chains and activates the IKK complex (Ea *et al.*, 2006; Li *et al.*, 2006) The inhibitors IκBs are then phosphorylated upon TNF stimulation at serine residues 32 and 36 by the activated IKK-complex. This modification prepares them for ubiquitinylation by the E3-ubiquitin-ligase, resulting in degradation by the proteasome. Free of its inhibitors, NF-κB is now activated and able to translocate into the nucleus for target gene transcription and expression. Termination of NF-κB signalling is also linked to RIP. The E3-ubiquitin-ligase CARP2 (**c**aspase-**a**ssociated **r**ing **p**rotein-**2**) and the ubiquitin-ligase A20 both target RIP for K-48 linked ubiquitination, resulting in proteasomal degradation of RIP. Removing RIP causes final downregulation of TNFα induced NF-κB signalling (Liao *et al.*, 2008; Wertz *et al.*, 2004).

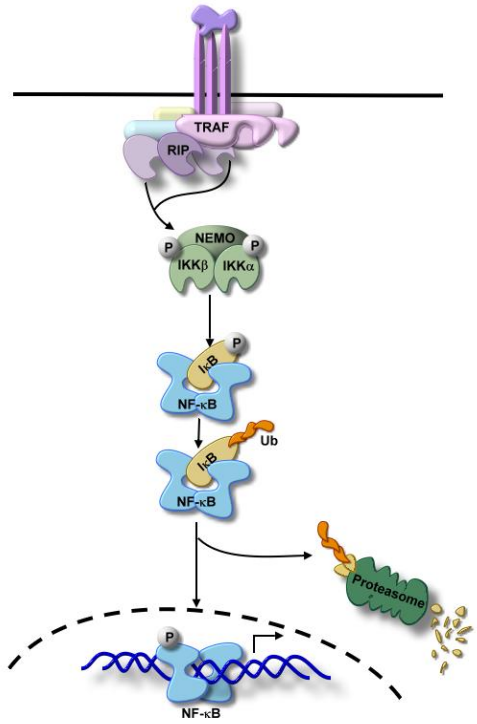

Figure 1.6: NF-κB signalling pathway
Following Receptor ligation, recruitment of receptor proximal adapter proteins and the TRAF-2/ RIP-1 complex leads to IKK activation. IKK consits of the subunits IKKα, IKKβ and NEMO which phopsphorylates the inhibitor protein IκB, prepares it for ubiquitinylation and results in proteasomal degradation of the protein. Phosphorylated NF-κB dimers translocate to the nucleus, binds to κB DNA elements and induces transcription of target genes. (Based on Hayden and Ghosh, 2008)

1.5.4. The MAP-kinase signalling

In order to complete the TNFα induced signalling cascades mediated by TNF-R1, the **m**itogen **a**ctivated **p**rotein-kinase (MAP-kinase) signalling pathway will be briefly represented in this chapter.
MAPKs are thyrosine/threonine kinases with functional implications in gene transcription, post-transcriptional regulation, apoptosis and cell cycle progression (Chang and Karin, 2001; Platanias, 2003). These kinases have been classified into three groups: the extracellular-signal regulated kinases (ERKs) ERK1 and ERK2, the p38 family (p38α, p83β, p38γ and p38δ) and the JUN amino-terminal kinases (JNKs) JNK1, JNK2 and JNK3. Recently identified MAPKs such as ERK3, ERK5, ERK7 and ERK8 have yet to be classified. The activation of these kinases is regulated by upstream kinases, known as MAPK kinases (MAPKKs), which phosphorylate thyrosine and threonine residues of all kinase groups. MAPKKs are in turn activated by their corresponding upstream kinases, known as MAPKK kinases (MAP3Ks) which are themselves activated by small GTPases. MAP3K function is regulated by guanine-nucleotide exchange factors (GEFs), which act as substrates for the receptor and non-receptor tyrosine kinases. This complex system of MAPKs facilitates the diversity of responses to different stimuli (Platanias, 2005). The MAP kinase signalling pathway is also involved in immune response and production of inflammatory cytokines. Via TLR signalling, activation of NF-κB and MAP kinases (p38 and JNK) lead to production of cytokines such as TNFα, IL-1 and IL-12 (Dong *et al.*, 2002; Kotlyarov *et al.*, 1999). TNFα itself, in turn, activates the p38 MAP kinase pathway and seems to be involved in bacterial killing. Mice deficient in MK2 (**m**itogen-activated protein **k**inase-activated protein kinase-**2**),

which is directly activated by p38-MAP kinase, show increased susceptibility to *L.m.* infection (Lehner *et al.*, 2002).

1.6. The signalling pathway of interferons

The most important interferon in innate and adaptive immunity is the cytokine IFNγ. Essential biological functions characterize this cytokine. It is critical for the immune response against viral and bacterial infections and for tumor control. Especially in the clearance of intracellular pathogens such as *L.m.*, IFNγ plays a predominant role (Murray, 1988; Portnoy *et al.*, 1989). IFNγ production by NK cells, $CD4^+$ and $CD8^+$ T-cells is induced after infection with microbes. IL-12 is a strong inducer of IFNγ release in NK cells and is liberated by macrophages during microbe infection. In macrophages, IFNγ activates the transcription of genes which encode enzymes that enhance bacterial killing. For example, IFNγ induces phagocyte oxidase and iNOS which synthesise ROS and RNI, respectively (see 1.3.3). Besides, IFNγ increases the expression of class I and II MHC molecules and other costimulatory factors on APCs. This action promotes recognition of infected cells by $CD8^+$ cytotoxic T-lymphocytes (Fruh *et al.*, 1999).

IFNγ is the sole component of the type II interferon group, in contrast to the type I group which consists of more members (IFNα, IFNβ, IFNε, IFNκ and IFNω). The latter show important biological functions in antiviral, antiproliferative and immunomodulatory areas. Type I and type II interferons also differ in the corresponding kind of receptors. Type I interferons bind to IFNα-receptor, composed of two subunits: IFNαR1 and IFNαR2. Both are associated with janus activated kinases (JAK´s) and tyrosine kinases (TYK). The kinase TYK2 is constitutively associated to IFNαR1, whereas JAK1 interacts with IFNαR2. Type II interferon IFNγ binds to IFNγ-receptor, which is also composed of two subunits, IFNγR1 and IFNγR2 (Pestka *et al.*, 2004). The IFNγR1 subunit associates with JAK1 and is required for both ligand binding and signalling. IFNγR2, on the other hand, is constitutively associated with JAK2 and is necessary mainly for signalling, thus playing a minor role in ligand-binding. IFNγ signalling starts with dimerisation of the receptor subunits, leading to autophosphorylation and activation of associated JAKs. The kinases then initiate the JAK-STAT (signal transducer and activator of transcription) signalling pathways. Figure 1.6 summarises the IFN signalling pathways with the proteins involved. In type I IFN receptor signalling, STAT2 is activated by tyrosine phosphorylation and, together with STAT1 and IRF9 (**I**FN-**r**egulatory **f**actor-**9**), forms ISGF3 (**I**FN-**s**timulated **g**ene **f**actor **3**) complexe. This complex translocates into the nucleus and binds specific elements, known as **I**FN-**s**timulated **r**esponse **e**lements (ISREs), located in the promoter regions of **I**FN-**s**timulated **g**enes (ISG). Promotor association induces gene transcription of IFN target genes. In addition, there are also many other STAT complexes consisting of dimers and heterodimers, based on combinations of STAT1,

STAT2, STAT3, STAT4, STAT5 and STAT6. Some of these can also bind to another type of promoter element, the IFNγ-activated site (GAS) element. In some promoter regions of ISGs, both GAS and ISRE are present allowing combinations of different STAT-containing complexes to mediate diverse responses (Aaronson and Horvath, 2002; Platanias and Fish, 1999; Platanias, 2005). Both type I and II IFNs are capable of inducing the formation of STAT1-STAT1 homodimers, which translocate into the nucleus, bind to GAS promoter elements and initiate gene transcription of ISGs. Biochemical modifications of STATs, such as phosphorylation, are required for the interaction with other proteins and optimal gene transcription. For instance, the phophorylation of STAT1 at serine 727 (Ser727) seems to be essential for full transcriptional activation. In mice expressing this STAT1 mutant increased murine mortality upon infection with *Listeria monocytogenes* is observed (Varinou *et al.*, 2003). Hence, STAT1 phosphorylation is relevant in IFNγ mediated innate immunity against intracellular bacteria.

Besides the classical JAK-STAT signalling pathway, other signalling cascades which contribute to the full generation of responses to interferons have been ascertained, including the mitogen-activated protein kinase (MAPK) p38 cascade and the phosphatidylinositol 3-kinase cascade.

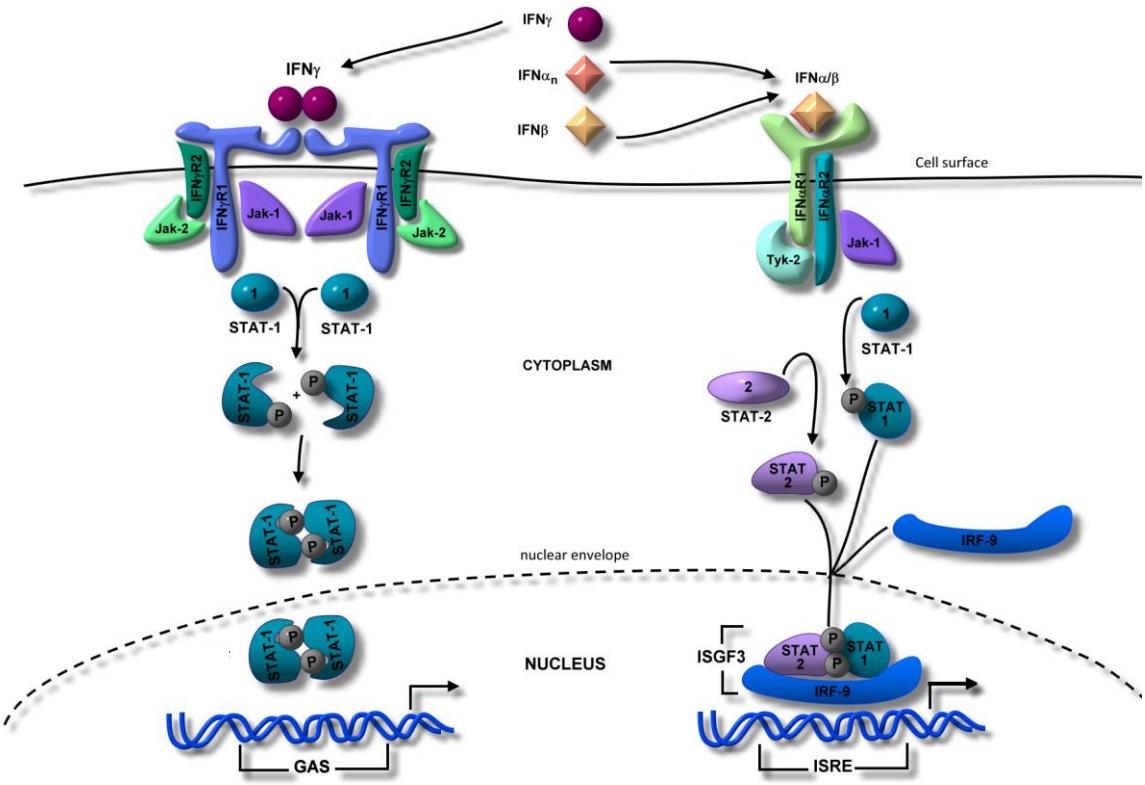

Figure 1.7: Type I and Type II interferon signalling and activation of the JAK-STAT pathway
Each type of IFN binds to a specific receptor. ***Type I*** *IFNs bind to IFNαR, consisting of IFNαR1 and IFNαR2. Activation of associated JAK1 leads to phosphorylation of STAT2 and STAT1, which together with IRF9, generate the ISGF3 complexes. These complexes translocate into the nucleus and bind to the promoter element ISRE, initiating gene transcription.* ***Type II*** *interferon IFNγ binds to the IFNγR, composed of IFNγR1 and IFNγR2. Phosporylation and activation of STAT1 leads to STAT1-STAT1 homodimer formation, which also translocates into the nucleus for binding to the promoter element GAS, initiating gene transcription (based on Shtrichman and Samuel, 2001).*

1.7. Objectives of this work

A considerable amount of our knowledge on how the immune system functions and deals with bacterial infections has been learned from experimental work with *Listeria monocytogenes* in mice. Murine listeriosis involves a complex interplay between host and pathogen, and its study has lead to the discovery of many essential factors in the immune response to bacteria. In the particular process of bacterial eradication, macrophages and the inflammatory cytokines IFNγ and TNFα have been shown to play a predominant role. However, the precise molecular mechanism of both cytokines for mediating their bactericidal activity is still not fully understood. Initially, TNFα and its binding receptor TNF-R1 came into focus as components of the bacterial eradication process because deletion of the receptor or its ligand resulted in complete loss of capacity to kill the pathogen *L.m.* in mice. Recent studies performed by our group revealed that TNF-R1 mediates its diverse cellular functions by internalisation-dependent and independent events. Receptor-internalisation allowed recruitment of several proteins to the receptor complex and notable among these were bactericidal molecules, such as the protease cathepsin D (CTSD). The precise molecular mechanism of how TNF-R1 may contribute to bacterial killing, as well as the specific role of receptor-internalisation in the process, was the objective of the present study. In particular receptor-internalisation was thought to be a potential mechanism for routing bactericidal components towards the bacteria-containing phagosome. The protease CTSD seemed to be a promising candidate for mediating bactericidal actions on the phagosome in this context. A mutual compartment of TNF-R1 and bacteria-containing phagosome was hypothesised as a mechanism for creating a bactericidal environment in the phagosomal compartment.

The encounter of TNF-R1 and bacteria-containing phagosome was to be analysed by several methods: confocal microscopy, electron transmission microscopy and Western blot. In order to investigate cytokine specific effects and molecular changes on *L.m.*-containing phagosomes, a new technical approach for the isolation of bacteria-containing vesicles was to be used and therefore needed to be adjusted to the pathogen *L.m*. and J774 macrophages. This new method is based on the magnetic labelling of bacteria, which requires pre-experimental workup in order to validate this labelling for the analyses planned in the present study. This method allows the analysis of specific changes on the bacteria-containing phagosomes upon cytokine stimulations or of effects based on knockout conditions. This opens new possibilities of finding other components involved in bacterial killing. Conclusively, this approach was to be applied with the aim of unravelling the molecular mechanism behind TNF-R1 signalling and its contribution to bacterial eradication. The overall hypothesis of this work is illustrated in figure 1.8.

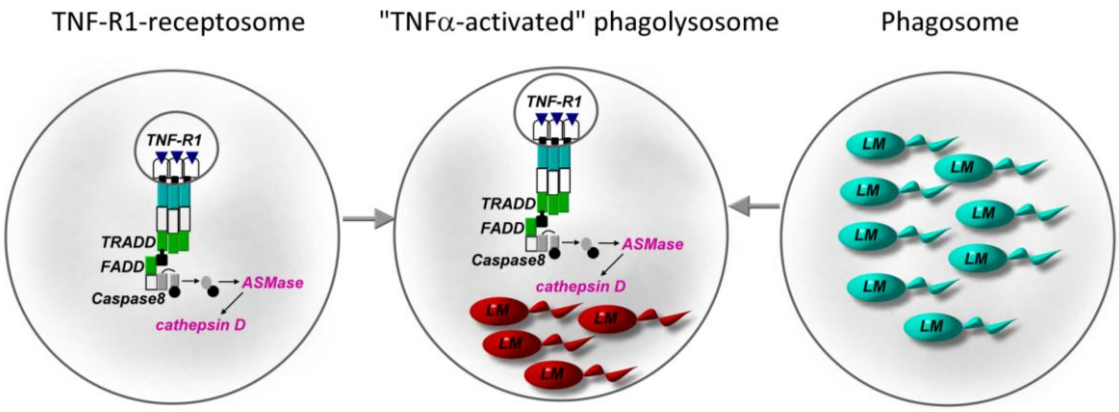

Figure 1.8 Hypothesis of TNF-R1 mediated eradication of intracellular bacteria
internalised TNF-R1 receptosomes contain activated CTSD and were hypothesised to fuse with L.m.-containing phagosomes. The Encounter of these two vesicles could build a" TNFα-activated phagolysosome" which might represent a compartment of bactericidal environment.

2. Material & Methods

2.1. Materials

2.1.1. Devices

Blaubrand® hemocytometer	Brand GmbH + Co KG Wertheim (Germany)
Branson Sonifier 450	Branson (Germany)
Blockthermostat BT 100	Kleinfeld Labortechnik (Germany)
Confocal microscpe LSM 510 META	Zeiss (Germany)
Eppendorf centrifuge 5415R	Eppendorf AG, Hamburg (Germany)
Eppendorf centrifuge 5804R	Eppendorf AG, Hamburg (Germany)
Eppendorf centrifuge 5810R	Eppendorf AG, Hamburg (Germany)
FACS CANTO II flow cytometer	BD Biosciences
Gel electrophoresis device	BioRad Labortatories GmbH, München (Germany)
Hera 240 Heraeus cell incubator	Haereus instruments GmbH, Osterode (Germany)
INTAS Chemilux Pro	INTAS Science imaging instruments GmbH
LEO 912AB	Zeiss, Oberkochen (Germany)
LYNX-microscopy tissue processor	LEICA
Laminar flow sterile cabinet (antair BSK)	Haereus instruments GmbH, Osterode (Germany)
Microplate reader model 680	BioRad Labortatories GmbH, München (Germany)
Mini PROTEAN electrophoresis system	BioRad Labortatories GmbH, München (Germany)
Pump, Minipuls 3	Gilson
Smart spec™ plus Spectrophotometer	BioRad Labortatories GmbH, München (Germany)
Ultracut-S ultramicrotome	LEICA, Bensheim (Germany)
Washer Tecan Hydroflex	
Western Blot device	BioRad Labortatories GmbH, München (Germany)

2.1.2. Consumables

Biozym filter tips (10 µL, 20 µL, 100 µL, 1mL)	Biozym Scientific GmbH, Oldendorf (Germany)
Cell culture flasks (75cm^2, 175 cm^2)	BD Biosciences GmbH, Heidelberg (Germany)
Cell culture flasks non treated	Nalge Nunc GmbH, Langenselbold (Germany)
Cell scraper (25 cm)	Sarstedt AG&Co, Nümbrecht (Germany)
Cell strainer (100 µm)	BD Biosciences GmbH, Heidelberg (Germany)

Coverslips, Human Fibronectin Cellware (2mm round coverslips)	BD Biosciences GmbH, Heidelberg (Germany), BioCoat, Cat#354088
Eppendorf cup (1.5 / 2 ml)	Eppendorf AG Hamburg (GER)
Falcon tubes (15 ml, 50 ml)	BD Biosciences GmbH, Heidelberg (Germany)
FACS tubes BD Falcon	BD Biosciences GmbH, Heidelberg (Germany)
PVDF Membran Westran CS, 0,45 µm	Hartenstein, Würzburg (Germany), Cat# PVD4
Petri dish (10 cm) non treated	BD Biosciences GmbH, Heidelberg (Germany) REF 351005
Serological pipettes (5 ml, 10 ml, 25 ml)	Sarstedt AG&Co, Nümbrecht (Germany)
Syringe filters (0.2 µm)	Pall corporation, Ann Arbor (USA)
Sterile filter botteltop 75 mm	Sarstedt AG&Co, Nümbrecht (Germany)
Syringe (1 ml, 2 ml, 5 ml, 10 ml, 25 ml)	Sarstedt AG&Co, Nümbrecht (Germany)
Sterilin Square plates	Sterilin Limited®, Cambridge (UK)
Tissue culture 10 cm Petri dish	BD Biosciences GmbH, Heidelberg (Germany) REF 353003
6-well cell culture plate	BD Biosciences GmbH, Heidelberg (Germany), Falcon 35 3047
12-well cell culture plate	BD Biosciences GmbH (Heidelberg, Germany), Falcon 353225
96-Well flat bottom cell culture plate	BD Biosciences GmbH, Heidelberg (Germany), Falcon 35 3072
96-well cell culture plate (non treated)	BD Biosciences GmbH, Heidelberg (Germany)
96-well Microplate MICROCOLON 200, medium binding flat-bottom	Greiner GmbH, Frickenhausen (Germany) Cat. No. 82050-716
Whatman paper	Millipore GmbH, Schwalbach, Germany Cat# 10401196

2.1.3. Chemicals and reagents

Acrylamid-Solution 4K (30% Mix 37.5 : 1)	Applichem Cat# A 1672.1000
Alexa Fluor® 488 streptavidin, 10 nm colloidal, gold conjugate	Invitrogen gmbH, Karlsruhe (Germany) Cat# A 32361
β-Mercaptoethanol	Merck KGaA, Darmstadt (Germany), REF 31350-010
β-Mercaptoethanol for cell culture	GIBCO /Invitrogen GmbH, Karlsruhe (Germany)

Benzonase; Nuclease	Novagen, Cat# 70664-3
Biotin-TNFα (rhTNFα/TNFSF2 Biotin Fluorokine® Kit)	R&D Systems, San Diego (California) Cat# NFTA0
BSA	AppliChem, Darmstadt (Germany), Cat# A1391.0100
DMEM (Dulbecco's Modified Eagle Medium)	GIBCO /Invitrogen GmbH, Karlsruhe (Germany) Cat# 41966-029
Cytochalasin D	Merck KGaA, Darmstadt (Germany), Cat# 250255-1MG
ECL Western Blotting substrate solution:	
SuperSignal West Pico Chemiluminescent Substrate	Pierce 34077
SuperSignal West Dura Chemiluminescent Substrate	Pierce 34076
Fetal calf serum (FCS)	Gipco, lonza, PAN Biotech
Genatmycin	Sigma-Aldrich® GmbH, Taufkirchen (Germany)
Lowry Reagent	BioRad Labortatories GmbH, München (Germany)
DC Protein Assay, Reagent A	Cat# 500-0113
DC Protein Assay, Reagent B	Cat# 500-0114
Mounting Medium, Vectashield with DAPI	LINARIS, Cat#H-1500
MagCellect streptavidin ferrofluid	R&D Systems, Minneapolis, MN, Cat #MAG999
Methanol	Merck KGaA, Darmstadt (Germany)
N-(1-Naphtyl)-ethylendiamine dihydrochloride	Applichem, Cat# A2782.0025
PageRuler™ Plus Prestained Protein Ladder	Fermentas, Cat #1811; Sizes 250, 130, 95, 72, 55, 36, 28, 17, 10 kDa
Paraformaldehyde	Sigma-Aldrich® GmbH, Taufkirchen (Germany)
Penicillin/Streptomycin (1000U/ml Pen., 10 mg/ml Strep.)	Pan Biotech GmbH, Aidenbach (Germany) P10-023500
Penicillin G	Sigma-Aldrich® GmbH, Taufkirchen (Germany)
Propanol	Merck KGaA, Darmstadt (Germany)
Proteinase inhibitor (Complete EDTA-free)	Roche Diagnostics GmbH, Penzberg (Germany) Cat# 04693132001
Recombinant mouse IFNγ (rmIFNγ)	Invitrogen GmbH, Karlsruhe (Germany), PMC 4033

Recombinant human TNFα (rhTNFα)	Knoll AG
10 x Roti^{R}-block concentrate	Roth, Cat# A151.2
Saponin	Sigma-Aldrich® GmbH, Taufkirchen (Germany)
Skimmed milk powder	Heiler Cenovis GmbH, Radolfzell (Germany)
Sodium nitrite	AppliChem, Cat# A7014.0250
Streptavidin-Cy5	Jackson Immunoresearch, West Grove, PA
Substrate Reagent A	BD Biosciences GmbH, Heidelberg (Germany) Cat# 51-2606KC
Substrate Reagent B	Cat# 51-2607KC
Sulfanilamide pure	AppliChem, Cat# A2226.0250
Tetracycline-hydrochloride	Sigma-Aldrich® GmbH, Taufkirchen (Germany)
Triton X-100	Sigma-Aldrich® GmbH, Taufkirchen (Germany)
Trypan blue 0.5% (w/v)	Biochrom AG, Berlin (Germany)

2.1.4. Kits

BD OptEIA ™ Mouse TNF ELISA Set II	BD Biosciences GmbH, San Diego (California) Cat# 55834
rhTNFα/TNFSF2 Biotin Fluorokine® Kit	R&D systems GmbH, Abingdon (UK) Cat# NFTA0

2.1.5. Buffers and solutions

Buffer A	0.25 M Sucrose, 15 mM HEPES, 0.5 mM MgCl2, pH 7.4
Blot buffer	25 mM Tris, 150 mM Glycin, 10 % (v/v) Methanol
Blocking-buffer	5 % skimmed milk powder (w/v) in TBS-T
ELISA Coating buffer	0.1 M sodium carbonate (8.4 g $NaHCO_3$; 3.56 g Na_2CO_3 q.s. to 1.0 L H_2O) (pH 9.5)
ELISA wash buffer	PBS with 0.05% (v/v) tween-20
ELISA assay diluent	PBS with 10% (v/v) FCS
ELISA stop solution	2N NH_2SO_4
Griess reagent A	1% sulfanilamide (w/v), 5% H3PO4
Griess reagent B	0.1% naphtyl-ethylenediamine dihydrochloride
Karnovsky´s fixative	2% paraformaldehyde, 2.5% glutaraldehyde, buffered in sodium cacodylate
KS-RIPA	50 mM Tris-Cl pH 7.4, 150 mM NaCl, 1 % Triton X-100, 5 mM EDTA, 10 % Glycerol, 10 mM K_2HPO_4

PBS	137 mM NaCl, 2.7 mM KCl, 10 mM Na2HPO4, 1.47 mM KH2PO4, pH 7.4
Red blood cell lysis buffer	150 mM NH_4Cl, 1mM $KHCO_3$, 0.1 mM Na_2EDTA, ad 500 ml dH_2O (pH 7.2-7.4) sterile filtrated.
SDS - PAGE running buffer	144g Glycin (192mM), 30g Tris (250mM), 10g SDS (1%) ad 1L bidest H_2O
2xSDS - PAGE loading buffer	125 mM Tris, 2 % (w/v) SDS, 10 % (v/v) β-Mercaptoethanol, 1 mM EDTA, 10 % (w/v) Glycerin, 0,01 % (w/v) Bromphenolblau, pH 6.8
5xSDS-PAGE loading buffer	TBS 150 mM NaCl, 50 mM Tris/HCl, pH 7.4
3.5 x SMHEM buffer	952 mM Saccharose, 3.5 mM $MgCl_2$, 7 mM HEPES ad 200 ml bidest H_2O, pH 7.2
Standard for Griess reagent	10 mM $NaNO_2$
TBS	150 mM NaCl, 50 mM Tris/HCl, pH 7.4
TBS/T	TBS mit 0.1 % (v/v) Tween-20

2.1.6. Cell culture and bacteria media

Cell culture medium:	DMEM supplemented with 10% (v/v) FCS, 1% (v/v) Pen./Strep.
BMDM-Medium:	DMEM supplemented with 10% (v/v) FCS, 10% (v/v) L929-CM, 1% (v/v) Pen./Strep., 50 µm β-mercaptoethanol
BHI (Brain heart infusion) broth	Merck KGaA, Darmstadt (Germany), (37 g in 1L)
BHI agar plates	Merck KGaA, Darmstadt (Germany), (37 g in 1L), 15 g Agar
Blood agar plates	Columbia-Agar (42 g in 1L), 8% Sheep blood

2.1.7. Mouse strains

C57BL/6 wildtype mice (Charles River Laboratories, Germany)

C57BL/6 TNF-R1 $^{-/-}$ (The Jackson Laboratory, Sacramento, California)

C57BL/6 IFNγR$^{-/-}$ (The Jackson Laboratory, Sacramento, California)

2.1.8. Cell lines

L929, murine aneuploid fibrosarcoma cell line ATCC# CCL-1™

J774 macrophages, murine reticulum cell sarcoma cell line, ATCC #TIB-67™

2.1.9. Bacterial strains

EGDe, *Listeria monocytogenes* wild-type strain, a friendly gift from Dr. J. Stritzker, Würzburg

L.m. Δhly strain, a friendly gift from Dr. J. Stritzker, Würzburg (Stritzker *et al.*, 2004)

2.1.10. Software

This manuscript was prepared with Microsoft Office Word 2003. Graphs and diagrams were prepared using Graph Pad Prism version 5.01. The list of references was compiled using Reference manager version 10. Software for other applications are indicated in the following.

For TEM: analySIS-Software EsiVision / Soft Imaging System GmbH, Münster.

For confocal microscopy: Zeiss LSM510 software

For ELISA washing steps: HydroControl-Software Version 1.0.1.0

For ELISA quantification: software Microplate manager (version 5.2)

For Flow cytometry: WinMDI Version 2.9

2.2. Cell biological methods

2.2.1. Cell culture and conditions

Cells were cultured using sterile reagents, pipettes, and vessels and employing the laminar flow sterile cabinet (antair BSK). Consumables and reagents are listed in 2.1.2 and 2.1.3. J774 macrophages were cultured in cell culture medium (DMEM supplemented with 10%FCS and 1% Pen./Strep) on non treated sterile flasks (Nunc). Cells were cultured at 37°C, 5% CO_2, and 95% humidity in HERA cell 240 Heraeus cell incubator (Heraeus instruments). J774 macrophages were split every 2-3 days and were split by gently scraping cells off the flask bottom with the use of a cell scraper.

2.2.2. Generation of bone marrow derived macrophages

For the generation of Bone marrow-derived macrophages (BMDM), mice were sacrificed by cervical dislocation, femura and tibiae were dissected and remaining tissue was removed. Bones were kept on ice in PBS. The following steps were done under the laminar airflow cabinet. Both ends of the intact bones were cut with scissors and bone marrow was flushed into a 50 ml Falcon tube until the bone cavity appeared white using PBS and a 0.45 mm syringe. Clots within the bone marrow suspension were disrupted by pipetting up and down several times. Cells were filtered with a 100 µm cellstrainer in order to remove other mouse material. The cells were centrifuged 300 x g for 8 min at 4°C. Supernatant was removed and pellets were resuspended in 5 ml red blood cell lysis buffer in order to destroy containing erythrocytes. Cells were washed three times with cold PBS, resuspended

in BMDM-medium and seeded on sterile tissue culture Petri dish to adhere fibroblasts overnight. On the next day non-adherent, immature progenitor cells were removed and seeded on sterilin square plates in 20 ml BMDM-medium containing 10% M-CSF supernatant from L929 cells (see 2.2.4). Medium containing this stimulation factor drives the progenitor cells to mature to macrophages. On day four, fresh BMDM-medium containing M-CSF supernatant of L929 cells was added. Mature macrophages were harvested on day seven. Cells were centrifuged at 300 x g for 5 min at 4°C, counted using dilutions with trypan blue solution and seeded on the appropriate culture dish. These cells were then used for isolation assays of *L.m.*-containing phagosomes, ELISA and NO detection. For infection studies, cells were always grown in DMEM medium without antibiotics. For isolation of *L.m.*-containing phagosmes, cells of five mice were pooled to obtain enough cells for four time points (15, 30, 60, 120 min p.i.), NO detection and ELISA assays. For the isolation of phagosomes, $2x10^7$ cells for every time point p.i. were seeded on non treated 10 cm Petri dish. For ELISA specific to mouse TNFα, $5x10^4$ cells were seeded on 96-well cell culture dish in triplicates and could adhere overnight. For NO detection, $1x10^5$ cells were seeded in triplicates also on 96-well culture dish.

2.2.3. Stimulation of Cells

Cells were seeded on an appropriate cell culture dishes in culture medium with or without antibiotics. Cells were either stimulated with the cytokines IFNγ, TNFα or with combination of both. Stimulation with IFNγ was carried out overnight. J774 macrophages were stimulated with 500 U/ml, whereas all BMDM with 200U/ml. Cells could adhere at least two hours on the surface of the cell culture dish before stimulation was started. Cells were seeded in one half of the volume of the desired end-volume and cytokine was added in the other half of the volume with the desired concentration to reach the final concentration. For TNFα stimulation, rhTNFα (100 ng⁄ml) was diluted in culture medium without antibiotics and added simultaneously with bacterial infection.

2.2.4. Generation of M-CSF containing supernatant (L929-CM)

M-CSF is highly expressed in L929 cell lines. L929 cell-conditioned medium (L929-CM) was used as the source of M-CSF employed for BMDM generation as described in 2.2.2. The cells were cultured in DMEM medium supplemented with 10%FCS and 1% Pen./Strep. Cells ($7x10^5$) were seeded in T-175 cell culture flasks and were able to grow seven days. Supernatant was collected and centrifuged at 1000 x g for 10 min at 4°C. In order to guarantee sterility, the supernatant was sterilized by filtrating through a 0.22 µm filter using a bottle top filter system and stored at -20°C.

2.2.5. Determination of cell numbers

Cells in single cell suspensions were counted using a Neubauer hemocytometer. In brief, cells were mixed with at least 50% (v/v) trypan blue and 10 µl of the mixture were placed in the space between the hemocytometer and the cover slip. Cell concentrations in the sample were calculated as described below. The mean value of four independent areas containing 50 to 100 cells counted was calculated, in order to minimize the variance.

One area with 16 squares: Cell number x dilution factor = cell number x 10^4 /ml

2.2.6. Bacterial growth assays

The bacterial growth assays were performed according to the protocol of Singh *et al*. with some modifications (Singh *et al.*, 2008). Infections of macrophages for in vitro growth assays were carried out at an MOI of 0.1. During the previous day, $5x10^4$ cells per well were seeded on 96-well cell culture dish in triplicates. Stimulation with IFNγ was performed overnight and addition of rhTNFα (100 ng/ml) was performed simultaneously with infection (see 2.2.3). Aliquots of mid-log phase bacteria (~5 x 10^8 *c.f.u.* /ml) were washed twice in PBS and used to infect macrophages in medium without antibiotics (see 2.3.1). For synchronisation of bacterial uptake, cells on 96-cell culture dishes were centrifuged 500 x g, at 15°C for 5 min. In order to remove extracellular bacteria, after 30 min infection at 37 °C, gentamycin (50 mg/ml) was added and the cells were incubated for another 30 min at 37 °C. Cells were then washed three times with 200 µl DMEM medium, and incubated for the indicated times in 100 µl fresh medium without antibiotics at 37 °C. Cells were lysed at 0, 2, 4, 6, 8h in 10 µl of 5% saponin in H_2O for 5 min. Medium (90 µl) was added, serial dilutions were plated on blood agar plates and colonies were counted the next day to determine c.f.u.

2.2.7. Determination of bacterial uptake

In order to determine the number of phagocytosed bacteria, $1x10^6$ cells were seeded on a 12-well cell culture dish in culture medium without antibiotics. For infection, wild-type strain EGDe and mutant strain *L.m.*Δhly were grown and labelled with LB as described in 2.3.2. Cells were infected at a MOI 10 and were centrifuged at 500 x g for 5 min at 15°C to synchronise bacterial uptake. Cells were infected for one hour as described in 2.3.1. After incubation supernatant was removed and cells were lysed with 50 µl of 5% saponin in H_20 for 5 min. 350 µl medium was added, serial dilutions were plated on blood agar plates and colonies were counted the next day to determine c.f.u.

2.2.8. Flow cytometry

In order to measure incorporation of LB into *L.m.*-membrane, bacteria were incubated with the indicated concentrations of LB overnight at 4°C. Bacteria were washed with 500 µl PBS and centrifuged (6000 x rpm, 10min, 4°C). LB-labelled bacteria were resuspended in 100 µl PBS and incubated with Cy5-conjugated streptavidin (SA) for 20 min at 4°C. Cy5-statined bacteria were washed with 500 µl PBS, centrifuged (6000 x rpm, 10min, 4°C) and resuspended in 500 µl PBS. Staining of bacteria was analysed in a FACS CANTO II flow cytometer (BD Biosciences). Data was processed using WinMDI Version 2.9.

2.2.9. Confocal microscopy and Immunofluorescence staining

For immunofluorescence staining, macrophages were plated on fibronectin coated coverslips in 6-well cell culture dishes, 12 hours before infection. For the monitoring *L.m*. translocation from the phagosome into the cytoplasm or for the staining of phagosomal compartment markers, cells were infected at MOI 3 with EGDe wild-type strain or the hemolysin negative mutant of *L.m.* (Δhly) (see 2.1.9). To obtain synchronised uptake, infected cells were centrifuged at 500 x g for 5 min at 15°C. After infection and incubation of the cells at 37°C, coverslips with infected cells were washed with PBS and fixed in 2% paraformaldehyde (pH 7.5) for 15 min at room temperature (RT), each time point and stimulation condition. Cells were then washed three times with 1 ml PBS per well. In order to obtain intracellular staining, the cells on coverslips were permeabilised with 1 ml of 0.1% Triton X-100 in PBS for 10 min at RT and washed twice with 1 ml PBS. To prevent unspecific antibody-binding, unspecific binding sites were blocked with 5% BSA in PBS for two hours at RT or overnight at 4°C. For actin staining phalloidin-FITC was used. After washing, phalloidin stock solution was diluted 1:500 into 1% BSA in PBS and the coverslips stained overnight at 4°C. Primary antibodies were added overnight at 4°C and secondary antibodies two hours at the next day in PBS with 1% BSA. The antibodies which were used for the translocation assays of *L.m*. out of the phagosome and for staining of phagosomal markers during the phagocytosis process are listed in table 2.1. Three washing steps for 5 min with 1 ml PBS on each well washed unbound antibodies away. Coverslips were mounted using mounting medium. Nuclei were stained with DRAQ5. Samples were analysed using confocal microscope LSM 510 META, (Zeiss). Microscope objective: Zeiss plan-apochromat 63x/1.4 Oil, Laser lines: 488 nm Argon ion laser; 543 nm Helium-Neon laser, 30 mW; 633 nm Helium-Neon laser, 15mW. Emission filters: BP 505-530; LP 560; META detector 745-799. Images were analysed using Zeiss LSM510 software.

Primary antibody			Secondary antibody		
Name	Brand	Dilution in PBS with 1% BSA	Name	Brand	Dilution in PBS with 1% BSA
α-*L.m.*	Acris Antibodies GmbH, BP1047	1:200	Goat anti-rabbit-Alexa 546/chicken anti-rabbit-Alexa 594	Molecular Probes®, A21085/A21442	1:200 or 500
α-Rab5	Santa Cruz Biotechnology, Inc., sc-46692	1:50	Goat anti-mouse-Alexa-FITC	Molecular Probes®., F2761	1:200 or 500
α-EEA1	Santa Cruz Biotechnology, Inc., sc-6414	1:50	Rabbit anti-goat-Alexa-FITC	Molecular Probes®., A10529	1:200 or 500
α-LAMP1	Santa Cruz Biotechnology, Inc., sc-8098	1:50	Rabbit anti-goat-Alexa-FITC	Molecular Probes®., A10529	1:200 or 500
Phalloidin-FITC	Sigma, P5282	1:500	-	-	-
DRAQ5™	Axxora GmbH, BOS-889-001-R200	1:30000 dilution in mounting medium	-	-	-

Table 2.1: Antibodies used for immunofluorescence staining

2.2.10. Transmission electron microscopy of infected cells and magnetically isolated phagosomes

BMDM were seeded on 6-well cell culture dish and infected with magnetically labelled *L.m.* (Δhly) as described in 2.3.2. Infected J774 cells and isolated phagosomes (see 2.2.14) were fixed in Karnovsky´s fixative overnight. The next steps were performed by Heiko Ingo Siegmund and with the help of Dr. Josef Schröder (Institute of pathology, Universitätsklinikum Regensburg, Germany). Samples were intersected to a size of 1-3 mm^3 and automatically processed by LYNX-microscopy tissue processor (LEICA). Samples were washed, post-fixed in 1% osmium tetroxide in destilled water, dehydrated in graded series of EtOH and embedded in Epoxy resin (EPON 812). After 48 h of heat polymerisation at 60°C, semithin (0.8 µm) sections were cut, stained with toluidine blue/fuchsin. After light microscopic *L.m*. selection, the epon block was trimmed for ultrathin sectioning. Ultrathin (60-80 nm) sections were prepared with a diamond knife on an Ultracut-S ultramicrotome (Leica, Bensheim). Sections were collected on copper grids and double contrasted with aqueous 2% uranyl acetate and lead citrate solutions for 10 min each. The sections were examined using a LEO912AB electron microscope (Zeiss, Oberkochen). Images were acquired by using analysis software (AnalySIS-Software EsiVision / Soft Imaging System GmbH, Münster) and images were assembled using Adobe Photoshop CS2.

2.2.11. Transmission electron microscopy of TNF-R1 trafficking and colocalisation with phagosomes

For TEM analysis $1x10^6$ J774 macrophages were seeded per well (6-well dish) in culture medium without antibiotics. Prior to ligand binding, cells were precooled for 15 min on ice. Biotin-TNFα (100 ng = 50 µl) and streptavidin-10 nm colloidal gold conjugate (500 ng = 16.4 µl) per sample were incubated one hour at RT. The biotin-TNFα-streptavidin colloidal gold-complexes were mixed with cold PBS and cells were incubated with 500 µl of this mixture for one hour at 4°C in order to mark TNF-R1 with the gold conjugate. Cells were washed twice with 1 ml PBS per well to remove unbound complexes. Control samples with marked TNF-R1 on the cell-surface were prepared for TEM after this step. Cells were detached from culture dish by rinsing with PBS, centrifuged at 2000 x rpm for 10 min at 4°C and, after discarding the supernatant, the cell-pellet was fixed with 1.5 ml Karnovsky´s fixative. For Colocalisation-analysis of *L.m*-containing phagsosomes with the receptor, the mutant strain *L.m.* Δhly was prepared as described in 2.3.2 and cells were infected with bacteria at a MOI 10. In order to synchronise phagocytosis, infected cells on a 6-well dish were centrifuged at 500 x g for 5 min at 15°C. Bacterial uptake and TNF-R1 internalisation started with shift to 37°C. After one hour of incubation, cells were moved to 4°C and supernatant was removed. Cells were detached from the culture dish by rinsing wells with PBS. Cells were centrifuged at 2000 x rpm for 10 min at 4°C. Supernatant was discarded and the cell-pellet was fixed with 1.5 ml Karnovsky´s fixative. Samples were then prepared for TEM and analysed as described in 2.2.10.

2.2.12. Fluorescence labelling of TNF-R1 and colocalisation with *Listeria monocytogenes.*

J774 macrophages ($1x10^5$) were seeded on fibronectin-coated coverslips placed in 6-well dish in culture-medium without antibiotics and cells could adhere overnight. For TNF-R1 fluorescence labelling, components of the rhTNFa/TNFSF2 Biotin Fluorokine® kit (R&D) were used. Prior to Receptor-ligand binding, 1.25 µl Streptavidin-FITC and 1.25 µl biotin-TNFα were incubated for one hour at RT in the dark. These complexes were mixed with PBS and cells on coverslips were incubated for one additional hour at 4°C with this mixture. Coverslips were washed three times with cold PBS in order to remove unbound complexes. For infection the mutant strain *L.m.* Δhly was grown and prepared as described in 2.3.1. Cells were infected at a MOI 3 simultaneously with initiating receptor-internalisation by shifting cells to 37°C. Prior to internalisation, infected cells on coverslips, placed in the 6-well dish were centrifuged at 500 x g, for 5 min at 15°C in order to synchronise bacterial uptake. These samples were then prepared for immunofluorescence staining as described in 2.2.9.

L.m. was stained with α-*L.m.* antibody and the secondary antibody goat-anti-rabbit Alexa-fluor546. Nuclei were stained with DRAQ5™ (for antibodies see table 2.1)

2.2.13. Magnetic labelling of TNF-Receptor and isolation of TNF Receptosomes in *Listeria monocytogenes*-infected macrophages

J774 macrophages ($2x10^7$) were seeded on a 10 cm cell culture Petri dish and could adhere overnight. Before magnetic labelling of the receptor, cells were infected with the hemolytic negative mutant of *L.m.* (Δhly) at a MOI 10 (see 2.3.1). In order to obtain synchronised uptake cells were centrifuged for 500 x g for 5 min at 15°C and subsequently incubated another 10 min at 37°C. Prior to receptor-ligand binding, biotinylated TNFα (200 ng) was incubated with streptavidin-magnetic beads (20 ng) (MagCellect streptavidin ferrofluid) for one hour at 4°C. This ligand complex was added to the infected cells and could bind to the receptor for one additional hour at 4°C in a volume of 5 ml PBS. Unbound complexes were washed away by rinsing cells twice with 10 ml PBS. Internalisation of the receptor-ligand complex was initiated by shifting cells to 37°C for one hour in order to obtain fusion events with bacteria containing phagosomes. Cells were subsequently incubated wither Buffer A containing 0.02% EDTA for 20 min at 4°C, resulting in the detachment of cells from the culture dish. Cells were collected in tubes and centrifuged for 10 min, 310 x g at 4°C. The supernatant was discarded and pellet was resuspended in 500 µl buffer A supplemented with Benzonase Nuclease (25 U/ml Novagen) and cytochalasin D (5 µg/ml Calbiochem) to degrade free DNA and to disrupt actin microfilaments. Macrophages membranes were then disrupted by sonication using a Branson Sonifier. Disrupted cells were centrifuged at 100 x g for 2 min, the supernatant was collected and the residual pellet was resuspended in a stepwise manner using smaller volumes (200 µl and 100 µl) of buffer A (containing Benzonase Nuclease and Cytochalasin D). This step was repeated three times. The supernatant (PNS) gained after different sonication steps was pooled and 85 µl were used for Western blot analysis and determination of protein content. PNS was then loaded on to the custom-built magnetic chamber for 30 min to collect the TNF-R1-containing vesicles, known as receptosomes (Tchikov, 2008). The loading tube in the magnetic chamber was rinsed with buffer A (containing protease inhibitor, roche complete) for collection of the non magnetic fraction (NM). After a further 10 min washing step of the magnetic fraction was collected by removal of the tube from the magnet field. The isolated magnetic fraction was then concentrated by centrifugation at 15000 x g for 15 min at 4°C. The pellet was resuspended in 85 µl Buffer A (containing Benzonase Nuclease and Cytochalasin D) and prepared for further analysis. Western blot samples were mixed with 5xSDS-PAGE loading buffer and denaturised at 95°C for 15 min. Sample-pellets for TEM were fixed with 1.5 ml Karnovsky´s fixative overnight.

2.2.14. Isolation of *Listeria monocytogenes*-containing phagosomes

In order to monitor the phagocytosis process of *L.m.* in macrophages, bacteria-containing phagosomes were isolated. Bacteria were prepared as described in 2.3.2. Magnetic labelled bacteria were exposed at a MOI 10 to macrophages for uptake. In order to synchronise phagocytosis, infected cells were centrifuged at 500 x g for 5 min. Subsequently, macrophages were infected certain periods of time. The endocytosis was stopped by shift to 4°C and incubated for 20 min with buffer A containing 0.02 % EDTA resulting in detachment of cells from the culture dish. Cells were washed with buffer A containing 0.02 % EDTA collected in tubes and centrifuged at 310 x g for 10 min, at 4°C. The supernatant was discarded and pellet was resuspended in 500 µl buffer A supplemented with Benzonase Nuclease (25 U/ml Novagen) and cytochalasin D (5 µg/ml Calbiochem) to degrade free DNA and to disrupt actin microfilaments. Cells were then disrupted by sonication using a Branson Sonifier 450 (Output 20, Constant Duty Cycle, and duration 30s). Disrupted cells were centrifuged 100 x g for 2 min, the supernatant was collected and the buffer A (containing Benzonase Nuclease and Cytochalasin D). This step was repeated three times. The supernatant (PNS) gained after different sonication steps was pooled and 85 µl were used for Western blot analysis and determination of protein content. The PNS was then loaded on to the magnetic chamber to collect phagosomes containing magnetic bacteria. These vesicles could attach for 30 min on the wall of a tube between two magnets. The loading tube in the magnetic chamber was then rinsed with Buffer A (containing protease inhibitor, roche complete) for collection of the non magnetic fraction (NM). After a further washing step of 10 min the magnetic fraction was collected by removal of the tube from the magnet field. The isolated magnetic fraction was then concentrated by centrifugation (15 000 x g, 15 min, 4°C). The pellet was resuspended in 85 µl Buffer A (containing Benzonase Nuclease and Cytochalasin D) and prepared for further analysis (Western blot or TEM).

2.2.15. Cell lysates

Cell lysates were used for analysing endogenous expression of signalling proteins after infection with labelled *L.m.* Lysates were obtained from $1x10^6$ J774 macrophages seeded on a 12-Well culture dish infected with *L.m.*Δhly labelled with different amounts of LB. Bacteria were prepared for infection and labelled with magnetic beads as described in 2.3.1 and 2.3.2. Macrophages were infected for one hour at 37°C. After removing the supernatant and washing with 1 ml PBS per well, cells were lysed using 100 µl KS-RIPA buffer. Cells were scraped off the bottom of the culture dish using a cell-scraper and lysate was transferred to an Eppendorf tube. Cells were homogenised in lysis-buffer (KS-RIPA containing complete protease-inhibitor from Roche) for 20 min on ice. Lysate was centrifuged (20 000 x g, 15 min, 4°C) and supernatant containing soluble proteins was transferred to a new Eppendorf tube. Protein concentration was determined using Lowry reagent (see 2.4.1). Samples

were mixed with SDS-PAGE loading buffer and denaturised for 5 min at 95°C. Samples were then used for Western Blot analysis.

2.3. Working with bacteria

2.3.1. Cultivation of bacteria and infection of macrophages

L. monocytogenes (EGDe and Δhly (Stritzker, 2004)) strains were cultured by picking one colony and transferring it into 4 ml BHI broth. On the following day, overnight cultures of bacteria were diluted 1:10 in fresh BHI broth and grown with shaking for additional three hours at 37 °C. Aliquots of mid-log phase bacteria (~5 x 10^8 *c.f.u.* /ml) were washed twice in PBS and used to infect macrophages in medium without antibiotics. Infected cells were centrifuged at 500 x g for 5 min at 15°C in order synchronise bacterial uptake. Infection was carried out at 37°C, 5% CO_2 and 95% humidity.

2.3.2. Magnetic and fluorescent labelling of bacteria

Bacteria were grown as previously described (2.3.1). Bacteria were incubated with Lipobiotin (LB) at the indicated concentrations in PBS overnight at 4°C. Bacteria were washed with 500 µl PBS and centrifuged (6000 x rpm, 10min, 4°C). For magnetic labelling bacteria were resuspended in 100 µl PBS and subsequently incubated with 7-14x10^8 magnetic beads (MagCellect streptavidin ferrofluid) per 2x10^8 bacteria, for 20 min at 4°C. After magnetic labelling, bacteria were immediately used for infection.

2.3.3. Generation of GFP-expressing *Listeria monocytogenes*

According to the protocol of Park and Stewart, an electroporation-mediated transformation with plasmid DNA was used for generation of GFP-expressing *L.m.* (Park and Stewart, 1990). Bacteria were prepared for electroporation as follows. Overnight cultures of *L.m.* wild-type strain EGDe and *L.m.* Δhly were diluted in fresh BHI broth and grown with shaking at 37°C until reaching OD_{600} = 0.5. Penicillin G (5µg/ml) was added at this time point and the incubation continued until OD_{600} = 0.8 was reached, normally after one additional hour of incubation. The bacteria-culture was placed on ice for 20 min. Cells were harvested by centrifugation (6000 × rpm, 10 min, 4°C) and washed twice with 10 ml ice-cold 3.5 x SMHEM buffer. The final pellet, scrupulously aspirated, was resuspended in 1ml ice-cold 3.5 x SMHEM buffer and 100 µl aliquots were frozen at -80°C. Aliquots were again defrozen for DNA transformation. A Plasmid encoding GFP under the control of the strong listeria **s**uper**o**xide **d**ismutase promoter (pSOD) was used. This plasmid was friendly provided by Dr. J. Strizker, University of Würzburg. Transformation was carried out with 4x10^6 transformants/µg DNA, field strength of 12kV/cm and pulse duration of 5 ms. After electroporation, bacteria were incubated at 30°C for 1.5

hours in BHI broth containing 500 mM sucrose and plated on BHI-agar plates containing 5 µg/ml tetracycline. Green fluorescent bacterial colonies could be picked the next day, were grown in BHI broth containing 5 µg/ml tetracycline and used for infection.

2.4. Working with proteins

2.4.1. Measuring of protein concentrations

Protein concentration was determined with Lowry-reagent (Bio-Rad DC Protein assay). Cell lysates' supernatant were analysed diluted in 25 µl H_2O total volume and mixed with 150 µl reagent A and 1 ml reagent B. The mixture was incubated for 10 min at RT and absorbance was measured at 750 nm using Smart spec™ plus Spectrophotometer. Serial dilution of BSA was used as standard control (0, 1, 2, 3, 5, 7, 9, 11 µg/ml). Correlations coefficient R^2 was constantly > 0.98.

2.4.2. SDS-PAGE

A method to separate proteins according to their size is SDS-polyacrylamide Gel electrophoresis (Laemmli, 1970). In order to assess only the primary structure, the secondary and tertiary structure of the proteins are dissolved with the detergent sodium dodecyl sulfate (SDS) and the reducing agent β-mercaptoethanol. Additionally, the negatively charged SDS associates with the proteins and leads them to the anode, when an electric field is applied. The density of the polyacrylamide network reduces the migration speed of every protein depending on its size. For electrophoresis the samples are loaded on the stacking gel where they are compressed by the glycine of the running buffer as soon as the electric field is launched. When the proteins pass into the resolving gel, they have all reached the same starting point and separate according to their size. For protein analysis the appropriate resolving gel was cast (10%, 12.5% and 15% acrylamid) and overlaid with propanol. After complete polymerisation, propanol was removed, 4% collection gel was filled into the rack, and the comb generating the slots for the samples was inserted. After polymerisation of the collection gel, the system was inserted into the apparatus and the basins containing the anode and the cathode were filled with SDS-PAGE running buffer. Mini Protean® Electrophoresis system (Bio-Rad Laboratories GmbH) was employed. The cationic basin covered the loading area of the gel. Samples were mixed with SDS-PAGE loading buffer and denaturised for 5 min at 95°C. The comb was removed and appropriate volumes of the samples, as well as 5 µl of molecular weight marker (PageRuler™), were transferred into the single slots of the gel. The gel electrophoresis was launched with 25 mA per gel, 200V and followed by Western blotting.

2.4.3. Western Blot analysis and immunological detection of proteins

Following separation in acrylamide gels, protein mixtures were transferred to polyvinylidene fluoride PVDF-membranes (45 µm) to analyse them for the presence of specific proteins by applying antibodies, a method known as immuno- or Western blotting (Towbin *et al.*, 1979). PVDF membranes were briefly equilibrated in methanol and, together with filter papers (whatman papers), sandwich pads and migrated acrylamide gels containing proteins were subsequently equilibrated in blot buffer and assembled in cassettes according to the manufacturer's instructions. The samples were transferred onto PVDF membranes using a tank blotting device in blot buffer at 350 mA and 100 V for 1h, kept at 4°C. Before labelling, the membranes were incubated in blocking buffer containing 5 % skimmed milk to block unspecific binding sites. Membranes were briefly washed again with TBS-T and afterwards dilutions of primary antibodies were prepared in 1x Roti®-block and applied overnight at 4 °C (see table 2.2). Membranes were washed with TBS-T three times for 10 min., followed by incubation with horseradish peroxidase (HRP)-conjugated secondary antibodies diluted in 1x Roti®-block for one hour at RT. After another three washes in TBS-T for 10 min, the PVDF membranes were exposed to ECL Western Blotting substrate solution (SuperSignal West Pico Chemiluminescent Substrate or SuperSignal West Dura Chemiluminescent Substrate) for 2 min at RT. Subsequently, chemiluminescent signals were visualised and detected by **C**harge-**c**oupled **D**evice (CCD) -Camera (INTAS Chemilux Pro). Images were acquired using ImageJ.

Primary antibody			Secondary antibody		
Name	Brand	Dilution in 1x Roti®-block	Name	Brand	Dilution in 1x Roti®-block
α-*L.m.*	Acris Antibodies GmbH, BP1047	1:1000	Goat anti-rabbit-HRP-conjugate	BioRad #172-1019	1:20000
α-mTNF-R1	Abcam ab19139	1:500			
α-Rab7	Cell signalling #2094				
α-iNOS	Cell signalling #2977				
α-GSK3β	Cell signalling #9315				
α-Nup62	BD Transduction laboratories #610498				
α-EEA1	Santa Cruz Biotechnology, Inc., sc-6415		Rabbit anti-goat-HRP-conjugate	BioRad #172-1034	1:3000
α-Actin	Santa Cruz Biotechnology, Inc., sc-1615				
α-LRG-47	Santa Cruz Biotechnology, Inc., sc-11075				
α-Rab5	Santa Cruz Biotechnology, Inc., sc-46692		Rabbit anti-mouse-HRP-conjugate	BioRad #1706516	1.3000
α-LAMP1	Developmental Studies, Hybridoma bank, Iowa 1D4B		Goat anti-rat-IgG light chain-HRP-conjugate	Jackson Immunoresearch #112-035-175	1:2000
α-CTSD	R&D systems MAB1029				

Table 2.2: Antibodies used for detection in Western Blot

2.4.4. ELISA for detection of TNFα

The principle of the **e**nzyme-**l**inked **i**mmuno**s**orbent **a**ssay (ELISA) method is the antibody-based antigen detection. For detection of mouse TNFα in cell supernatant, the Mouse TNF ELISA set II (BD OptEIA™) was used. A capture antibody for mouse TNFα was directly coated to the surface of a flat bottom medium binding 96-well Microplate according manufacturer's instructions. Coating with capture antibody required buffers free of other proteins using coating buffer and was performed overnight at 4°C. Wells were aspirated and washed three times with 300 µl per well with wash buffer. Thereafter, plates were incubated with 200 µl assay diluent, one hour at RT. This blocking step is required to saturate all protein binding sites of the well and to avoid unspecific antibody binding in the following procedures. The supernatants were discarded and the antigen containing

sample was generated as follows. Cells ($5x10^4$) were seeded on a 96-well flat-bottom cell culture dish when analysing J774 macrophages and on a non treated flat bottom 96-well culture dish analysing BMDM. Stimulation of cells and infection with the mutant strain of *L.m.* ∆hly was carried out at a MOI 3 as described in 2.2.3 and 2.3.1., respectively. Cell culture supernatant was harvested, diluted and transferred to the microplate, where target proteins were retained by the capture antibody. Samples were diluted 1 to 2 in DMEM medium and measured in triplicates. Following several washing steps, the detection antibody labelled with biotin was diluted in assay diluent containing blocking protein and added to the microplate where it bound to the captured antigen. Each well was washed 5 times with 300 µl of wash buffer. Subsequently, wells were incubated with enzyme reagent (streptavidin-HRP). The detection was based on enzymatic activity due to the incubation with a substrate solution (1:1 mixture of substrate reagent A and B, 100 µl per well) for 30 min at RT. Reaction was stopped with 50 µl of stop solution per well. Educts of those reactions were measured at 450 nm. Absolute quantification was performed employing a standard serial dilution of known antigen concentrations. The detection limit was 15.6 pg/ml. Correlations coefficient was constantly > 0.98. Washing steps were carried out with the Washer Tecan Hydroflex using HydroControl-Software Version 1.0.1.0. Absorbance was measured at 450 nm employing Microplate reader model 680 (BioRad) and quantification was carried out with use of the software Microplate manager (version 5.2).

2.4.5. Detection of NO - Griess reagent

Griess reagents A and B were used to detect NO concentrations in the supernatant of cells. Supernatant was obtained from $1x10^5$ cells seeded on a 96-well culture dish in triplicates in 250 µl medium without antibiotics. Cells were stimulated overnight as described in 2.2.3. and infected at a MOI 3 with the mutant strain *L.m.* ∆hly (see 2.3.1). Cells were incubated at 37°C for 24 and 48 hours. For detection of released NO, 100 µL of supernatant were transferred to a 96-well plate. Standard for the Griess reagent was diluted 1 to 100 in medium to generate the highest standard concentration of 100 µg/ml followed by 7 log2 dilutions in medium. Medium was used as blank control. Standard and samples were measured in triplicates. Griess reagents A and B were equally mixed and 100 µl were transferred in each case to the 100 µl sample or standard. OD was measured at wavelength 490 nm, employing Microplate reader model 680 (Bio Rad). The detection limit of this method was 1.56 µM. Correlations coefficient was constantly > 0.98. Quantification was carried out using the software Microplate manager (version 5.2).

3. Results

3.1. Bacterial propagation in J774 macrophages - the role of IFNγ and TNFα for infection control

The cytokine dependent molecular mechanisms which drive bacterial restriction of growth in macrophages remain to be elucidated. Given the fact that both TNF-R1 and IFNγ deficient mice are highly susceptible to infection with the intracellular bacteria *listeria monocytogenes* (*L.m.*) (Huang *et al.*, 1993; Pfeffer *et al.*, 1993), a role for both cytokines in a synergistic manner was considered in *L.m.* eradication. Based on our and others´ observations, TNFα is more likely to play a critical role in the process of eliminating bacteria, in an IFNγ mediated context. Already in 1989, Portnoy and his group defined a synergistic interplay of these two cytokines based on infection studies with mouse peritoneal macrophages (Portnoy *et al.*, 1989) . *L.m.* was found to be restricted in the phagosome during infection in IFNγ stimulated macrophages and a decrease of bacteria number over a time period of eight hours was observed. TNFα alone had no bactericidal properties and promoted an enhanced bacterial killing only in combination with IFNγ . These early studies could also be confirmed by others, which substantiated the role of TNFα in bacterial killing. For instance, neutralising antibodies against TNFα in IFNγ stimulated macrophages led to inhibition of toxoplasmastatic activity (Langermans, 1992). In order to establish a system for bacterial killing without the need of elaborate primary cell culture, the murine macrophages cell line J774 was used for initial infection studies in this work. This cell line was originally isolated in 1986 and deposited by P. Ralph (Ralph *et al.*, 1976). In order to monitor cytokine specific effects on bacterial killing, a convenient protocol was found in the publication of Singh *et al.* (Singh *et al*., 2008). TNFα binds and activates two distinct cell surface receptors, TNF-R1 and TNF-R2. Since this work was focused on the role of TNF-R1 in bacterial eradication, an intent to exclude TNF-R2 signalling was carried out by using recombinant human TNFα (rhTNFα). According to Tartaglia *et al.*, human TNFα only binds and activates murine TNF-R1, but not TNF-R2 (Tartaglia *et al.*, 1991).

Using this protocol, our findings regarding TNFα did not completely coincide with experiments performed with peritoneal macrophages (Portnoy *et al.*, 1989). Macrophages were infected with a low bacterial number of wild-type strain of *L.m.* (EGDe) and monitored over a time period of eight hours. Bacterial load was determined under different cytokine stimulation conditions. The replication of *L.m* remained uncontrolled in unstimulated (Medium) and TNFα treated macrophages. On the other hand, incubation with IFNγ resulted in restriction of growth, confirming Portnoy´s data (figure 3.1). However, the combination of both cytokines (IFNγ and TNFα) could not lead to the phenomenon of enhanced decrease of bacterial load. Since IFNγ stimulated macrophages respond to

bacterial components with TNFα production (Nathan, 1987; Nedwin *et al.*, 1985), addition of recombinant TNFα may not enhance the IFNγ mediated effect in this particular system. Therefore, supernatant of infected macrophages were taken and analysed with an enzyme-linked immunosorbant assay (ELISA) against mouse TNFα to obtain the actual amount of the cytokine in this system. As early as 60 min post infection (p.i.), high amounts of up to 500pg/ml TNFα were measured independent of whether the wild-type strain (EGDe) or the avirulent mutant strain Δhly had been used for infection (figure 3.2). Not only IFNγ stimulated, but also unstimulated macrophages secrete TNFα upon infection, likely to be a consequence of Toll-like-receptor (TLR) signalling. These data demonstrate that TNFα release cannot be separated from infection in any case. IFNγ mediated effects are consequently always synergistic effects of both cytokines and only working with macrophages deficient in TNF or its receptor could give indication of pure IFNγ effects.

In IFNγ stimulated macrophages, murine TNFα which can bind and activate TNF-R2 is released. These signalling events are probably negligible, as TNF-R2 is mainly activated by the transmembrane form of TNFα (Grell *et al.*, 1995), however an eventual influence of TNF-R2 was kept in mind.

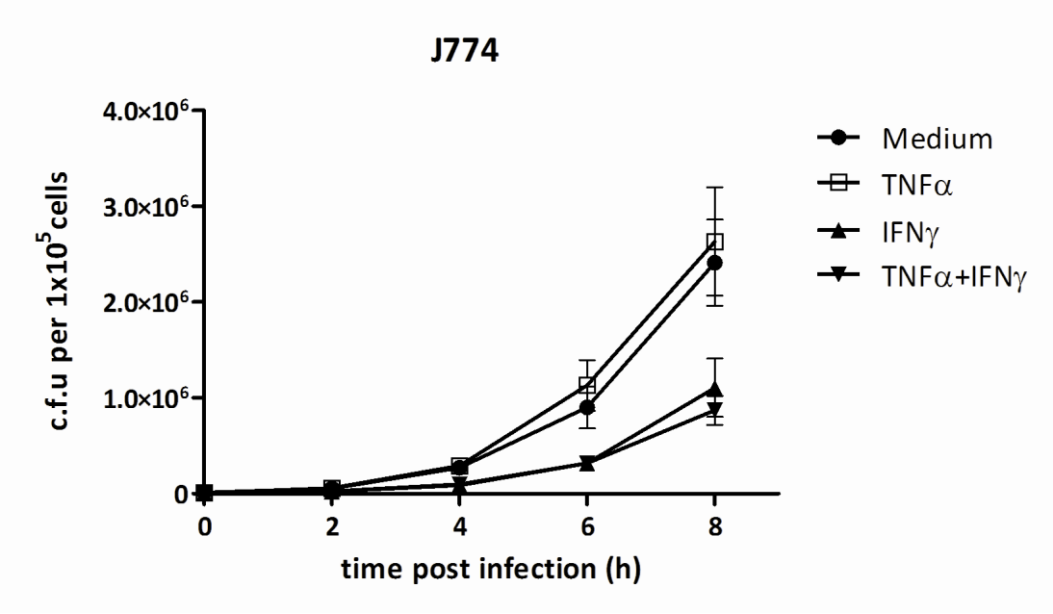

Figure 3.1: Growth of Listeria monocytogenes in J774 macrophages under different cytokine stimulation
Growth of L.m. in J774 macrophages was monitored. Cells were incubated with rmIFNγ (500 U/ml) overnight before infection and exposed to wild-type strain EGDe at a MOI of 0.1 for indicated time periods. At the time of infection, rhTNFα (100 ng/ml) was added and was present at all times. A short incubation with gentamycin (30 min, 50 µg/ml) removed extracellular bacteria. Cells were washed three times, supplemented with new medium and shifted to 37°C for the indicated time periods. The cells (5x10^4 per well) were lysed at each time point shown and serial dilutions were plated to obtain the c.f.u. (colony forming units). Data points represent means from three individual experiments ± SE; MOI = multiplicity of infection

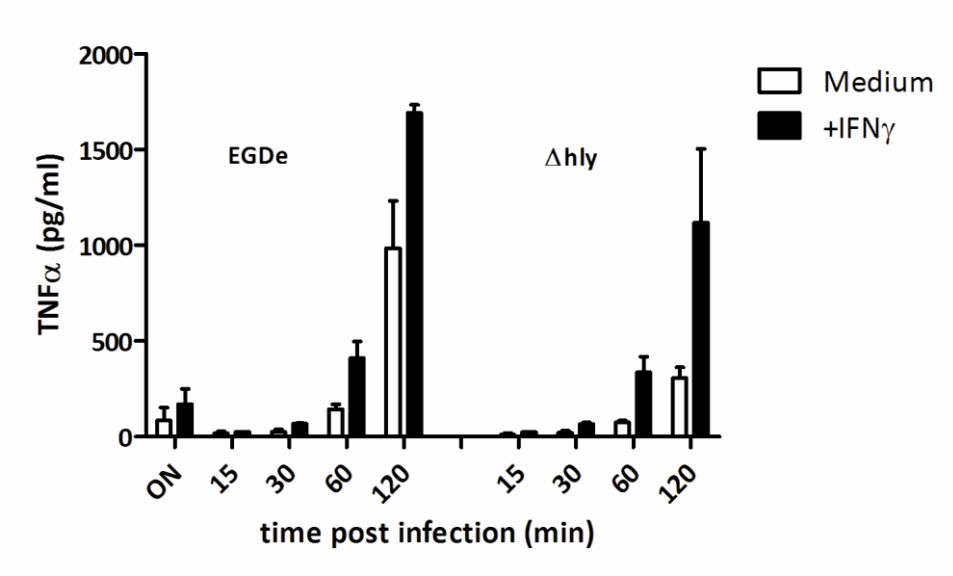

Figure 3.2: TNFα -secretion of J774 macrophages during infection with Listeria monocytogenes
TNFα production during infection was analysed. J774 macrophages were stimulated with or without rmIFNγ (500U/ml) overnight (ON) and supplemented with new medium for infection. Cells were exposed at a MOI 3 to the wild-type strain EGDe and the hemolysin-negative mutant Δhly for the indicated periods of time. To analyze the amount of TNFα, supernatants were harvested at the indicated time points after infection. TNFα amounts were determined with an ELISA specific to mouse-TNFα. Data represent means and SD of three individual experiments.

The method of confocal microscopy was used to confirm the cytokine specific effects on bacterial growth restriction at a cellular level. As described in 1.2, *L.m.* escapes from the phagosome and polymerizes host actin for intercellular movement and spreading, providing phalloidin staining as a convenient tool to see whether bacterial growth is impaired or not. After translocation into the cytoplasm bacteria start to propagate and originally red stained bacteria appear green due to positive actin-staining by phalloidin-FITC. This staining allows differentiating between those bacteria escaped into the cytoplasm (green) and those which still reside in the phagosome (red). In the early phase of infection, escape from the phagosome occurs approximately within the first 30 min following phagocytosis (Myers *et al.*, 2003). Therefore images at 30 min indicate the number of bacteria at the beginning of infection, ensuring that all cells were infected with comparable bacterial loads. After two hours p.i., virtually all bacteria in unstimulated (Medium) macrophages had escaped from the phagosome and almost all bacteria formed the characteristic actin "comet tail", allowing the pathogen to enter the neighbouring cells. In the case of TNFα stimulated macrophages, similar effects were observed. Bacterial factors prevailed and *L.m*. could enter the cytoplasm resulting in uncontrolled bacterial growth, indicated by red stained bacteria carrying a green actin "comet tail". However, macrophages stimulated with IFNγ seem to limit phagosomal escape, detected by delay in actin polimerisation of the few bacteria which had actually translocated. Concomitantly, some bacteria remained in the phagosome, indicated by red staining and rendering the observations

Portnoy had described in his work in consequence of IFNγ stimulation. Addition of TNFα to IFNγ treated macrophages showed no changes in phagosomal ecscape in comparison to IFNγ stimulated cells and this corresponds with the data presented in figure 3.1. Taken together, these findings are consistent with the early work of Portnoy regarding IFNγ. The exact role of TNFα in bacterial growth restriction remains yet to be determined. Infection studies with TNF-R1 $^{-/-}$ macrophages will elucidate the contribution of TNFα to bacterial elimination in more detail (see 3.6.3).

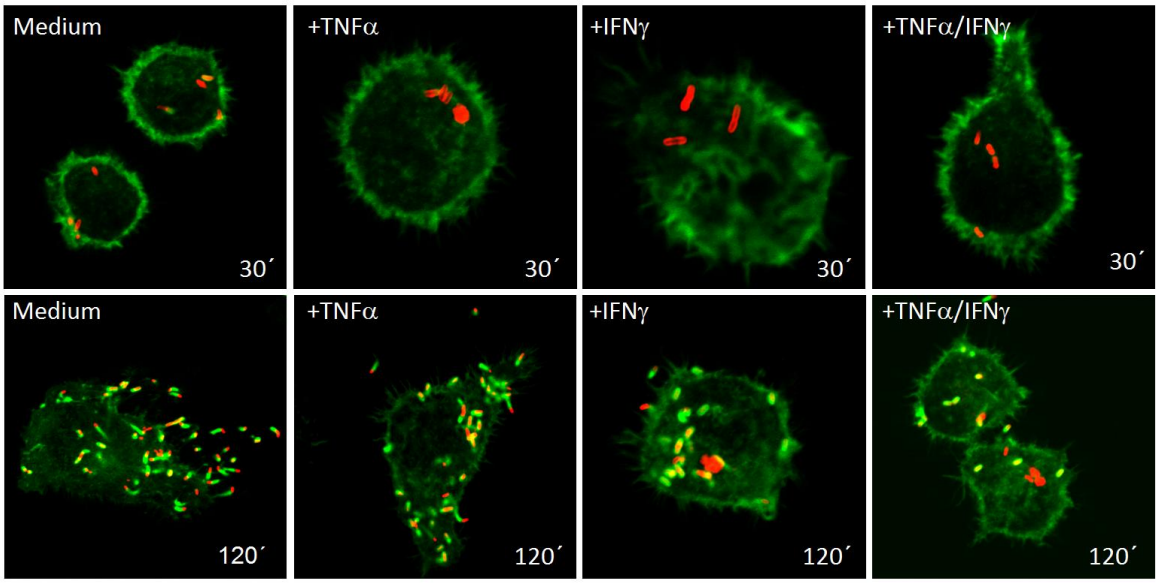

Figure 3.3: Confocal microscopy of Listeria monocytogenes in J774 macrophages
Actin polymerisation of L.m. in J774 macrophages was monitored. Cells were seeded on coverslips and stimulated with or without rmIFNγ (500 U/ml) overnight. At the time of infection, rhTNFα (100 ng/ml) was added. Cells were infected at a MOI 3 with the wild-type strain EGDe for indicated time periods. Cells were fixed with 2 % paraformaldehyde for 15 min, preparing them for immunofluorescence staining. To obtain intracellular staining, cells were permeabilised with 0.1 % Triton X-100. Actin: phalloidin-FITC (green); L.m.: Alexa546 (red).

3.2. Tumor necrosis factor receptor 1 - localisation in infected J774 macrophages

Previous work of our group revealed that internalisation of TNF-R1 is required for signal transduction events of the apoptotic pathway and that a number of proteins can only be found in association with the internalised "receptosomes" (see 1.5.1). Interestingly, these receptor vesicle compartments were demonstrated to fuse with vesicles of the *trans*-Golgi-network containing CTSD and acid sphingomyelinase (ASMase). These enzymes appear on the matured receptor compartment in their activated form approximately 30-60 min after internalisation (Schneider-Brachert *et al.*, 2004). Given the fact that TNF-R1 is essential for the eradication of intracellular bacteria and based on the importance of internalisation for recruitment of effector proteins to the receptor, we hypothesized a mutual compartment containing bacterial phagosomes and TNF-R1-receptosomes. The fusion of both of these subcellular compartments could display a mechanism to direct bactericidal components of TNF-R1 multiprotein-complex to the phagosome and might enlighten the biological function of TNF-R1 internalisation. To demonstrate that this hypothetical compartment of receptor and phagosome indeed exists, the first method employed was confocal microscopy.

A ligand-based staining with a combination of biotin-hTNFα and streptavidin-FITC (green) allowed staining of TNF-R1 and its internalisation. The application of recombinant human biotin-TNFα (rhTNFα) ensured that only TNF-R1, not TNF-R2 was bound and stimulated (see 3.1). To obtain fusion events of bacterial phagosomes and TNF-R1 complexes, macrophages were infected with the hemolysin negative mutant strain of *L.m.* (Δhly). In contrast to the wild-type strain EGDe, this mutant stays in the phagosome and does not escape from the phagosome for replication in the cytoplasm (see 1.2), which makes it convenient for this type of assay. Previous receptor-internalisation studies showed that most internalised complexes concentrate after 60 min in the inner cell. The activated form of CTSD was found to accumulate between 30-60 min on the TNF-R1 complex (Schneider-Brachert *et al.*, 2004). Therefore, a 60 min period of TNF-R1 internalisation with simultaneous infection was chosen as a valid time point for monitoring fusion events. Indeed, TNF-R1 complexes (green) were found to be localised very close to single bacteria (red). This was observable over a series of sections with 0.5 µm diametre screening through one single cell (figure 3.4A, TNF-R1 indicated by white arrows). Figure 3.4B displays another infected cell, with closer detail to a single bacterium. Green TNF-R1 complexes colocalise with the pathogen, shown in higher magnification at the lower panel of figure 3.4B. From this data we concluded that an encounter of TNF-R1 compartment and the phagosome seems to be likely. Since immunofluorescence staining has limited resolution for sections thinner than 0.5 µm, a further step was taken in order to contrast and therefore confirm these findings with electron microscopy.

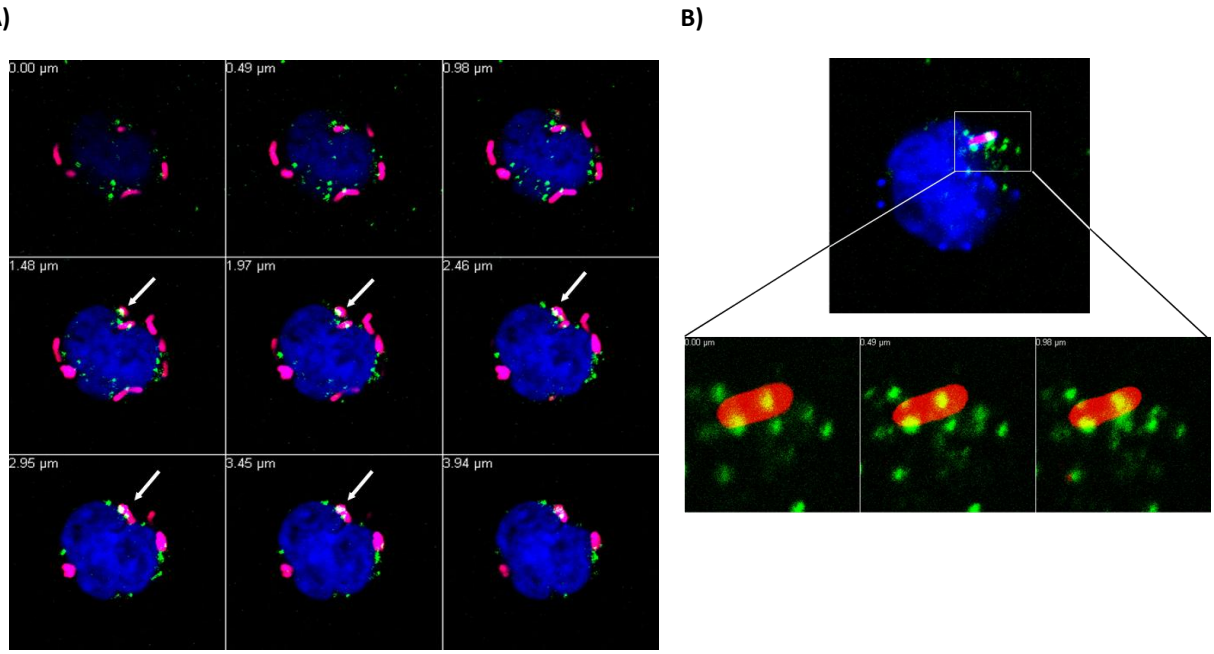

Figure 3.4: Analysis of TNF-R1 localisation in Listeria monocytogenes infected J774 cells
In order to obtain fusion events of TNF-R1 and L.m., J774 macrophages were seeded on coverslips. Biotin-rhTNFα (1.25 ng) and Streptavidin-FITC (12.5 ng) were pre-incubated for 60 min and TNF-R1 was labelled with these complexes for additional 60 min at 4°C in the dark. After three washing steps with PBS cells were shifted to 37°C and infected at a MOI 3 with L.m. (Δhly) for 60 min. Internalisation was stopped with a shift to 4°C.
***A)** and **B)** Cells were fixed with 2 % paraformaldehyde for 15 min, preparing them for immunoluorescence staining. For intracellular staining, cells were permeabilised with 0.1 % Triton X-100. Nuclei :Draq5 (blue);L.m.: Alexa 594 (red); TNF-R1: Biotin-TNFα/SA-FITC (green).*

Since labelling with biotin-TNFα and streptavidin-FITC worked successfully for immunofluorescence staining, a similar method was selected for electron microscopy and TNF-R1 was ligand based stained with a complex of human biotin-TNFα/Streptavidin-gold. Prior monitoring of J774 macrophages at 4°C was necessary to ensure that TNF-R1 is initially located on the cell surface. Internalisation process was induced by a temperature shift to 37°C and is required to localise gold-labelled TNF-R1 to the phagosomal compartment. In figure 3.5A, a representative macrophage shows gold labelled TNF-R1 on its cell surface. The square-shaped area outlined in black was depicted for higher magnification. White arrows indicate the gold-labelled TNF-R1 (figure 3.5B). Subsequently, macrophages were infected with the listeriolysin negative mutant strain of *L.m.* Δhly. The darker, oval and circular, well-defined structures in figure 3.5 C-F represent phagocytosed bacteria. Shift to 37°C obtained internalisation of gold-labelled TNF-R1, indicated by white arrows. After 60 min of incubation, nearly all analysed bacterial phagosomes had started to fuse (Figure 3.5C) or in some cases already contained several of these TNF-R1 complexes inside the phagosomal compartment (Figure 3.5 C-F). Based on confocal and electron microscopic data, these results illustrate for the first time that TNF-R1 fuses with *L.m.*-containing phagosomes and that the proposed hypothetical compartment of phagosome and TNF-R1-receptosome is indeed an existing one.

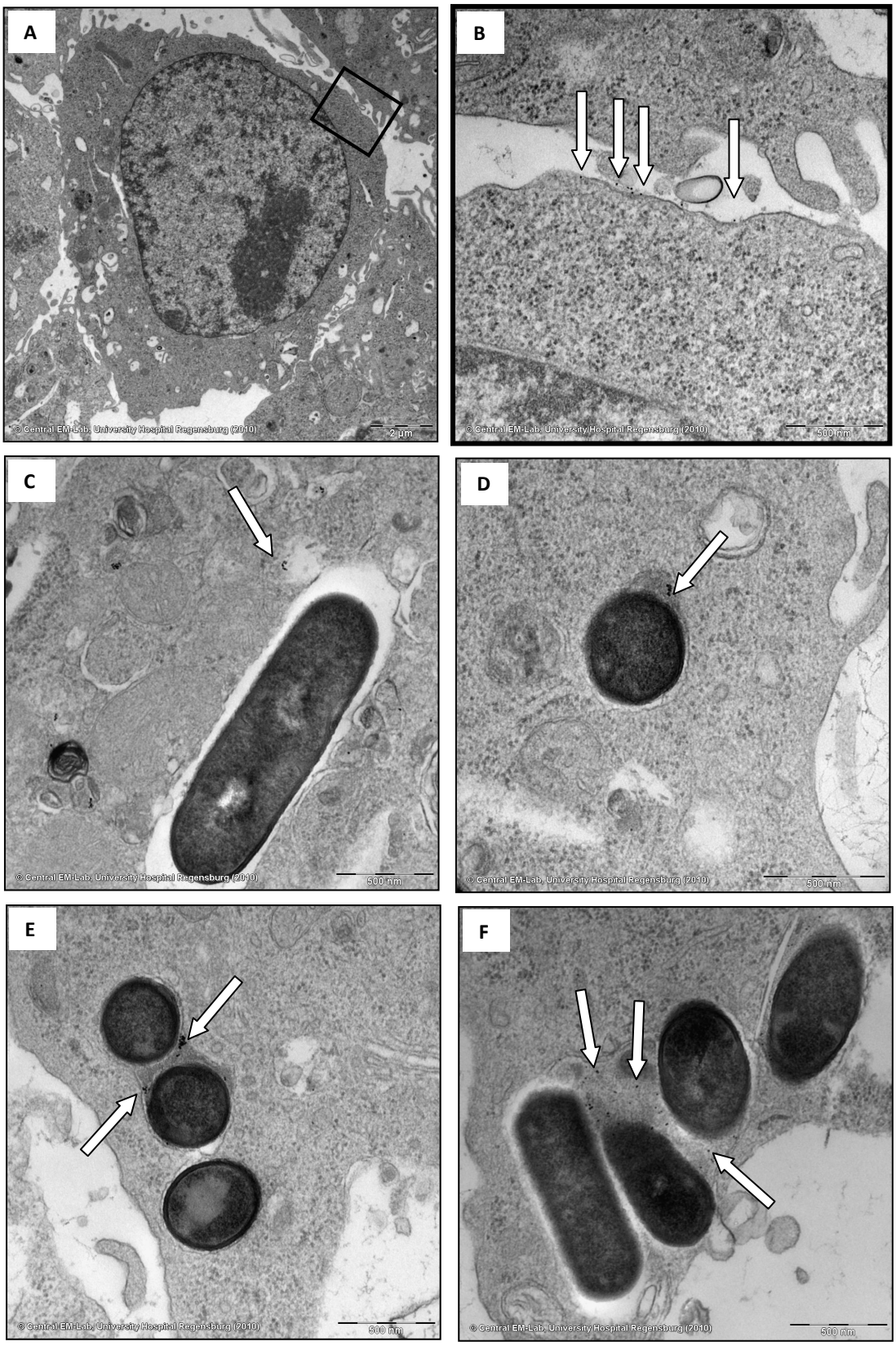
A
© Central EM-Lab, University Hospital Regensburg (2010)
2 µm
B
© Central EM-Lab, University Hospital Regensburg (2010)
500 nm
C
© Central EM-Lab, University Hospital Regensburg (2010)
500 nm
D
© Central EM-Lab, University Hospital Regensburg (2010)
500 nm
E
© Central EM-Lab, University Hospital Regensburg (2010)
500 nm
F
© Central EM-Lab, University Hospital Regensburg (2010)
500 nm

Figure 3.5 (on previous page): TEM pictures of TNF-R1 and Listeria monocytogenes in J774 macrophages
To obtain fusion events of L.m-phagosomes and TNF-R1-receptosomes, cells were seeded on 6-well-plates and could adhere overnnight. Biotin-hTNFα (100 ng) and streptavidin-gold (SA-gold) (500 ng) were pre-incubated for 60 min and TNF-R1 was labelled with these complexes for an additional 60 min at 4 °C.
***A)-B)** After three washing steps with PBS cells were softly removed by rinsing the wells with 1 ml cold PBS. Cells were centrifuged 10 min at 2000 x rpm and the pellet was fixed with Karnovsky´s fixative and prepared for electron microscopy**. C)-F)** After three washing steps with PBS, cells with the biotin-TNFα/SA-gold complex were infected at an MOI 3 with L.m.Δhly and plates were centrifuged for 5 min, 15 °C, 500 x g to synchronize the uptake. The cells were then incubated for 60 min at 37°C and after incubation softly removed by rinsing the wells with cold PBS and fixated as described previously.*

3.3. Analysis of *Listeria monocytogenes*-containing phagosomes – a new method of phagosome isolation

Considering TNF-R1 to be part of the phagosomal compartment, it was consequently of special interest to study in detail which signalling components of TNF-R1 contribute to the mechanism of bacterial killing. This question implied to go further into the examination of subcellular compartments, especially the bacteria-containing phagosomes. There are many different protocols available for the isolation of phagosomes. In this work, a new promising method established by C. Steinhäuser in the group of Dr. Norbert Reiling in Borstel was applied.

Based on immunomagnetic labelling, this protocol allowed the isolation of intact bacteria-containing compartments. To date, this method has only been employed for *mycobacteria*- and *clamydia*-containing phagosomes in primary bone marrow macrophages, which implied the need of pre-experimental workup in order to transfer the protocol to *L.m.* and J774 macrophages. The system was then validated for these macrophages and basic conditions for host and pathogen were controlled. In comparison to other methods which usually rely on density gradient centrifugation (Desjardins, 1994), this is a very fast and efficient protocol (detailed in figure 3.7).

Prior to phagosomal isolation, bacteria were incubated with a specific biotinylated lipopeptide termed Lipobiotin (LB) (see figure 3.6). LB incorporates into the bacterial membrane, generating biotinylated bacteria. These modified bacteria were coupled with streptavidin magnetic beads and exposed to J774 macrophages for bacterial uptake. Infected cells attached to a 10 cm dish were centrifuged in order to achieve synchronized phagocytosis. Vesicular trafficking was initiated by shifting infected macrophages to 37°C and was halted by moving them back to 4°C. Cells were detached with the use of EDTA-containing buffer A and collected in tubes. Macrophages were centrifuged and resuspended in buffer A, which contained cytochalasin D and Benzonase Nuclease. The mycotoxin cytochalasin D inhibits actin polimerisation and disrupts actin microfilaments, decreasing interaction of vesicles with cytoskeletal proteins. Benzonase Nuclease degrades free DNA. Subsequently, cells were softly disrupted by sonication at 4°C to keep vesicles in shape, generating the fraction of the post nuclear supernatant (PNS). Stepwise centrifugation gradually removed

residual intact cells. The PNS fraction was loaded onto the custom-built magnetic chamber which is based on a high magnetic field (2 Tesla) from strong permanent magnets (Neodymium-Iron-Baron magnets). Application of magnetic *L.m.*-containing vesicles to the magnetic field results in specific enrichment of these phagosomes. After 30 min attachment, the loading tube was rinsed with buffer A for 10 min resulting in the collection of the non magnetic fraction (NM). Further washing steps increased the purity of the magnetic fraction (M). This fraction was obtained after release of the tube from the magnetic field. These particular fractions were used for analysis by western blot or transmission electron microscopy (TEM). For detailed steps of this method see figure 3.7.

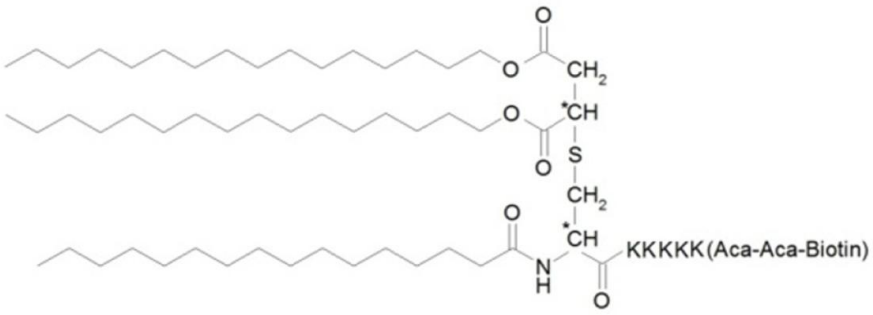

Figure 3.6: Biochemical structure of Lipobiotin
triacetylated,biotinylated lipopeptides termed Lipobiotin (LB, PHC-KKKKK(Aca-Aca-Biotin) x 3TFA, N-Palmitoyl-S-(1,2-bishexadecyloxy-carbonyl)ethyl-[R]-cysteinyl-[S]-lysyl-[S]-lysyl-[S]-lysyl-[S]-lysyl-[S]-lysine(ε-aminocaproyl-ε-aminocaproyl-biotinyl) x 3 CF3COOH, Molecular mass 2018 • 342.1) (Hoff, 2002)

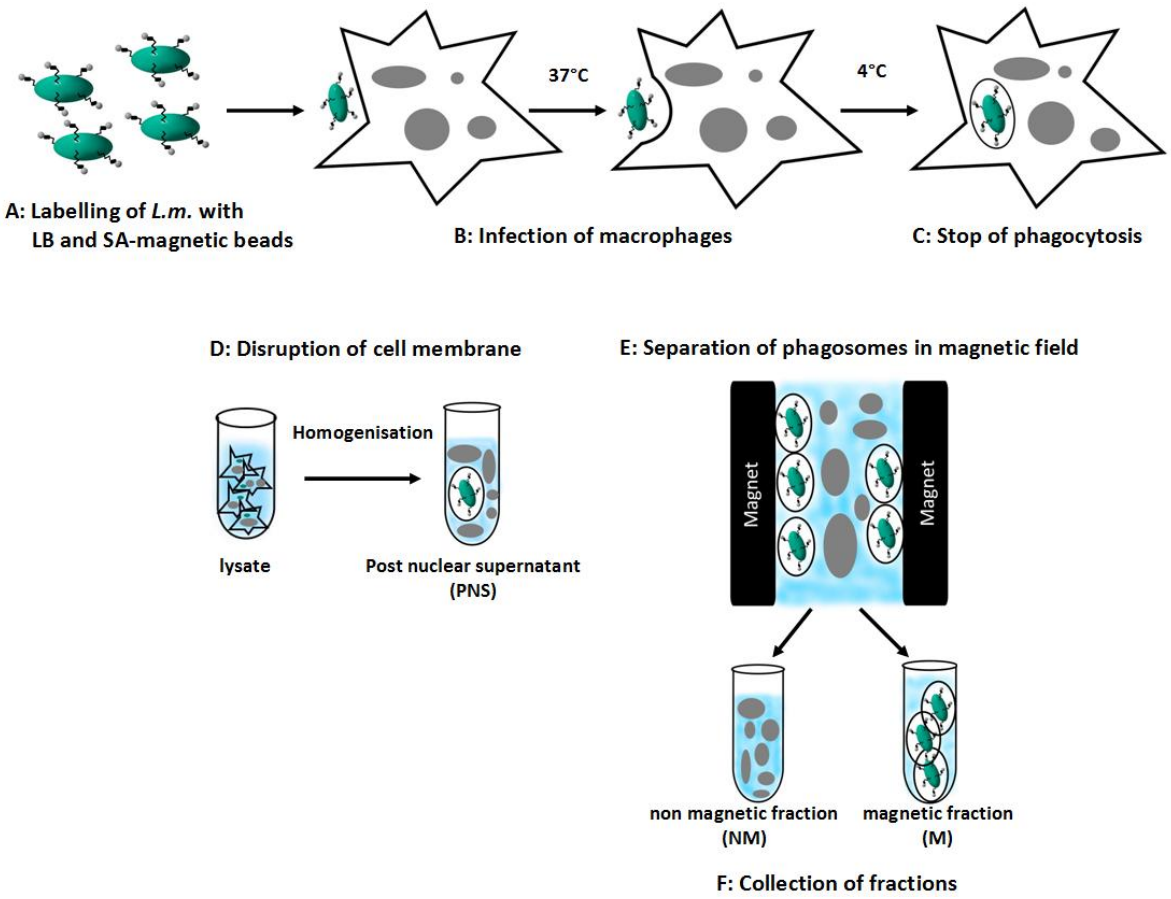

Figure 3.7: Isolation of Listeria monocytogenes-containing phagosomes
In order to monitor the phagocytosis process of L.m. in macrophages different infection periods were chosen. For each measuring point 2x10^7 cells were seeded on a 10 cm cell culture dish. ***A)*** *Bacteria were incubated with LB (10 µg/ml) overnight. On the following day, bacteria were labelled with streptavidin magnetic and* ***B)*** *exposed at a MOI 10 to macrophages for uptake.* ***C)*** *Endocytosis was stopped by shifting cells to 4°C and incubation with buffer A containing 0.02 % EDTA resulted in detachment of cells from the culture dish. Cells were washed with buffer A containing 0.02 % EDTA, collected in tubes and centrifuged. The supernatant was discarded and pellet was resuspended in 500 µl buffer A supplemented with Benzonase Nuclease (25 U/ml) and cytochalasin D (5 µg/ml) to degrade free DNA and to disrupt actin microfilaments.* ***D)*** *Cells were then disrupted by sonication using a Branson Sonifier. Disrupted cells were centrifuged, the supernatant was collected and the residual pellet was resuspended in a step wise manner using smaller volumes (200 µl and 100 µl) of buffer A containing Benzonase Nuclease and Cytochalasin D. This step was repeated three times. The supernatant (PNS) gained after different sonication steps was pooled and were used for Western blot analysis and determination of protein content.* ***D)*** *PNS was then loaded on to the magnetic chamber to collect phagosomes containing magnetic bacteria. These vesicles could attach for 30 min on the wall of a tube between two magnets.* ***E)*** *The loading tube in the magnetic chamber was then rinsed with Buffer A (containing protease inhibitor, roche complete) for collection of the non magnetic fraction (NM). After a further washing step of 10 min the magnetic fraction was collected by removal of the tube from the magnet field. The isolated magnetic fraction was collected and prepared for further analysis (Western Blot or TEM).*

3.3.1. Incorporation of Lipobiotin into *Listeria monocytogenes* membrane

According to the protocol of C. Steinhäuser, *L.m.* was incubated with LB and small magnetic particles (magnetic beads). To validate the specific incorporation of LB into *L.m.* membrane, these bacteria were incubated with decreasing amounts of LB, subsequently coupled with Cy5-conjugated streptavidin (SA-Cy5) and prepared for flow cytometric analysis. Both strains, *L.m.* wild-type EGDe and listeriolysin mutant (Δhly), showed positive staining with Cy-5 (figure 3.8), suggesting LB can be used for labelling bacteria with magnetic beads. It is worth noting, that also lower concentrations of LB were sufficient for magnetic labelling of bacteria. In this work a concentration of 10 µg/ml was used to ensure high degree labelling. In order to achieve magnetic labelled bacteria for the isolation protocol, the first step, specific incorporation of LB into *L.m.* bacterial wall was demonstrated.

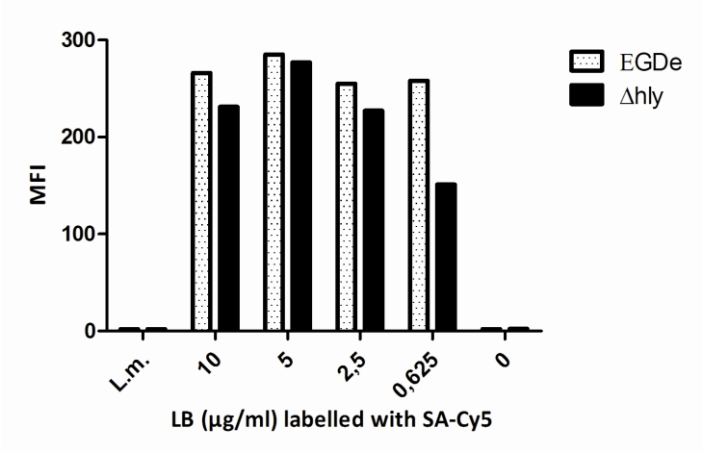

Figure 3.8: flow cytometric analysis of LB incorporation in L.m. membrane
In order to demonstrate specific incorporation of LB into the bacterial wall, L.m. strains were incubated with decreasing amounts of LB as indicated at 4°C overnight. After washing with PBS, bacteria were stained with SA-Cy5 (1:160) for 20 min at 4°C. Flow cytometric analysis was performed on the FACS Canto II cytometer and shows positive stained bacteria dependent on decreasing LB concentrations. MFI = mean fluorescence intensity.

3.3.2. Influence of Lipobiotin on *Listeria monocytogenes* life cycle

Modifying the bacterial membrane with LB may affect the general life cycle of *L.m.* in macrophages. In order to exclude an impairment of growth and virulence potential of *L.m.* evoked by LB, several control experiments were performed. One of the primary steps of infection, bacterial uptake, was monitored in J774 macrophages. Both *L.m.* strains EGDe and Δhly were incubated with decreasing concentrations of LB and exposed to J774 macrophages for engulfment (Figure 3.9). At 60 min p.i., cells were lysed and the ratio of LB modified to unmodified bacteria was determined. In general, the bacterial uptake seemed to be slightly reduced with high concentrations (5-10 µg/ml) of LB for both

L.m. strains. This difference in comparison to untreated bacteria was minimal and bacteria were able to enter the host cells. The second important step in listerial life cycle is the translocation out of the phagosome into the cytoplasm, where replication starts (see 1.2). In order to see whether LB alters the invasive potential of *L.m.,* LB modified EGDe strain was monitored for replication ability and actin polimerisation after infection. J774 macrophages were exposed to wild-type strain EGDe incubated with decreasing concentrations of LB. Cells were lysed and number of viable bacteria 120 min p.i. was determined. All bacteria replicated similarly and bacterial load increased independently of any LB concentration (figure 3.10A). These results were supported by using confocal microscopy. Actin staining by phalloidin-FITC allowed differentiation between translocated and phagosome retained bacteria. In J774 macrophages, virtually all LB incubated bacteria (red) were able to enter the cytoplasm and showed actin polymerisation, demonstrated by a green actin tail (Figure 3.10A). These findings appear more in detail when a single cell is observed at higher magnification (figure 3.10B). Nearly all bacteria maintained their replication potential and formed the characteristic actin "comet tail" (figure 3.10B). In conclusion, LB did not affect the virulence and life cycle of *L.m*. Magnetic labelling of bacteria with the help of LB is possible without a loss of infective potential.

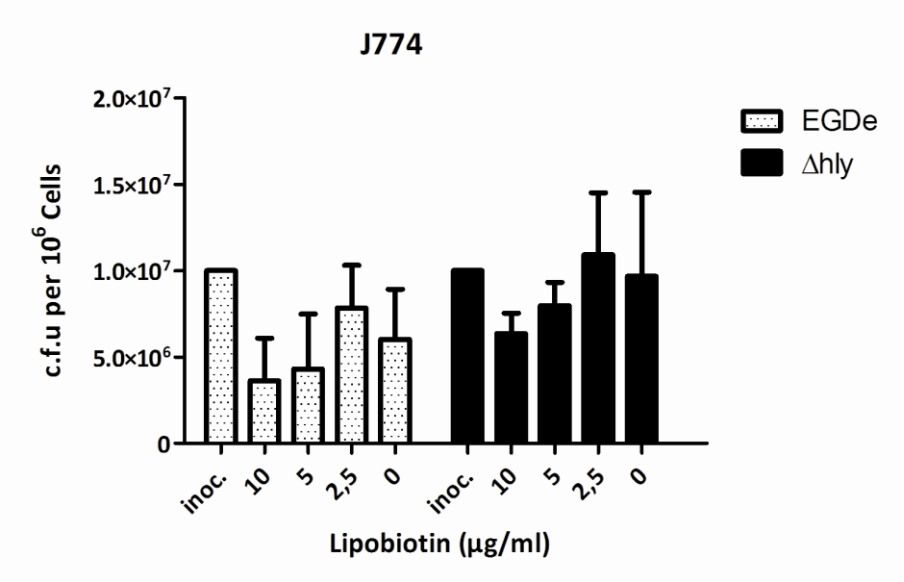

Figure 3.9: Influence of Lipobiotin on bacterial uptake in J774 macrophages
In order to monitor bacterial uptake, 1x10^6 cells were infected at a MOI 10 with EGDe and ⊿hly strain incubated with different concentrations of LB as indicated. At 60 min p.i., cells were lysed and serial dilutions were plated to obtain c.f.u. inoc. = inoculum. Data represent means and SD of three independent experiments.

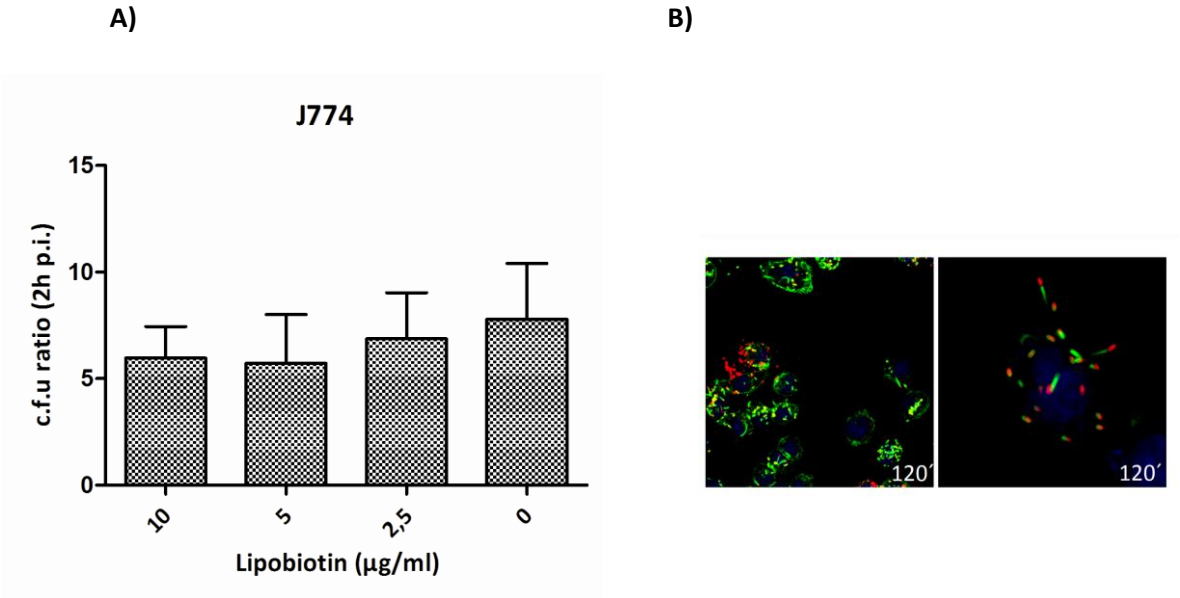

Figure 3.10: Impact of Lipobiotin on Listeria monocytogenes life cycle
A) *In order to monitor listeria life cycle, 5x10^4 macrophages were infected at a MOI 3 with wild-type strain of L.m. (EGDe). Bacteria were incubated with different concentrations of LB as indicated. After 120 minutes p.i., cells were lysed and serial dilutions were plated to obtain the c.f.u. Data represent means of two independent experiments. Means and SD are shown as the ratio of c.f.u at 2h to c.f.u at 0h.*
B) *Actin polymerisation of L.m. in J774 macrophages was monitored 120 min p.i. using confocal microscopy. Bacteria were labelled with 10 µg/ml LB. Cells were fixed with 2 % paraformaldehyde and were permeabilised with 0.1 % Triton X-100 for intracellular staining. Nucleus: Draq5 (blue); Actin: phalloidin-FITC (green); L.m.: Alexa546 (red).*

3.3.3. Influence of labelled bacteria on macrophages

To establish LB as a valid method for magnetic labelling, influences of this modification on the pathogen itself and its host cell needed to be determined. Lipopeptides and lipoproteins are known to activate the innate immune system by triggering TLRs on macrophages and other immune cells (Jin, 2008). Activation of macrophages by TLRs usually results in NF-κB signalling which induces TNFα-release. This provides the determination of TNFα production as a convenient readout for enhanced activation of those macrophages. The cytokine IFNγ enhances the signalling effects mediated by these receptors and TNFα release increases depending on duration of bacterial exposure. The amount of released TNFα was measured with an ELISA specific to murine TNFα during infection with both strains of *L.m.* (EGDe and Δhly), at different time points p.i. Compared to unlabelled bacteria, magnetically labelled *L.m.* induced a slight increase of TNFα production which was independent of IFNγ, p.i. time point and the particular strain (figure 3.11A and B). These differences were inconsiderable for both strains.

To determine differences in the activation status of J774 macrophages upon infection with magnetic labelled bacteria, the p38 MAP kinase signalling pathway was monitored. This signalling pathway is

activated by several stimuli, including IFNγ and TNFα (see 1.5.4). P38 MAP kinase phosphorylation served as indication for activation and was analysed by Western blot (Figure 3.11C). Incubation of wild-type (EGDe) or mutant strain (Δhly) of *L.m*. with decreasing concentrations of LB caused no enhanced p38 phosphorylation in comparison to lysates of J774 macrophages infected with unlabelled bacteria. P38-expression served as loading control and a lysate of cells stimulated with 10 ng/ml LPS was used as positive control. According to these data, J774 macrophages were not activated by this specific pathogen modification, allowing magnetic labelling to monitor cytokine specific effects on the bacterial phagosomes also.

A)

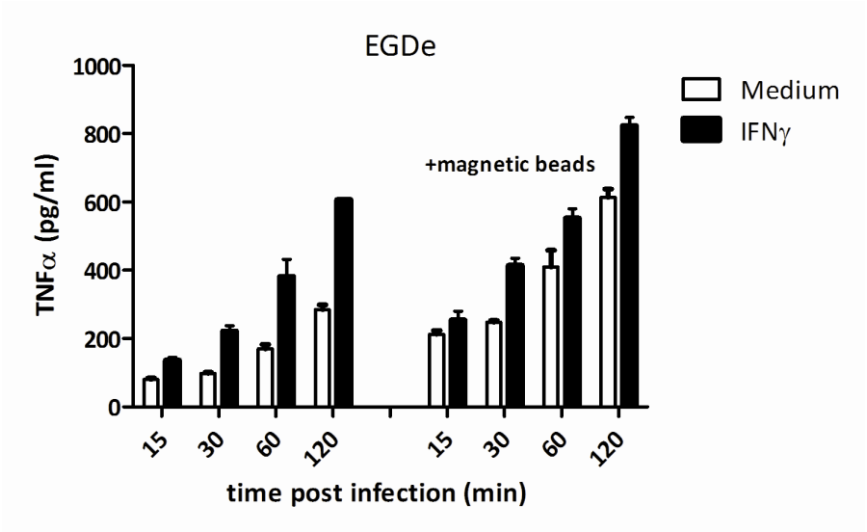

B)

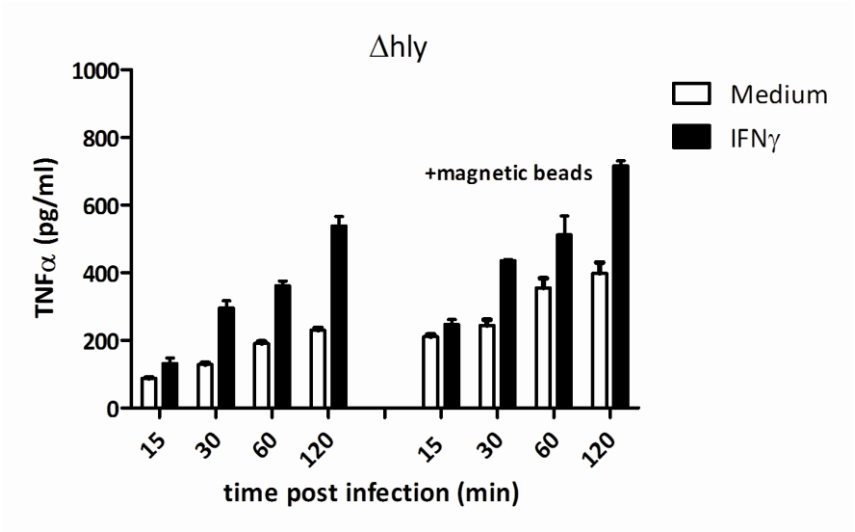

C)

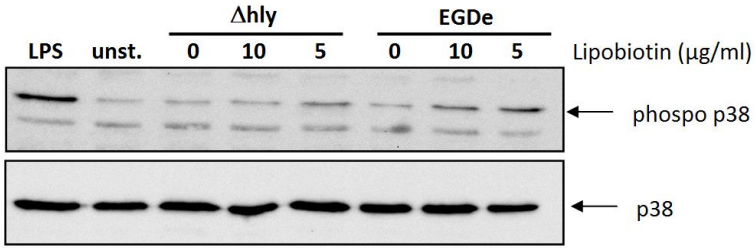

Figure 3.11: Activation status of J774 macrophages after infection with labelled bacteria
A) *and* ***B)*** *In order to analyse the activation status of infected macrophages, J774 macrophages were stimulated with rmIFNγ (500 U/ml) overnight and supplemented with new medium for infection. Cells were infected at a MOI 3 with the wild-type strain EGDe and the hemolysin-negative mutant Δhly labelled with or without magnetic beads. To analyse the amount of TNFα, the supernatant was harvested for the indicated time points p.i. TNFα amounts were determined with an ELISA specific to mouse-TNFα. Data show means and SD of triplicate cultures from one representative experiment.*
C) *In order to monitor p38 phosphorylation in Western blot analysis, cells were infected for 60 min at a MOI 10 with magnetically labelled bacteria. Different concentrations of LB were used as indicated. To obtain samples for Western blot, cells were lysed with RIPA buffer. Positive control = cells treated with 10 µg/ml LPS; negative control (unst.) = completely unstimulated cells. An antibody specific for phosphorylated p38 obtained the activation status of the cells; the second blot against p38 was used as loading control.*

3.3.4. Magnetic labelling of *Listeria monocytogenes*

LB was shown to be a convenient tool to specifically modify *L.m*. and subsequently label them with magnetic beads. The magnetic label can then be employed to isolate *L.m.*-containing phagosomes. **T**ransmission **e**lectron **m**icroscopy (TEM) was used to reveal the constitution of magnetically labelled bacteria and the phagosomes in the cells. The mutant strain *L.m.*Δhly was labelled with LB and streptavidin magnetic beads, and exposed to J774 macrophages for 15, 60 and 120 min. The TEM picture in figure 3.12A represents a single cell infected with magnetically labelled *L.m.* and the square-shaped area outlined in black was depicted for higher magnification of the pathogen within the cell (3.12B).The bacterium carrying magnetic beads on the surface (white arrow) is surrounded by the phagosomal membrane and at this stage no morphological impairment is visible. Interestingly, LB seems not to cover the whole bacterium. Only a few spots carry the magnetic beads and it is also notable that the microbeads seem to bind with a minimal space between beads and the bacterial surface. At this stage, the origin of this minimal space between magnetic beads and bacterial membrane is not yet clear, but this can also be observed with mycobacteria (work from Dr. Norbert Reiling´s laboratory). Monitoring further phagosomal maturation stages (15, 30 and 120 min p.i.), the magnetic beads lose their contact to the bacteria completely and detach from the bacterial membrane, probably due to phagosomal acidification. Nevertheless, the magnetic beads (white arrows) remain in the bacteria-containing phagosome and do not leave the compartment at any time during intracellular trafficking and phagosomal maturation (Figure 3.12 C-E). Following the protocol

of phagosome isolation (see 2.2.14), these cells were subsequently disrupted by sonication, allowing disruption of the host cell membrane without any harm to the intracellular membranes. These samples were loaded onto the magnetic chamber for phagosome separation and were further analysed by TEM. Monitoring the magnetic fraction with its whole content (figure 3.12F) demonstrated the high enrichment of bacteria containing phagosomes after the isolation process and confirmed the impressive efficiency of this new protocol. In order to study the constitution of the isolated vesicles, pictures in higher magnification were examined. Isolated phagosomes after 15 min p.i. showed electron translucent compartments, which are characteristic for early phagosomes (Figure 3.12G) in contrast to the microscopic dense structures of late phagosomes at 60 min p.i. (figure 3.12H). Both pictures show that there is no observable impairment of the phagosomal membrane and that the magnetic beads are still contained in the phagosomal lumen (white arrows). Therefore, this method allows the isolation of intact bacteria-containing vesicles in all maturation stages. Additionally, the constitution of magnetic labelled bacteria in macrophages and isolated phagosomes was anlaysed dependent on different stimulation patterns. A set of TEM pictures of infected cells and phagosomes isolated after stimulation is shown in 7 and 7.2. Virtually no difference regarding membrane constitution was observed, whether the cells were stimulated with TNFα, IFNγ or with a combination of both.

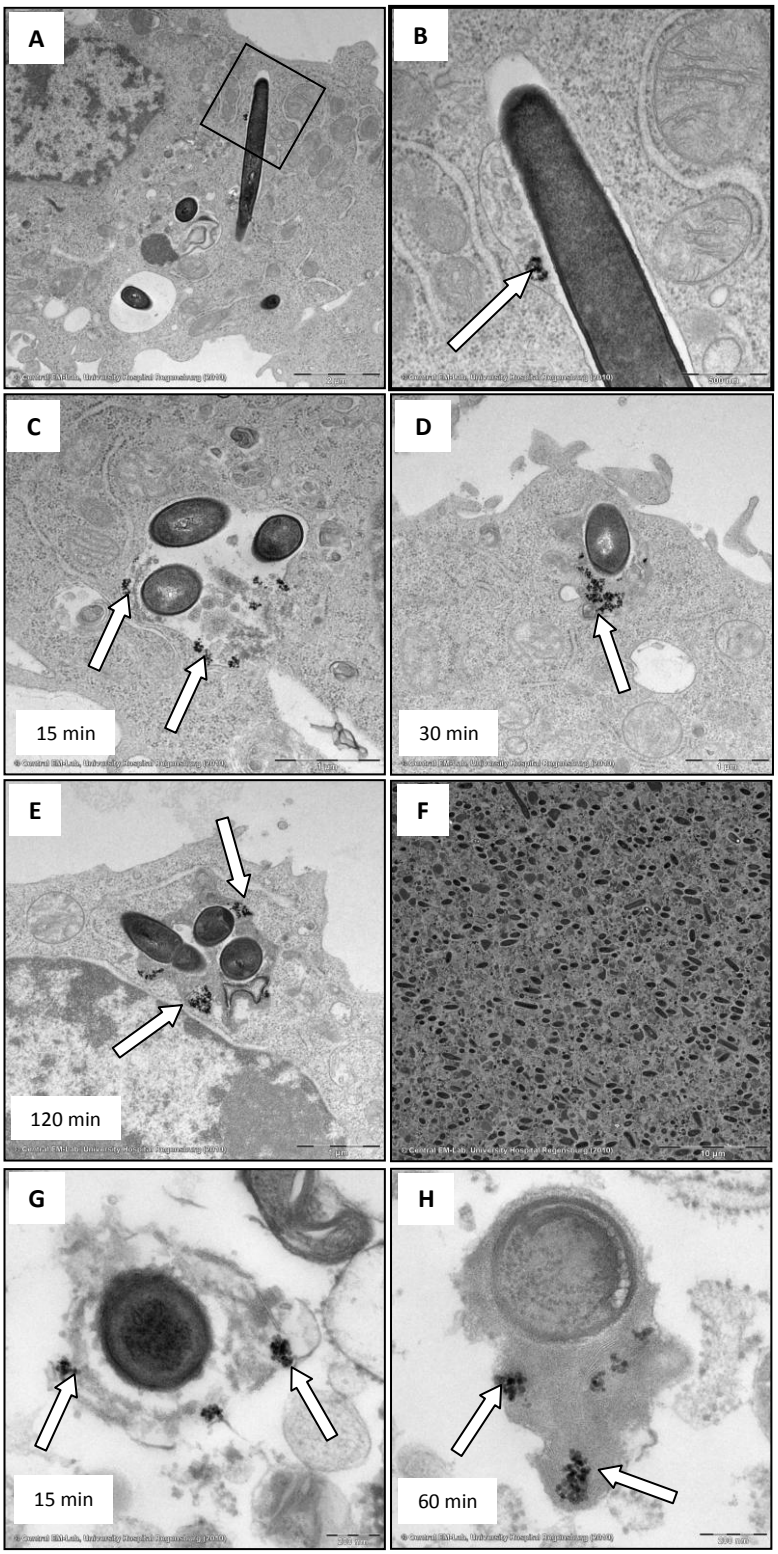

Figure 3.12: TEM of magnetically labelled Listeria monocytogenes and isolated phagosomes
In order to determine constitution of magnetically labelled L.m. and isolated phagosomes, L.m.⊿hly was labelled with 10 µg/ml LB and streptavidin magnetic beads. J774 macrophages were infected for indicated periods of time. ***A)-E)*** *Cells were centrifuged for 10 min 2000 x rpm and the pellet was prepared for electron microscopy with Karnovsky´s fixative. Magnetic label is on the surface of the bacteria.* ***F)-H)*** *Infected cells were softly disrupted by sonication and phagosomes isolated in the magnetic chamber as described in 3.3. The magnetic fraction was centrifuged for 15 min with 15000 x g and the pellet was fixated for electron microscopy as described above.*

3.3.5. Protein distribution after phagosome separation

The established protocol for isolation of *L.m.*-containing phagosomes was finally used to examine particular phagosomal proteins. During the phagosomal separation process, four different fractions are gained: the lysate, the postnuclear supernatant (PNS), the non magnetic fraction (NM) and the magnetic fraction (M) (see 3.3). The lysate consists of whole cells infected with the pathogen, the PNS is obtained after sonication, the NM emerges from the washing step in the magnetic chamber and the M is the final fraction released from the magnet. All of these fractions reflect different stages of the purification process and show various proteins in different intensities in Western blot, which can be used to determine the purity of fractions and the success of phagosomal isolation. Western blot analysis revealed the protein composition of bacteria containing phagosomes obtained from IFNγ treated J774 macrophages, 120 min p.i. (figure 3.13). In order to compare these fractions, every lane was loaded with the same amount of protein (8 µg). In accordance with the TEM data (figure 3.12F), the high enrichment of bacteria containing phagosomes in the magnetic fraction could be confirmed at a molecular level. This is indicated by the high intensity of *L.m.* specific protein in comparison to the faint intensity in the three other fractions (lysate, PNS and NM). Since TNF-R1 was thought to be a component of *L.m*.-containing phagosomes, the receptor was also detectable with a specific antibody in the magnetic fraction, supporting previous data displayed in this work (see 3.2). Notably, the antibody against mTNF-R1 detected two lanes of similar molecular weight, the upper lane representing the specific band. This finding was confirmed by immunoprecipitation and Western blot of cell lysates from TNF-R1 knockout macrophages. As phagosomes undergo maturation process, several different marker proteins appear, indicating the maturation stage of the phagosome. For details see 1.3.4. Early markers such as the protein EEA1 (**E**arly **E**ndosome **A**ntigen **1)** were not detectable in a late phase of infection (two hours p.i.). However, small GTPases like Rab5 and Rab7 were enriched in the magnetic fraction. Late endosomal maker LAMP1 and activated aspartyl protease CTSD were also detectable in higher amounts, suggesting fusion events with vesicles of the *trans*-Golgi network (TGN). The IFNγ inducible GTPase LRG-47 which has been described as an important protein in mediating resistance to *L.m.* (Collazo *et al.*, 2001), also appeared in enhanced intensity. Another IFNγ-inducible protein, the **i**nducible **n**itric **o**xide **s**ynthase (iNOS) was hardly detectable in any fraction. The protein nucleoporin p62 (Nu p62) was used as quality indicator, not expecting to find any nuclear protein in phagosomal compartments. For the same purpose, glycogen synthase kinase-3 β (GSK3β) was used as a representative cytoplasmatic soluble protein and also should not be involved in the phagosomal maturation process. Both proteins were considerably diminished in the magnetic fraction. These data demonstrate the specificity of the new method to characterise the protein composition of phagosomes. Confocal microscopy was used to confirm and

visualize the Western blot data by monitoring two proteins of the early (figure 3.14A) and late (figure 3.14B) phase of phagosomal maturation, respectively. EEA1 (green) is detected 15 min p.i. surrounding the bacterium (red) and Rab5 (green) also colocalises with *L.m*. (red) during the early phase of infection. In this work, GFP-expressing *L.m.* were generated to study the recruitment of lysosomal marker proteins to the phagosomes. LAMP1 was shown to appear on *L.m*.-containing phagosomes during the late phase of infection (60 min p.i.), representing the phagolysosomal compartment.

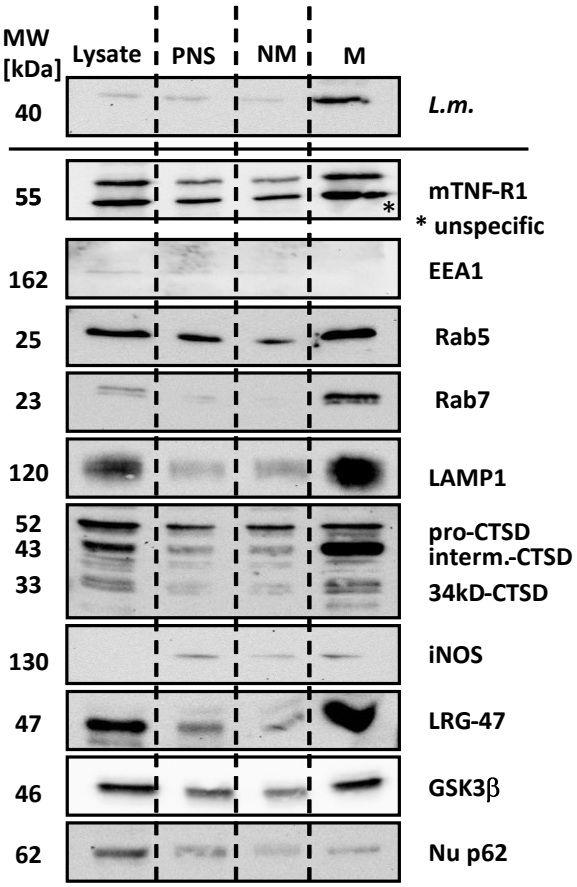

Figure 3.13: Western blot analysis of isolated phagosomes
In order to determine protein composition of isolated phagosomes, J774 macrophages were stimulated with 500 U/ml rmIFNγ and infected at a MOI 10 with magnetically labelled L.m (Δhly) for 120 min. Cells were softly disrupted by sonication and prepared for magnetic separation as described in 3.3. All fractions were collected and prepared for Western blot analysis. Every lane was loaded with 8 µg of total protein to compare protein composition. PNS = post nuclear supernatant, NM = non magnetic fraction; M = magnetic fraction; CTSD = cathepsin D; Nu p62 = Nucleoporin p62; GSK3β = Glycogen synthase kinase-3β; MW = molecular weight; kDa = Kilodalton

A)

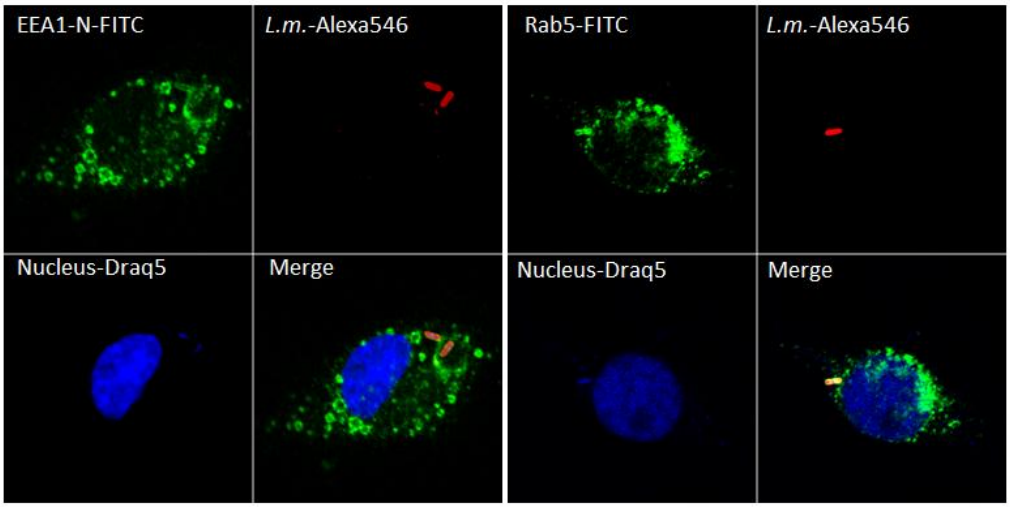

B)

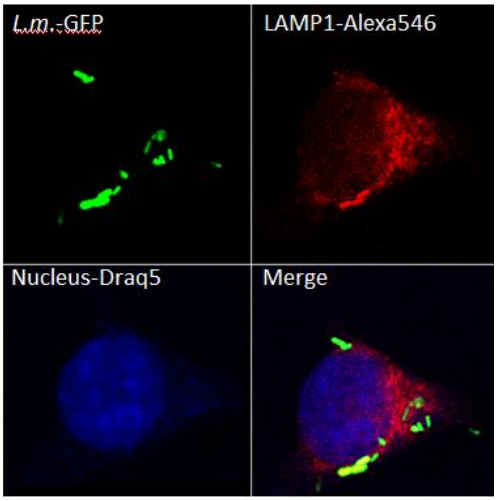

Figure 3.14: Confocal microscopic analysis of phagosomal proteins

In order to monitor protein recruitment to L.m.-containing phagosomes, J774 macrophages were seeded on coverslips and infected at a MOI 3 with EGDe wild-type strain. Cells were fixed with 2 % paraformaldehyde and permeabilised with 0,1 % Triton X-100 for intracellular staining. ***A)*** *Cells were monitored 15 min p.i. Nuclei: Draq5 (blue); L.m.: Alexa 594 (red) and EEA1/Rab5: FITC (green).*

B) *Cells were infected with GFP expressing L.m. (EGDe) at a MOI 3 and incubated for 60 min. Cells were prepared for immunofluorescence staining as described above. L.m.: GFP (green); LAMP1: Alexa546 (red).*

3.4. Phagocytosis of *Listeria monocytogenes* by J774 macrophages - the influence of cytokines to protein composition of phagosomes

During infection, the phagosomal maturation process is driven by recruitment of different proteins and fusion events. This can either be influenced by cytokines released from the host or by the phagocytosed pathogen itself in order to evade the phagolysosomal compartment. The new isolation protocol was used to examine alteration in protein composition on the phagosomal compartment during its maturation process. Different time points after infection and influences of different stimuli on components of endocytic trafficking were monitored. To study the time specific changes, *L.m.*-containing phagosomes at four different time points (15, 30, 60 and 120 min) p.i, were isolated and analysed by Western blot. In order to control the experimental settings, samples before magnetic isolation PNS were compared to samples of the magnetic fraction. Samples of unstimulated (**A**), TNFα stimulated (**B**), IFNγ (**C**) and double IFNγ-TNFα stimulated (**D**) J774 macrophages infected with *L.m.*Δhly were analysed (figure 3.15). All lanes were loaded with the same amount of protein (8 µg) to obtain comparable conditions.

The high enrichment of *L.m.*-specific protein in the magnetic fraction demonstrated the successful isolation of bacteria-containing phagosomes and this remained rather unchanged for all performed assays, regardless of any stimulation condition. Remarkably, unstimulated cells (figure 3.15A) showed a time-dependent enrichment of mTNF-R1 in magnetic fraction, which probably reflects the previous shown fusion events of TNF-R1-receptosomes with the phagosome. However, TNFα-release first needs to be induced (see 3.1), which in consequence may lead to the delayed internalisation and recruitment of TNF-R1 to the phagosome. TNFα stimulated cells, by contrast, differ from untreated cells in terms of composition of TNF-R1 on the phagosomal compartment (figure 3.15B). The magnetic fraction at 15 min p.i. showed identical quantities of mTNF-R1 protein as the magnetic fraction at 120 min p.i. This is likely due to the presence of high amounts of TNFα from the beginning of infection and simultaneous onset of TNF-R1 internalisation. Comparable to TNFα stimulated macrophages, IFNγ treated macrophages indicated similar amounts of TNF-R1 on the magnetic fraction, with no time-dependent delay of recruitment. IFNγ is known to enhance TNFα release upon infection and this was also demonstrated in this work (see 3.1). Probably sufficient amounts of TNFα were produced to start internalisation of TNF-R1 very early during infection. In general, double stimulation with IFNγ -TNFα exhibited no differences to IFNγ stimulated macrophages. Nevertheless, specific recruitment of TNF-R1 to the phagosome seemed to be a consistent event during infection, suggesting that TNF-R1-signalling contributes to bacterial fate in the phagosomal compartment.

The small GTPases Rab5 and Rab7 which regulate endocytic trafficking were also found in high amounts in the magnetic fraction. Rab5 is known to be a representative of early phagosomes and

Rab7 of late ones. Surprisingly, no time specific alteration of intensity was recognisable, irrespective of any treatment. Markers of the phagolysosomal compartment such as LAMP1 were also found as early as 15 min p.i. with no changes in later time points. It is not yet clear why these markers accumulate at these time points. Previous of work of Sturgill-Koszycki found similar early recruitment of LAMP1 in IgG-bead containing phagosomes (Sturgill-Koszycki *et al.*, 1996). The aspartyl-protease CTSD appears in three forms, comprising pro-CTSD (53 kDa), the intermediate form (43 kDa) and the 34 kDa mature form which represents the activated protease (described in 1.3.5). Cytokine specific effects on the activation-status of CTSD were striking. Cytokine treated macrophages seemed to induce processing of CTSD, indicated by arising of the mature 34 kDa form. Most surprisingly, TNFα stimulation alone was also sufficient to induce CTSD activation (Figure 3.16A). Furthermore, time-dependent increase of both intermediate and activated forms in the phagosome containing sample (magnetic fraction) may indicate cytokine involvement, in particular TNFα, to CTSD activation. This correlation between cytokine dependent presence of TNF-R1 on the phagosome and specific CTSD activation raises the assumption that signalling events via TNF-R1 may contribute to this. LRG-47 is a recently discovered GTPase suggested to be involved in bactericidal processes. It is an IFNγ responsive protein and was found only on IFNγ treated macrophages, demonstrating the applicability of this novel approach to monitor cytokine specific effects on phagosomes. The purity of all fractions was controlled by the detection of the nuclear protein nucleoporin p62 and the cytoplasmatic protein GSK3β. In all isolated magnetic samples these proteins disappeared or were at least considerably diminished compared to the PNS samples, indicating the purity of the magnetic fractions.

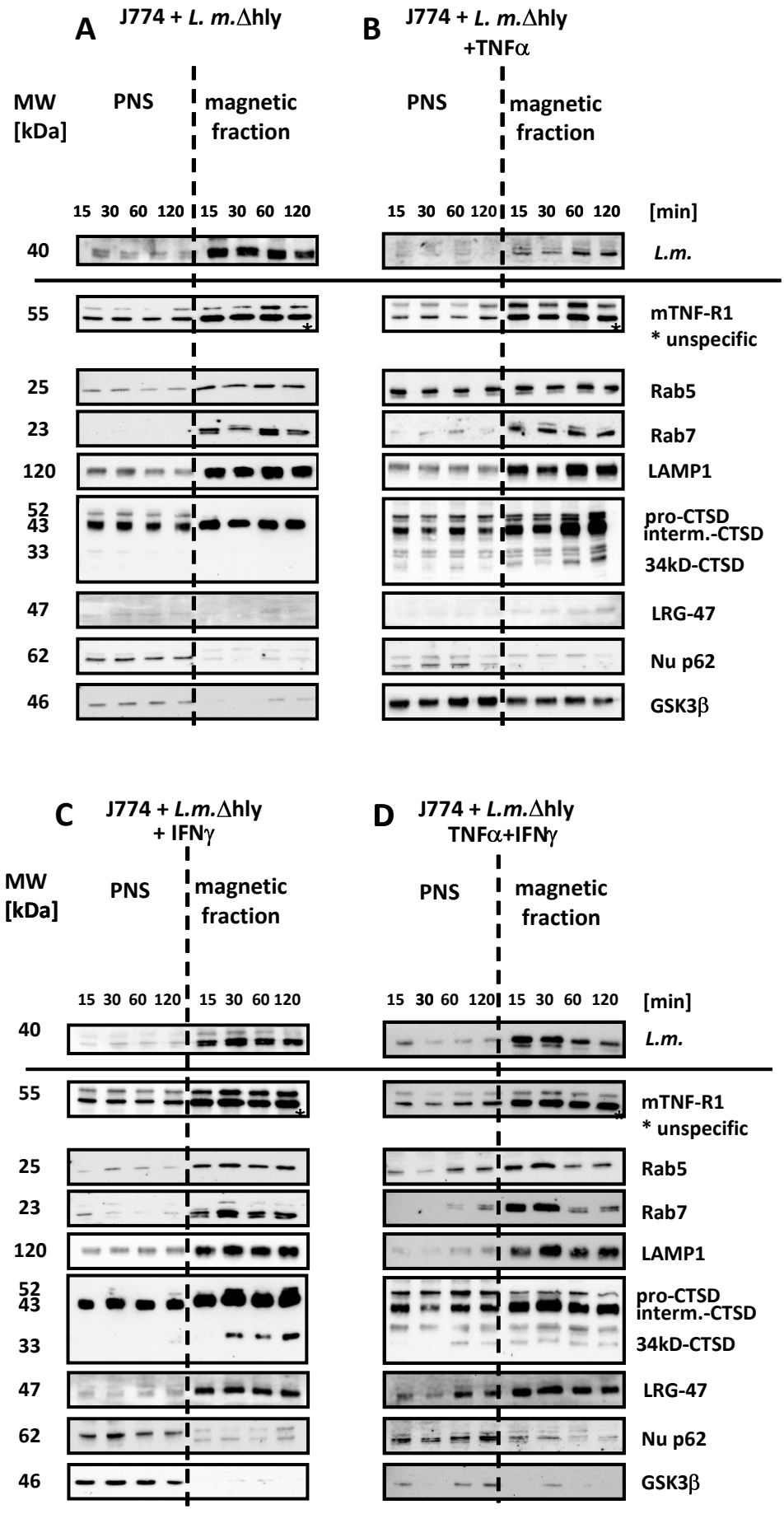
A
J774 + L. m.Δhly
MW [kDa]
PNS
magnetic fraction
15 30 60 120 15 30 60 120
40
55
25
23
120
52
43
33
47
62
46
L.m.
mTNF-R1
* unspecific
Rab5
Rab7
LAMP1
pro-CTSD
interm.-CTSD
34kD-CTSD
LRG-47
Nu p62
GSK3β
B
J774 + L. m.Δhly +TNFα
PNS
magnetic fraction
15 30 60 120 15 30 60 120
[min]
C
J774 + L.m.Δhly + IFNγ
D
J774 + L.m.Δhly TNFα+IFNγ

Figure 3.15 (on previous page): Western blot analysis of isolated phagosomes under different cytokine stimulations
In order to monitor protein composition of phagosomes, J774 macrophages were seeded on 10 cm cell culture dishes. ***A)*** *Cells were not treated.* ***B)*** *Cells were stimulated with 100 ng/ml rhTNFα during infection.* ***C)*** *Cells were pre-incubated with 500 U/ml rmIFNγ overnight and* ***D)*** *Cells were pre-incubated with 500 U/ml rmIFNγ overnight and stimulated with 100 ng/ml rhTNFα during infection. All cells were infected at a MOI 10 with magnetically labelled L.m (Δhly) for indicated time periods (15, 30, 60 and 120 minutes). Cells were then softly disrupted by sonication and prepared for magnetic separation as described in 3.3. All fractions were collected and prepared for Western blot analysis. Every lane was loaded with 8 µg of total protein to compare protein composition. One representative out of three individual preparations for each stimulation and time point is shown. PNS = post nuclear supernatant; CTSD = cathepsin D; Nu p62 = Nucleoporin p62; GSK3β = Glycogen synthase kinase-3β; MW = molecular weight; kDa = Kilodalton*

3.5. Tumor necrosis factor Receptor 1 - a new component of the *Listeria monocytogenes*-containing phagosome

Based on the results presented in the preceding chapters, it seemed likely that TNF-R1-containing vesicles fuse with *L.m.*-containing phagosomes upon TNFα stimulation. In order to confirm this new result and demonstrate the importance of TNF-R1 internalisation, another experiment was performed to prove the existence of this combined compartment. TNF-R1 complexes were magnetically isolated out of *L.m.* infected macrophages and these samples were analysed for the presence of *L.m.* To ensure that fusion events arise in consequence of TNF-R1 internalisation, bacterial uptake and ligand binding to the receptor were performed in sequential order. J774 macrophages were exposed to *L.m.*Δhly for 10 min and phagocytosis was stopped by shift to 4°C, preparing cells for magnetic labelling of TNF-R1. Subsequently, ligand based labelling with Biotin-TNFα and Streptavidin (SA)-magnetic beads was applied to render magnetic receptor-isolation via the custom-built magnetic chamber. After bacterial uptake (10 min p.i.), TNF-R1 internalisation was initiated by shifting the cells to 37°C. The internalisation process of 60 min duration was halted by moving cells to 4°C.

In order to exclude unspecific engulfment of magnetic particles by macrophages and to ensure that only compartments with magnetic TNF-R1 were isolated, a control experiment was performed, as follows. *L.m* infected macrophages were incubated 60 minutes at 4°C with magnetic beads alone. Cells were washed twice with PBS to remove unbound particles and cells were subsequently shifted to 37°C for 60 min in order to see whether unspecific uptake of magnetic particles occurred. These cells were further prepared for vesicle isolation. The protein composition of these magnetically isolated TNF-R1 containing compartments and fractions of the control experiment were analysed by Western blot (figure 3.16 right and left, respectively). In the control experiment, a magnetic fraction (M) could not be isolated, so unspecific engulfment of magnetic particles was excluded. The successful isolation of TNF-R1 complexes was confirmed by detection of enriched mTNF-R1 specific protein in the magnetic fraction compared to amounts in lysate, PNS and NM. The appearance of

L.m. specific protein in magnetic fraction validated the specific compartment of *L.m.*-containing phagosome and TNF-R1, underlining the results of several other techniques used in this work. Furthermore, this experiment suggested that internalisation is an indispensable event for recruitment of TNF-R1 to the bacteria-containing phagosome. Concomitantly, enrichment of phagosomal marker protein Rab7 in the magnetic fraction identified these isolated TNF-R1-contaning complexes as vesicles. Most notably, only in this fraction the mature active form of CTSD (34 kDa form) was detectable. These data correspond perfectly to the observation of TNFα mediated CTSD activation, already presented in 3.3.6. A correlation between CTSD activation and specific recruitment of TNF-R1 to the bacteria-containing phagosome seems to be likely.

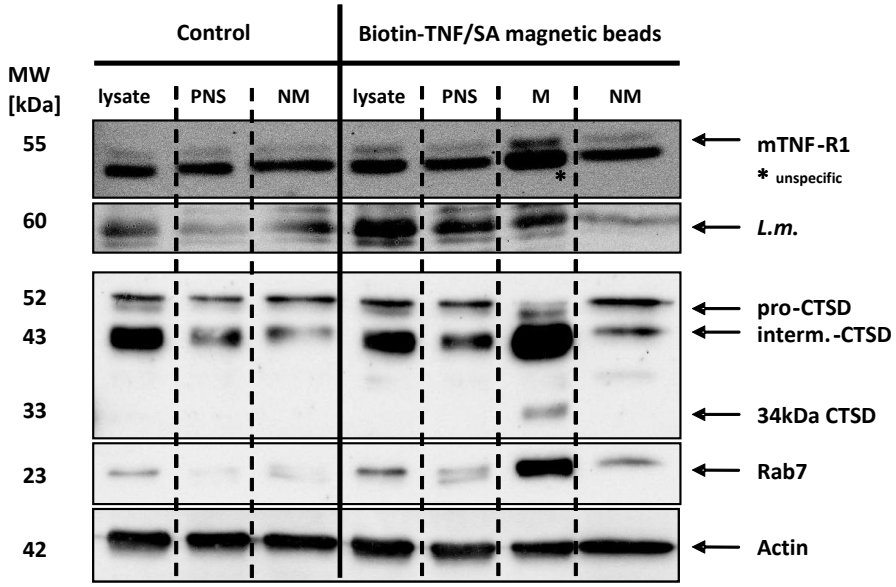

Figure 3.16: Isolation of mTNF-R1 containing compartments
Magnetically isolated TNF-R1-receptosomes of J774 macrophages were analysed. Cells were seeded on 10 cm cell culture dish and could adhere overnight. Macrophages were then infected at a MOI 10 with L.m.⊿hly for 10 min. Phagocytosis was stopped by shifting to 4°C. Biotin-rhTNFα (200 ng) and SA-magnetic beads (20 ng) were pre-incubated for 60 min. These complexes could bind to TNF-R1 for another 60 min at 4°C. Cells were washed twice with 10 ml PBS to remove unbound complexes. Internalisation was started by shifting to 37°C and terminated after 60 minutes by reverting to 4°C. Control cells were incubated with 20 ng magnetic beads for 60 min at 4°C and washed twice with 10 ml PBS. Cells were moved to 37°C for 60 min and phagocytosis was terminated by shift to 4°C. Both samples were prepared for magnetic isolation as described previously. Every lane was loaded with 8 µg of total protein to compare protein composition. Actin was used as loading control. Lysate = whole cell lysate; PNS = post nuclear supernatant; NM = non magnetic fraction; M = magnetic fraction; CTSD = cathepsin D; MW = molecular weight; kDa = kilodalton.

3.6. Contribution of TNF-R1 signalling to primary macrophages

The findings described above regarding TNF-R1 implied to perform experiments with TNF-R1 knockout macrophages (BMDM TNF-R1$^{-/-}$). Control experiments were initially performed with primary **b**one **m**arrow **d**erived **m**acrophages (BMDM) from wild-type mice (WT). Additionally, bone

marrow derived macrophages from IFNγR deficient mice (BMDM IFNγR$^{-/-}$) were monitored in order to separate specific effects caused by IFNγ from those of TNFα.

3.6.1. Bacterial propagation in wild-type macrophages - the role of TNFα and IFNγ for infection control

To validate the cytokine specific effects raised in J774 macrophages, BMDM from wild-type mice were generated and infected with *L.m*. strain EGDe. The bacterial propagation was monitored over a time period of eight hours. Similar to J774 macrophages, bacterial growth was not altered by TNFα stimulation. By contrast, IFNγ stimulation of macrophages restricted the pathogen in growth and double stimulation (IFNγ-TNFα) could not enhance any listericidal properties of these primary macrophages either (figure 3.17A). However, the effect of IFNγ was more distinct compared to J774 macrophages and showed statistical significance ($p<0.001$). When monitoring bacterial increase eight hours p.i., TNFα stimulation allowed up to 3-4-fold higher increase of bacterial number than IFNγ stimulated cells. Double stimulation of cells resulted in a slow growth of bacteria, comparable to in IFNγ stimulated cells (figure 3.17B). To analyse autocrine TNFα release, the amount of present TNFα during different time periods of infection was measured by ELISA specific to mouse TNFα (figure 3.18). Both strains of *L.m.* (EGDe and Δhly) induced production of almost equal amounts of TNFα, which differs from infected J774 macrophages. Compared to the mutant strain, EGDe induced an elevated release in J774 macrophages (see figure 3.2). However, the permanent presence of TNFα upon IFNγ stimulation and during infection complicates the examination of TNFα specific impact to the bacterial eradication process. Experiments in TNF-R1 deficient macrophages will enlighten the specific effects of these two cytokines in more detail (see 3.6.3).

Confocal microscopy was used to control bacterial translocation into the cytoplasm as an indication of growth impairment in these primary cells. Monitoring an early time point p.i. (30 min) demonstrated that all cells were infected under equal conditions, as all cells contained the same bacterial load at the beginning (figure 3.19). Monitoring the time point 120 min p.i. revealed the cytokine based effects on the life cycle of *L.m.* The green phalloidin-staining indicates that bacteria could escape from the phagosome and are still capable to replicate. Bacteria stained in red are inhibited to evade the phagosome and probably stay there for degradation. Unstimulated (Medium) and TNFα treated cells allowed phagosomal escape of *L.m*. (red bacteria with green actin tail), whereas IFNγ and combination of IFNγ and TNFα effectively prevented bacterial escape into the cytoplasm. In these cells there was no evidence of bacterial actin polymerisation, only red bacteria were observable. These findings correlate with those observed in J774 macrophages.

A)

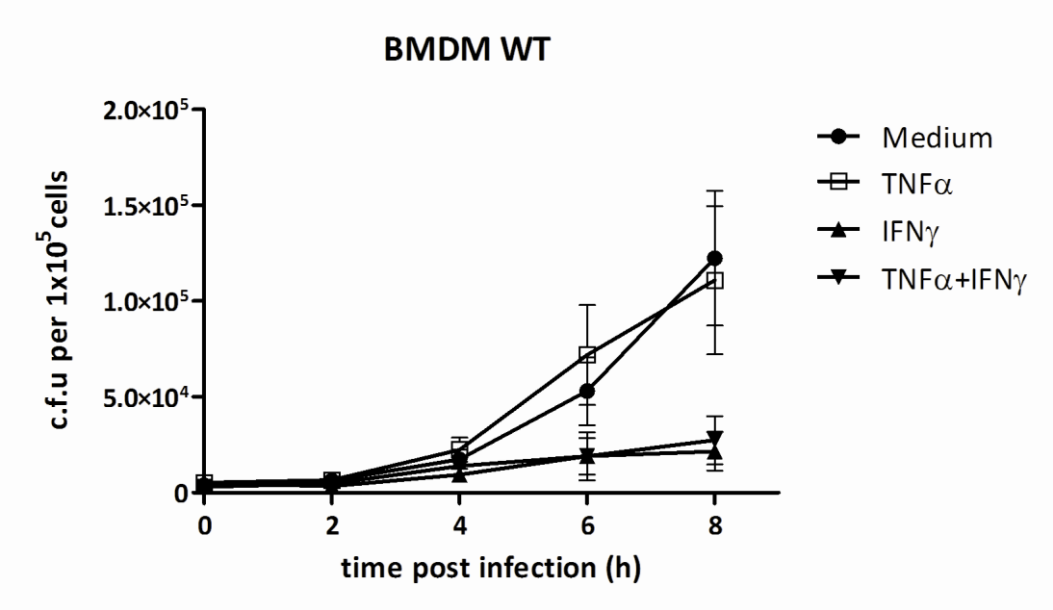

B)

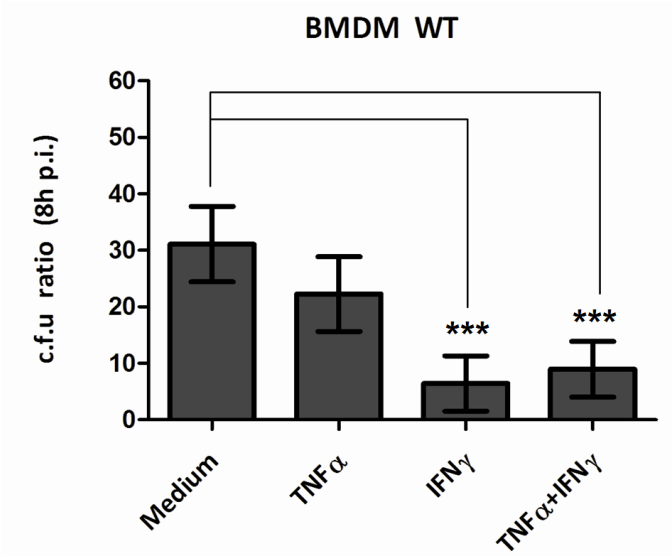

Figure 3.17 : Growth of Listeria monocytogenes in BMDM WT under different cytokine stimulations
Growth of L.m. in BMDM WT was monitored. Cells were infected with wild-type strain EGDe at a MOI 0.1 and incubated with rmIFNγ (500 U/ml) overnight. At the time of infection, rhTNFα (100ng/ml) was added and was present at all times. A short incubation with gentamycin (30 min, 50 µg/ml) removed extracellular bacteria. Cells were washed three times and shifted to 37°C for the indicated time periods. The cells (5x10^4 per well) were lysed at each time point shown and serial dilutions were plated to obtain the c.f.u.; BMDM = bone marrow derived macrophages; WT = wild-type
A) *Bacterial load at all indicated time points of infection is shown. Data points represent means from three individual experiments ± SD.*
B) *Bacterial growth restriction was monitored under different cytokine conditions. Data represent means and SD of three individual experiments. Means are shown as the ratio of c.f.u at 8h to c.f.u at 0h ± SD; ***P<0.001*

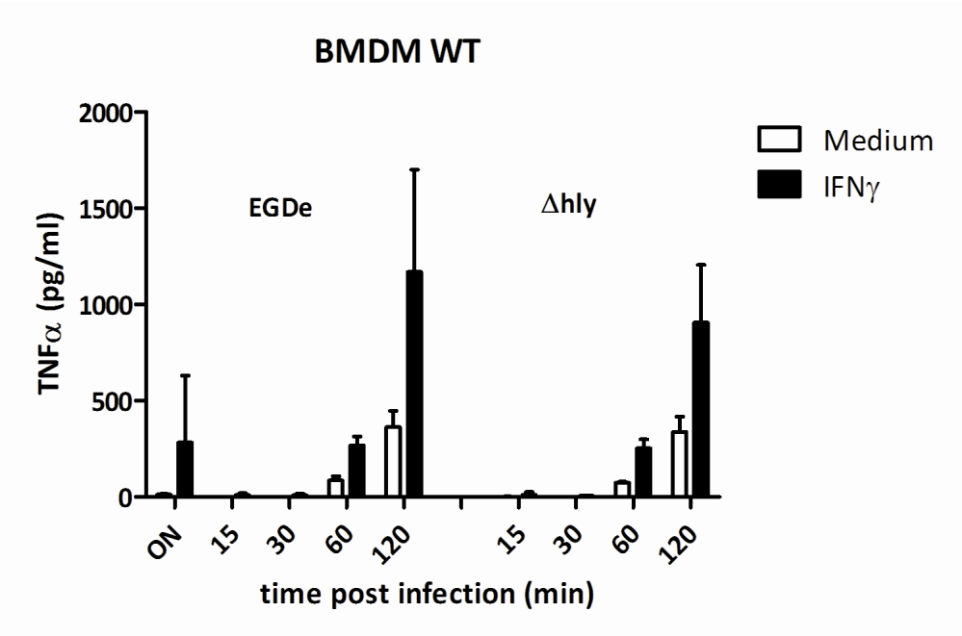

Figure 3.18: TNFα -secretion of BMDM WT during infection with Listeria monocytogenes
TNFα production during infection was monitored. BMDM WT were stimulated with or without rmIFNγ (200 U/ml) overnight (ON) and supplemented with new medium for infection. Cells were infected at a MOI 3 with the wild-type strain EGDe and the hemolysin-negative mutant Δhly. To analyze the amount of TNFα, supernatants were harvested at the indicated time points p.i. TNFα amounts were determined with an ELISA specific to mouse-TNFα. Data represent means and SD of three individual experiments. BMDM = bone marrow derived macrophages; WT = wild-type

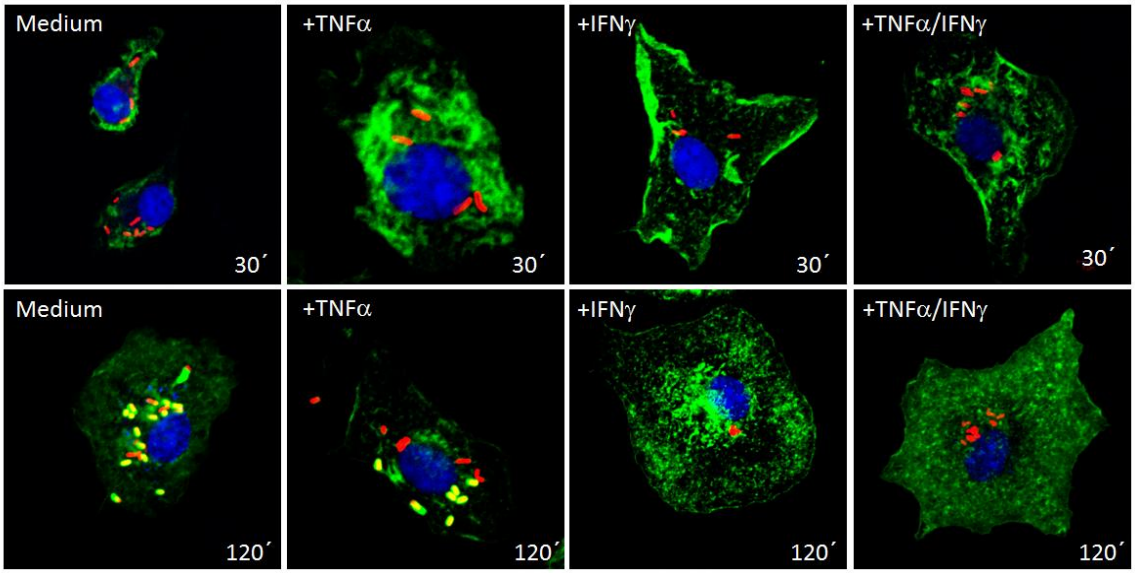

Figure 3.19: Confocal microscopy of Listeria monocytogenes in BMDM WT
Actin polymerisation of L.m. in BMDM WT was monitored. Cells were seeded on coverslips and stimulated with or without rmIFNγ (200 U/ml) overnight. At the time of infection rhTNFα (100 ng/ml) was added. Cells were infected at a MOI 3 with the wild-type strain EGDe for indicated time periods. Cells were fixed 2 % with paraformaldehyde for 15 min, preparing them for immunofluorescence staining. To obtain intracellular staining, cells were permeabilised with 0.1 % Triton X-100. Nuclei: Draq5 (blue); Actin: phalloidin-FITC (green); L.m.: Alexa546 (red). BMDM = bone marrow derived macrophages; WT = wild-type

3.6.2. The influence of cytokines to the protein composition of phagosomes from wild-type macrophages

The phagosomal protein composition of primary macrophages was analysed using the new phagosome isolation protocol. Specific alterations of proteins of the phagosomal maturation process were examined by Western blot. In order to illustrate the dynamics of intracellular trafficking during infection, components of early and late stages of phagosome maturation were examined, similar to experiments with J774 macrophages (see 3.4). Unstimulated (**A**) TNFα stimulated (**B**) and IFNγ stimulated (**C**) wild-type macrophages were exposed to the mutant strain *L.m.*Δhly for indicated periods of time and prepared for phagosomal isolation. Western blot analysis of PNS and magnetic fraction showed enrichment of *L.m.* specific protein, indicating successful solation of *L.m.*-containing phagosomes. The comparison of PNS to the magnetic fraction gave evidence for this (figure 3.20). Regarding TNF-R1 however, slight differences to J774 macrophages could be observed. TNF-R1 seems to appear irrespective of any cytokine treatment very early and with no alteration in amount on the phagosomal compartment. Nevertheless, in bone marrow derived macrophages TNF-R1 was shown to be a component of the phagosomal compartment, confirming our previous data (see 3.4 and 3.5). Markers which have been reported to indicate endocytic maturation stages were not altered as a consequence of phagocytosis duration. The early endosomal marker Rab5 and the markers Rab7 and LAMP1, both constituents of the late phagosome, showed no changes in amounts at different time points p.i. This correlates with data from J774 macrophages (see 3.4). Regarding CTSD, however, differences to J774 macrophages appeared. Unstimulated macrophages showed CTSD activation, indicated by the evidence of the 34 kDa active form in the magnetic fraction. This was similar to TNFα and IFNγ treated cells and a consistent increase of processed CTSD from early to late time points p.i. can be observed, disregardless to any stimulation condition. Whether this was due to fusion events with lysosomes containing mature CTSD or to a direct processing on the phagosome cannot be discerned.

The IFNγ inducible GTPase LRG-47 was only evident in the IFNγ treated macrophages and purity control markers nucleoporin p62 and GSK3β appeared in the magnetic fraction compared to PNS in less intensity. Taken together, these data differ from the findings in J774 macrophages. In primary macrophages CTSD activation did not seem to be cytokine dependent induced. At this point it is worth noting that these primary cells control bacterial propagation better than J774 macrophages. This fact may explain the differences that arose in the experiments with primary cells as compared to the J774 cell line. Double stimulation (TNFα and IFNγ) evinced no further insights in cytokine derived effects in J774 macrophages and was therefore not determined for primary cells.

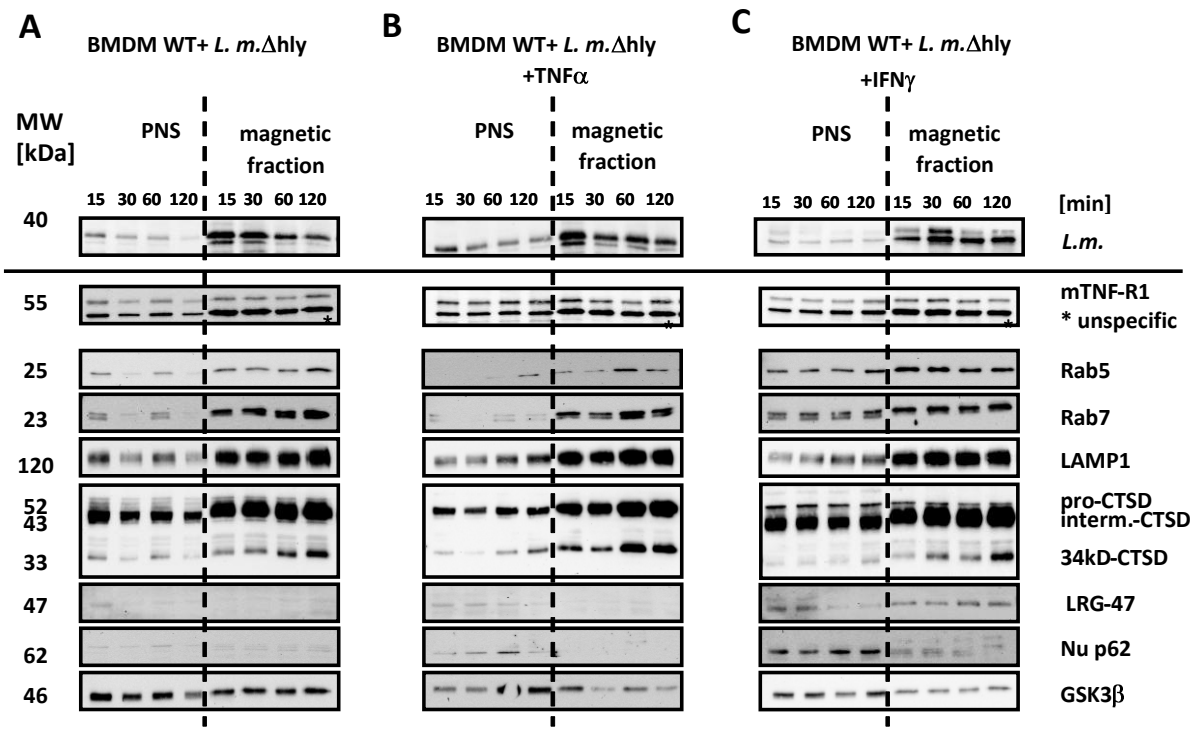

Figure 3.20: Western blot analysis of isolated phagosomes under different cytokine stimulations
Protein composition of isolated phagosomes in BMDM WT was monitored. ***A)*** *Cells were not treated.* ***B)*** *Cells were stimulated with 100ng/ml rhTNFα during infection* ***C)*** *Cells were pre-incubated with 200 U/ml rmIFNγ overnight. All cells were infected at a MOI 10 with magnetically labelled L.m.Δhly for indicated time periods (15, 30, 60 and 120 min). Cells were then softly disrupted by sonication and prepared for magnetic separation as described in 3.3. All fractions were collected and prepared for Western blot analysis. Each lane was loaded with 8 µg of total protein to compare protein composition. One representative out of two individual preparations is shown. PNS = post nuclear supernatant. BMDM = bone marrow derived macrophages; WT = wild-type; CTSD = cathepsin D; Nu p62 = Nucleoporin p62; GSK3β = Glycogen synthase kinase-3β; MW = molecular weight; kDa = Kilodalton.*

3.6.3. Bacterial infection control in TNF-R1$^{-/-}$ macrophages

Previous studies have demonstrated that TNF-R1 is an important factor for eradication of *L.m.* (Pfeffer, 1993). In order to elucidate the role of TNFα and its receptor TNF-R1 for bacterial load restriction in detail, macrophages derived from TNF-R1 deficient mice were generated. Influences of TNFα and IFNγ in limiting bacterial replication were analysed under TNF-R1 knockout conditions. These primary macrophages were exposed to the *L.m.* EGDe over eight hours in order to determinate bacterial load. In comparison to macrophages monitored thus far, a different picture arises with TNF-R1 knockout macrophages (figure 3.21A). Untreated and TNFα treated cells could not restrict pathogen growth, but IFNγ stimulation did not lead to an inhibition of bacterial replication either. Only a slight reduction of bacterial number was observed, though in less extent than in IFNγ stimulated BMDM from WT mice (see figure 3.17). This phenomenon becomes more apparent when comparing bacterial number in macrophages eight hours p.i. Only minimal, but not statistically significant differences ($p>0.05$), arose upon IFNγ treatment compared to the medium control (figure 3.21B). IFNγ mediated restriction of bacterial growth did not seem to work in absence of TNF-R1. This suggests that TNF-R1 is needed to maintain the bactericidal effect of IFNγ. Furthermore, this finding was not due to lower TNFα production in these cells. ELISA specific to mouse TNFα could show that TNF-R1$^{-/-}$ macrophages produce amounts of TNFα comparable to wild-type macrophages and that IFNγ enhanced the cytokine release upon infection (figure 3.22).

By using confocal microscopy, this loss of IFNγ mediated bacterial growth restriction was more evident. Phalloidin-staining was used as a marker for bacterial escape and *L.m.* replication capability. Pictures of 30 min time point p.i. indicate that bacterial load was equivalent at the beginning of infection. Unrestricted cytosolic invasion of *L.m.* was observed 120 min p.i., in unstimulated and TNFα stimulated TNF-R1$^{-/-}$ macrophages. Nearly all bacteria (red) carried the characteristic actin "comet tail" (green). IFNγ treated TNF-R1$^{-/-}$ macrophages indicated similar observations and inhibition of phagosomal escape was not observable. Some of the monitored bacteria were positive for actin staining, indicating their translocation into the cytoplasm (figure 3.23). IFNγ and the combination of TNFα and IFNγ was not sufficient to retain *L.m.* within the phagosome, which is likely caused by the missing TNF-R1 signalling.

A)

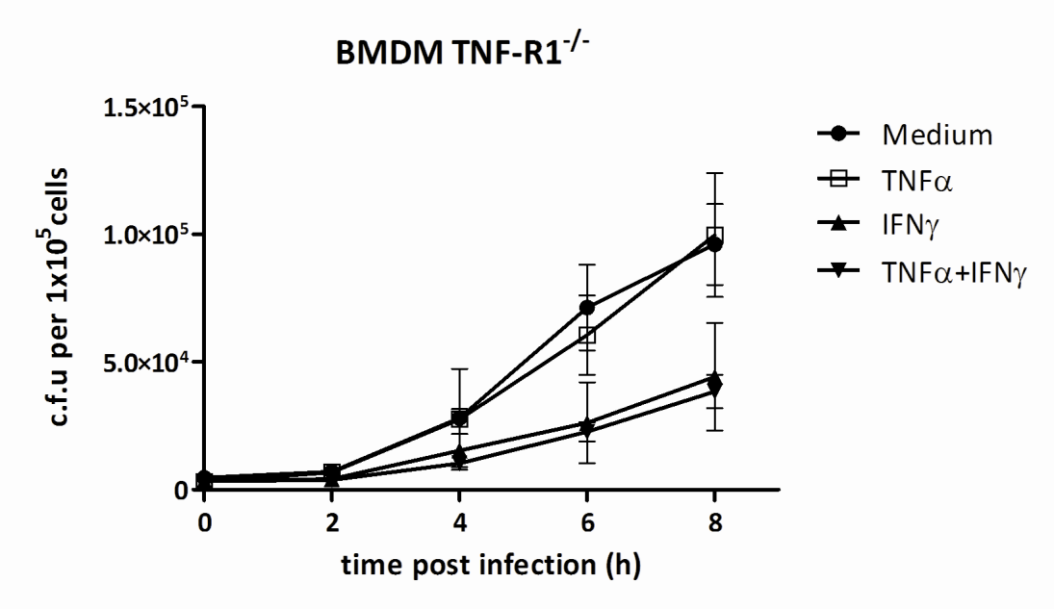

B)

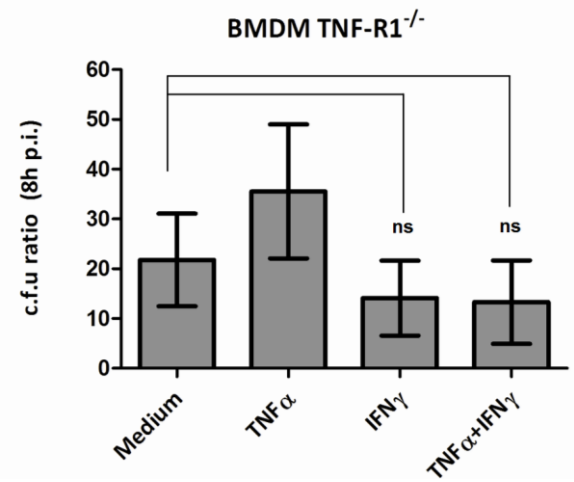

Figure 3.21: Growth of Listeria monocytogenes in BMDM TNF-R1$^{-/-}$ under different cytokine stimulations
Growth of L.m. in BMDM TNF-R1$^{-/-}$ was monitored. Macrophages were infected with wild-type strain EGDe at a MOI 0.1 and incubated with rmIFNγ (500 U/ml) overnight. At time of infection rhTNFα (100 ng/ml) was added and was present at all times. A short incubation with gentamycin (30 min, 50 µg/ml) removed extracellular bacteria. Cells were washed three times and shifted to 37°C for the indicated time periods. The cells (5x10^4 per well) were lysed at each time point shown and serial dilutions were plated to obtain the c.f.u.; BMDM = bone marrow derived macrophages
***A)** Bacterial load at all indicated time points of infection is shown. Data points represent means from three individual experiments ± SD.*
***B)** Bacterial growth restriction was monitored under different cytokine conditions. Data represent means and SD of three individual experiments. Means are shown as the ratio of c.f.u at 8h to c.f.u at 0h ± SD; ns = not significant p>0.05.*

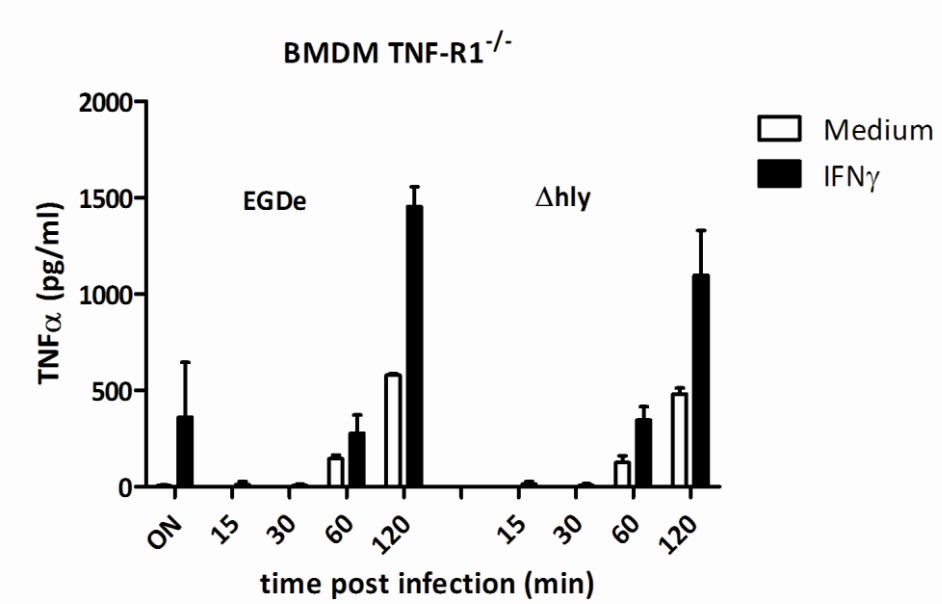

Figure 3.22: TNFα -secretion of BMDM TNF-R1$^{-/-}$ during infection with Listeria monocytogenes
TNFα production during infection was monitored. BMDM TNF-R1$^{-/-}$ were stimulated with or without rmIFNγ (200U/ml) overnight (ON) and supplemented with new medium for infection. Cells were infected at a MOI 3 with the wild-type strain EGDe and the hemolysin-negative mutant Δhly. To analyze the amount of TNFα, supernatants were harvested at the indicated time points post infection. TNFα amounts were determined with an ELISA specific to mouse-TNFα. Data represent means and SD of three independent experiments. BMDM = bone marrow derived macrophages.

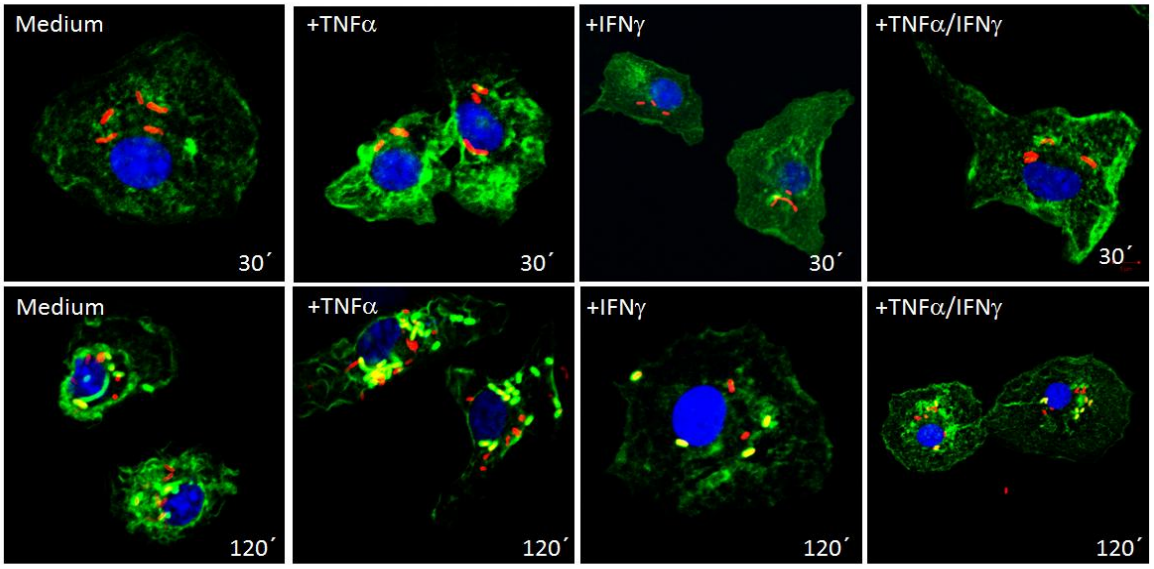

Figure 3.23: Confocal microscopy of Listeria monocytogenes in BMDM TNF-R1$^{-/-}$
Actin polymerisation of L.m. in BMDM TNF-R1$^{-/-}$ was monitored. Cells were seeded on coverslips and stimulated with or without rmIFNγ (200 U/ml) overnight. At the time of infection rhTNFα (100 ng/ml) was added. Cells were infected at a MOI 3 with the wild-type strain EGDe for indicated time periods. Cells were fixed with 2 % paraformaldehyde for 15 min, preparing them for immunofluorescence staining. To obtain intracellular staining, cells were permeabilised with 0.1 % Triton X-100. Nuclei: Draq5 (blue); Actin: phalloidin-FITC (green); L.m.: Alexa546 (red). BMDM = bone marrow derived macrophages; WT = wild-type.

3.6.4. The influence of cytokines to protein composition of phagosomes from TNF-R1$^{-/-}$ macrophages

From the data above it was clear that TNF-R1 in some way influences the phagosomal environment in IFNγ stimulated macrophages. In order to characterise phagosomes of TNF-R1 deficient macrophages biochemically, again phagosome isolation was performed using the new established protocol. Western blot analysis of PNS and the magnetic fraction after isolation revealed the specific protein composition of the isolated phagosomes at 15, 30, 60 and 120 min p.i. under different cytokine stimulations. Isolated phagosomes of unstimulated (**A**), TNFα stimulated (**B**) and IFNγ treated (**C**) macrophages from TNF-R1 deficient mice were examined by Western blot (figure 3.24). *L.m.* specific antigens were highly enriched in the magnetic fraction demonstrating efficient isolation of bacteria-containing vesicles. TNF-R1 specific protein was not detectable in any fraction, confirming the knockout status in these cells, as well as the specificity of this applied antibody for murine TNF-R1. Remarkably, the endocytic vesicle marker Rab5 seemed to be absent on phagosomes of TNF-R1 deficient macrophages and appeared only in IFNγ stimulated cells. This is very surprising because Rab5 is an important key player in phagosome-endosome fusion (Alvarez-Dominguez *et al.*, 1996), and Rab5a had been implicated in listericidal activity (Alvarez-Dominguez and Stahl, 1999; Prada-Delgado *et al.*, 2005). Additionally, Rab5a was described as an IFNγ inducible GTPase (Alvarez-Dominguez *et al.,* 1996; Prada-Delgado *et al.*, 2001), which may be the reason why Rab5 was only detectable in the IFNγ stimulated magnetic fraction. The specific antibody to Rab5 used in this work detects all isoforms (Rab5a, Rab5b and Rab5c), therefore it is possible that Rab5a might be displayed here. Until now, this seemed to be a unique effect of TNF-R1$^{-/-}$ cells in response to *L.m*. infection; therefore this might be of further interest. Late endosomal marker Rab7 and lysosomal marker LAMP1 arose with no changes in intensity, which corresponds to data with macrophages from wild-type mice. Regarding CTSD activation, similar effects to wild-type macrophages could be observed. CTSD appeared in its mature processed form (34 kDa) in all preparations, irrespective of any cytokine treatment. However, a slight increase from 15 to 120 min p.i. presumes that fusion events with vesicles containing processed CTSD may occur. Nevertheless, a TNF-R1 dependent CTSD activation in primary macrophages seems unlikely considering the data of this chapter. The IFNγ responsive GTPase LRG-47 only appeared in the magnetic fraction of IFNγ treated cells, which does not seem to be affected by the absence of TNF-R1. Nucleoporin p62 and GSK3β indicated the quality of the preparations and displayed a diminished intensity in the magnetic fraction compared to PNS.

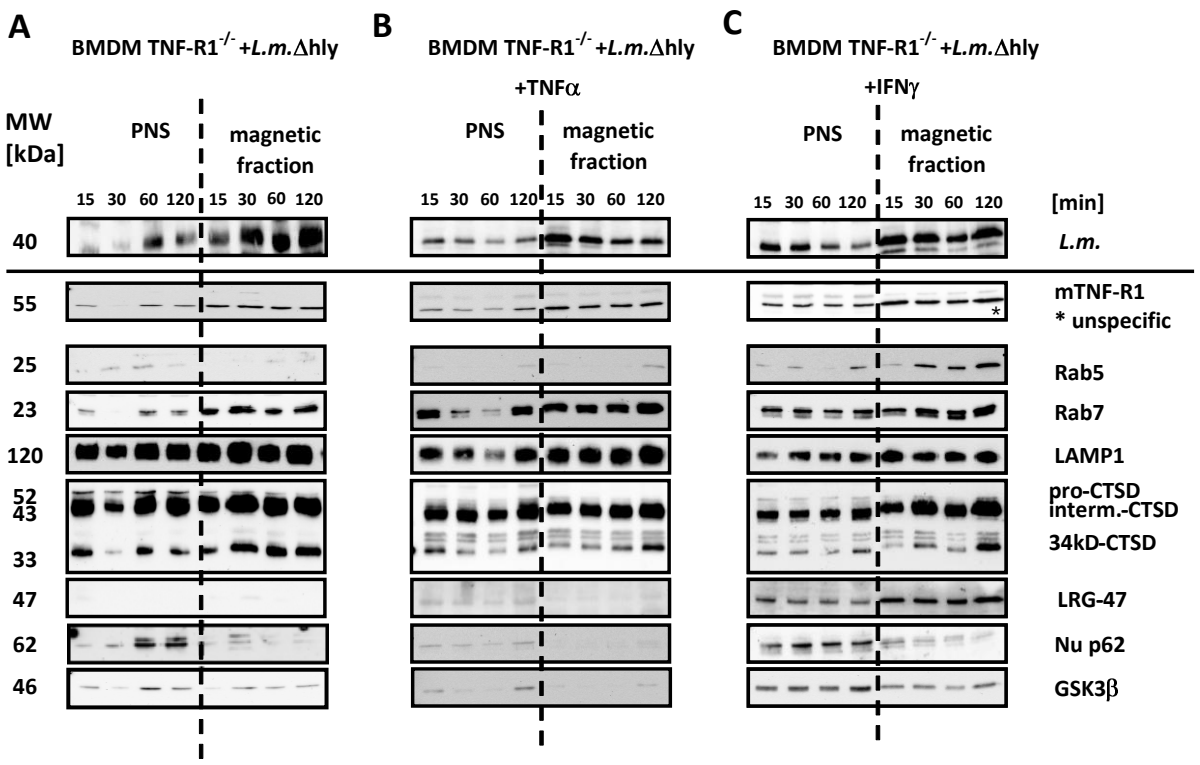

Figure 3.24 : Western blot analysis of isolated phagosomes under different cytokine stimulations
Protein composition of isolated phagosomes in BMDM TNF-R1$^{-/-}$ was monitored. ***A)*** *Cells were not treated* ***B)*** *Cells were stimulated with 100 ng/ml rhTNFα during infection* ***C)*** *Cells were pre-incubated with 200 U/ml rmIFNγ overnight. All cells were infected at a MOI 10 with magnetically labelled L.m (Δhly) for indicated time periods (15, 30, 60 and 120 minutes). Cells were then softly disrupted by sonication and prepared for magnetic separation as described in 3.3. All fractions were collected and prepared for Western blot analysis. Each lane was loaded with 8 µg of total protein to compare protein composition. One representative out of two independent preparations is shown. BMDM = bone marrow derived macrophages; PNS = post nuclear supernatant; M = magnetic fraction. CTSD = cathepsin D; Nu p62 = Nucleoporin p62, GSK3β = Glycogen synthase kinase-3β; MW = molecular weight; kDa = Kilodalton*

3.6.5. Bacterial infection control in IFNγR $^{-/-}$ macrophages

Mice lacking the IFNγ-receptor are significantly compromised in their ability to generate an effective immune response against intracellular microbes, including the pathogen *L.m.* (Huang, 1993). Interestingly, this work could show for the first time that TNF-R1 is an essential component of this IFNγ mediated restriction of listerial infection. In order to confirm IFNγ specific effects seen in the previous experiments performed with wild-type and TNF-R1$^{-/-}$ primary macrophages, macrophages from IFNγ Receptor (IFNγR) deficient mice were generated and tested for their listericidal activity. Subsequently, these macrophages were exposed to wild-type strain EGDe and their ability to control bacterial infection under cytokine treatment was monitored for over eight hours (figure 3.25). No difference arose whether cells were treated with IFNγ, TNFα or in a combination of both. The pathogen could replicate unrestricted in any case, although these cells do express TNF-R1 and can respond to TNFα stimulation. TNFα production upon infection was not impaired and the amount of

produced cytokine resembled those of TNF-R1$^{-/-}$ and wild-type macrophages. However, IFNγ treatment could not enhance the production any longer (figure 3.26). Replication ability of the pathogen was monitored in macrophages via confocal microscopy (figure 3.27). Phalloidin-based actin staining allowed the differentiation between bacteria retained within the phagosome with those that had escaped into the cytoplasm. Similar to previous data, TNFα could not retain the *L.m.* within the phagosome, resembling the medium control. In these macrophages 120 min p.i., virtually all bacteria (red) developed green actin "comet tails". Unlike wild-type macrophages, they do not respond to IFNγ treatment. This results in completely uncontrolled pathogen replication, indicated by detection of actin-positive bacteria (red bacteria with green tail). In sum, infection studies with IFNγR$^{-/-}$ macrophages confirmed that TNFα alone is insufficient for infection control and that IFNγ is essential to obtain suppression of phagosomal escape during listerial infection.

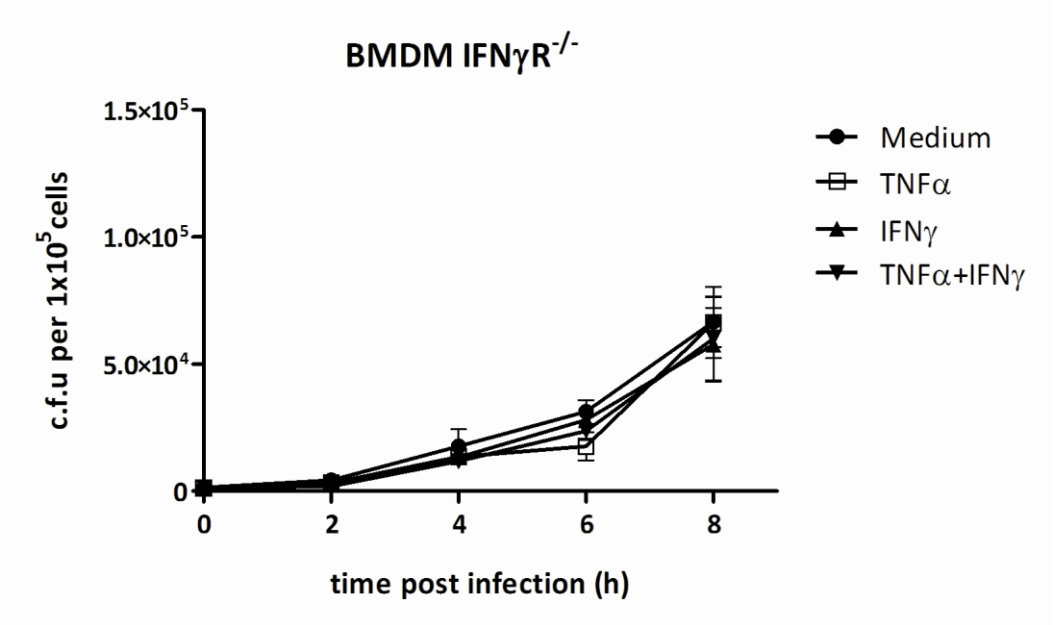

Figure 3.25: Growth of Listeria monocytogenes in BMDM IFNγR$^{-/-}$ under different cytokine stimulations
Growth of L.m. in BMDM TNF-R1$^{-/-}$ was monitored. Macrophages were infected with wild-type strain EGDe at a MOI 0.1 and incubated with rmIFNγ (500 U/ml) overnight. At time of infection rhTNFα (100 ng/ml) was added and was present at all times. A short incubation with gentamycin (30 min, 50 µg/ml) removed extracellular bacteria. Cells were washed three times and shifted to 37°C for the indicated time periods. The cells (5x10^4 per well) were lysed at each time point shown and serial dilutions were plated to obtain the c.f.u.; BMDM = bone marrow derived macrophages.

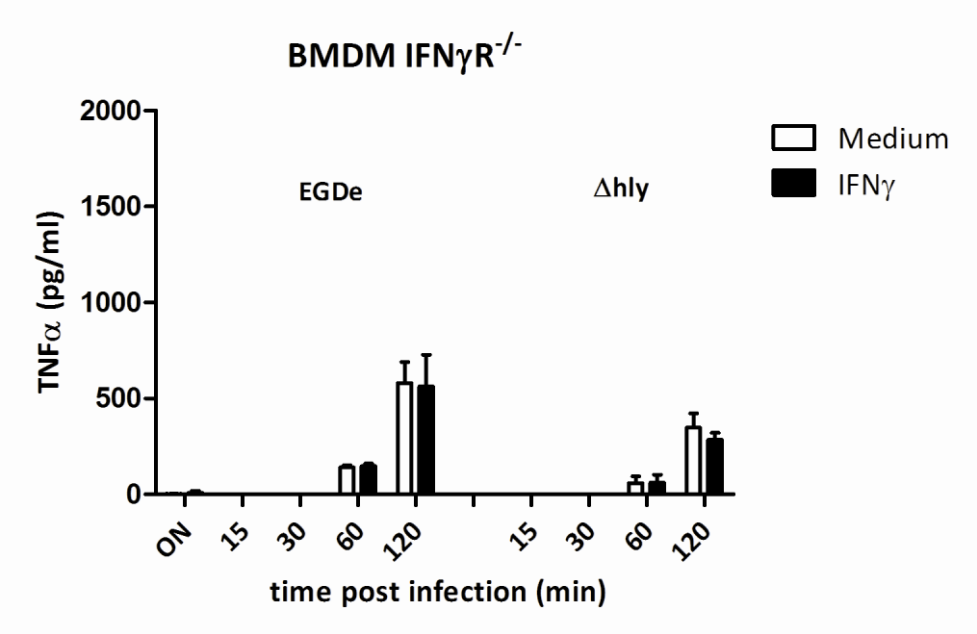

Figure 3.26: TNFα -secretion of BMDM IFNγR$^{-/-}$ during infection with Listeria monocytogenes
TNFα production during infection was monitored. BMDM IFNγR$^{-/-}$ were stimulated with or without rmIFNγ (200 U/ml) overnight (ON) and supplemented with new medium for infection. Cells were infected at a MOI 3 with the wild-type strain EGDe and the hemolysin-negative mutant Δhly. To analyse the amount of TNFα, supernatants were harvested at the indicated time points p.i. TNFα amounts were determined with an ELISA specific to mouse-TNFα. Data represent means and SD of two independent experiments. BMDM = bone marrow derived macrophages.

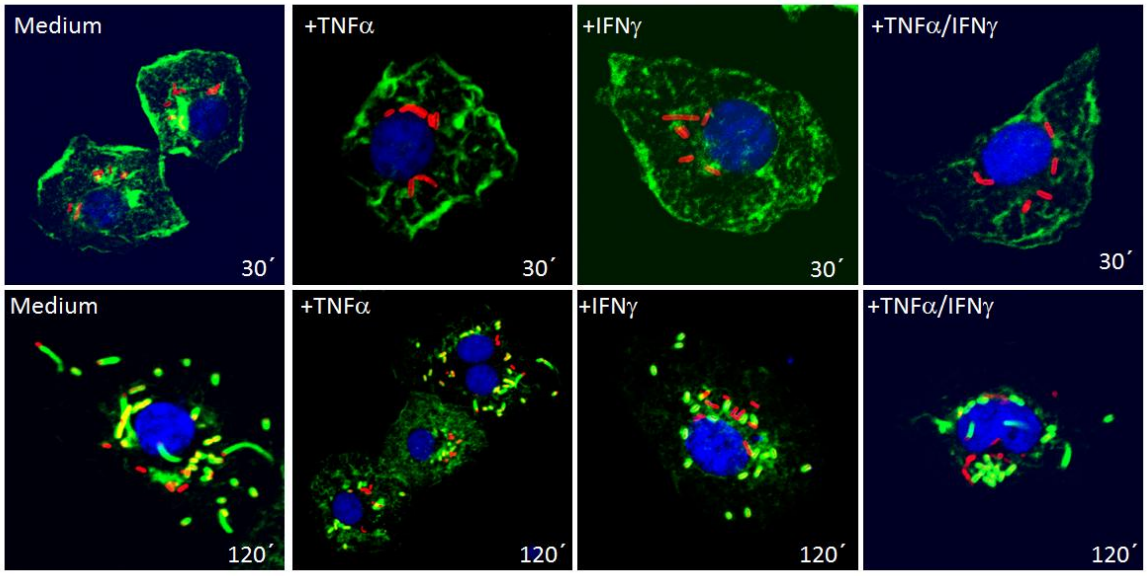

Figure 3. 27: Confocal microscopy of Listeria monocytogenes in BMDM IFNγR$^{-/-}$
Actin polymerisation of L.m. in BMDM IFNγR$^{-/-}$ was monitored. Cells were seeded on coverslips and stimulated with or without rmIFNγ (200 U/ml) overnight. At the time of infection rhTNFα (100 ng/ml) was added. Cells were infected at a MOI 3 with the wild-type strain EGDe for indicated time periods. Cells were fixed with 2 % paraformaldehyde for 15 min, preparing them for immunofluorescence staining. To obtain intracellular staining, cells were permeabilised with 0.1 % Triton X-100. Nuclei: Draq5 (blue); Actin: phalloidin-FITC (green); L.m.: Alexa546 (red). BMDM = bone marrow derived macrophages.

3.6.6. Protein composition of phagosomes from IFNγR$^{-/-}$ macrophages

In order to validate the results that arose in the previous chapters, IFNγR$^{-/-}$ macrophages were monitored for specific alteration in the protein composition of phagosomes. The novel method of phagosome isolation was used to obtain bacteria-containing vesicles and the emerged PNS and magnetic fraction were analysed by Western blot, respectively (figure 3.28). The high intensity of *L.m.* specific antigen in the magnetic fraction indicates the effective phagosome isolation. TNF-R1 expression and internalisation did not seem to be impaired in IFNγR$^{-/-}$ macrophages. Detectable amounts were apparent in the magnetic fraction, regardless of any stimulation and infection duration. The GTPase Rab5 was hardly detectable on the phagosome containing fraction (magnetic fraction) and in contrast Rab7 and LAMP1 did appear. Both the intermediate (43 kDa) and mature (34 kDa) forms of CTSD arose in remarkably high intensities, irrespective of any stimulation. The fact that these IFNγR$^{-/-}$ macrophages exhibited such a prominent CTSD activation was intriguing. With regard to literature, CTSD is a decisive protein in the eradication process of *L.m.* (Carrasco-Marin *et al.*, 2009; Cerro-Vadillo *et al.*, 2006). These findings could not be confirmed in this study, as Western blot data indicated otherwise. Uncontrolled bacterial replication was observed despite high amounts of activated CTSD within the phagosome. Additionally, earlier reports indicated an IFNγ driven recruitment of lysosomal proteins like CTSD and LAMP1 to the phagsosome (Prada-Delgado *et al.*, 2001). This could not be confirmed either, as similar or even higher amounts of phagosomal CTSD and LAMP1 appeared in IFNγR$^{-/-}$ knockout macrophages compared to wild-type macrophages. In sum, the reported CTSD importance for bacterial restriction seems to be questionable considering the data of these experiments.

The IFNγ inducible GTPase LRG-47 was not expressed, regardless of any stimulation condition as it was to be expected. The purity of the preparation was controlled by detection of nucleoporin p62 and GSK3β, both of which arose in less intensity in the magnetic fraction.

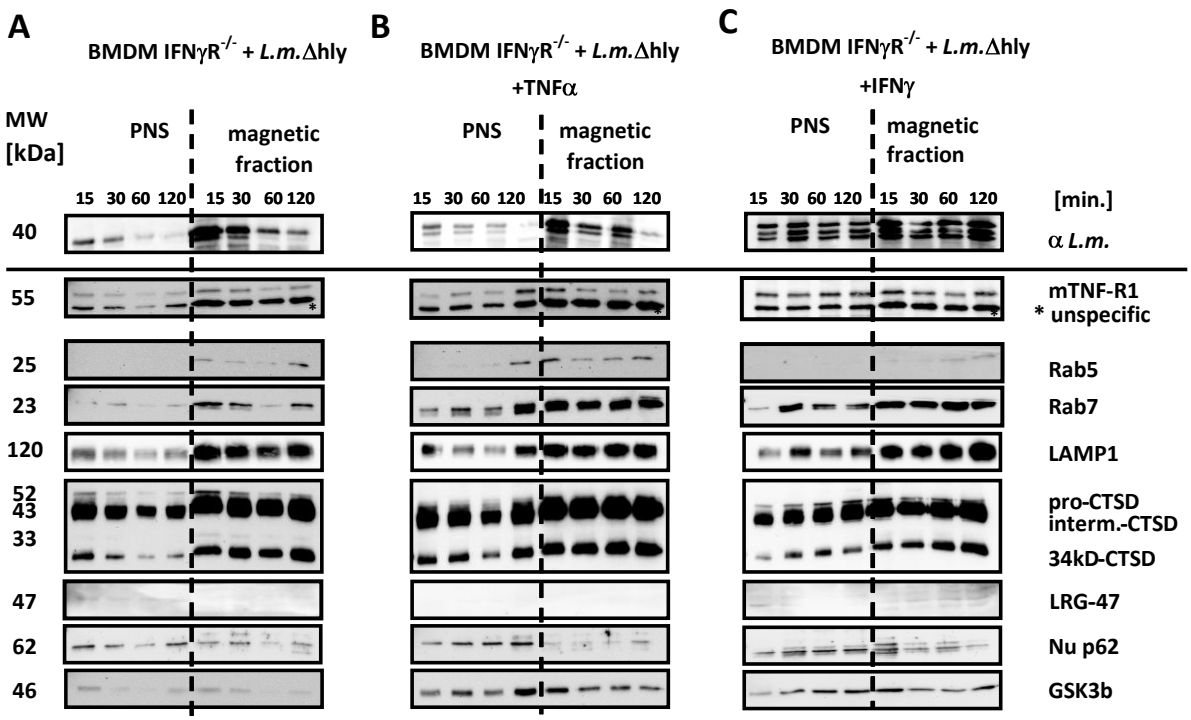

Figure 3.28: Western blot analysis of isolated phagosomes in dependence of different cytokine stimulation
Protein composition of isolated phagosomes in BMDM IFNγR$^{-/-}$ was monitored. ***A)*** *Cells were not treated* ***B)*** *Cells were stimulated with 100 ng/ml rhTNFα during infection* ***C)*** *Cells were pre-incubated with 200 U/ml rmIFNγ overnight. All cells were infected at a MOI 10 with magnetically labelled L.m (Δhly) for indicated time periods (15, 30, 60 and 120 minutes). Cells were then softly disrupted by sonification and prepared for magnetic separation as described in figure 3.6. All fractions were collected and prepared for western blot analysis. Every lane was loaded with 8 µg of total protein to compare protein composition. BMDM = bone marrow derived macrophages; PNS = post nuclear supernatant; CTSD = cathepsin D; Nu p62 = Nucleoporin p62, GSK3β = Glycogen synthase kinase-3β; MW = molecular weight; kDa = Kilodalton.*

3.6.7. Inducible nitric oxide synthase (iNOS) as effector molecule for eradication

An additional mechanism, through which IFNγ exerts its antimicrobial effects against pathogens, is the generation of reactive oxygen- and nitrogen-derived intermediates (ROI and RNI, respectively). ROI such as superoxide anions, hydroxyl radicals and hydrogen peroxide are generated as a result of the incomplete reduction of oxygen during respiratory metabolism (Turrens, 1980). Activated macrophages produce NO by iNOS and ROI by the NADPH oxidase complex. Both enzymes are critical in the host defense against *L.m.* (Shiloh *et al.*, 1999). Additionally, NO production was suggested to be necessary for *L.m.* killing, revealed by experiments with TNFα/LT-$\alpha^{-/-}$ bone marrow derived macrophages (Muller *et al.*, 1999). Therefore it was examined whether iNOS recruitment is altered by cytokine stimulation or if it is dependent on TNF-R1 signalling. Using the samples of isolated phagosomes generated in 3.6.2 and 3.6.4, specific iNOS recruitment was monitored by Western blot considering different stimulation conditions (figure 3.29: unstimulated (**A**), TNFα stimulated (**B**) and IFNγ stimulated (**C**) BMDM WT and BMDM TNF-R1$^{-/-}$, respectively). The enzyme iNOS did not seem to be a component of the *L.m.*-containing phagosomes at any of the time points monitored during infection, both in TNF-R1$^{-/-}$ macrophages and WT macrophages. The positive control (contr.) which accompanied each Western blot determined that this was not due to a non-functional antibody. In order to exclude general impairment of RNI generation in these cells, nitric oxide (NO) production was measured during infection at 24 and 48 hours p.i. using Griess reagent (figure 3.30). All cells were infected with the hemolysin negative mutant of *L.m*. (Δhly) to avoid death of macrophages due to uncontrolled replication of bacteria. An impairment of NO production in TNF-R1$^{-/-}$ macrophages when compared to WT was not observable. IFNγ stimulation induced NO release in both cell types (TNF-R1$^{-/-}$ and WT macrophages) upon infection, whereas IFNγR$^{-/-}$ macrophages exhibited no induction upon IFNγ stimulation. These data exclude iNOS recruitment via TNF-R1 to *L.m*.-containing phagsosomes at early time-poinst p.i.

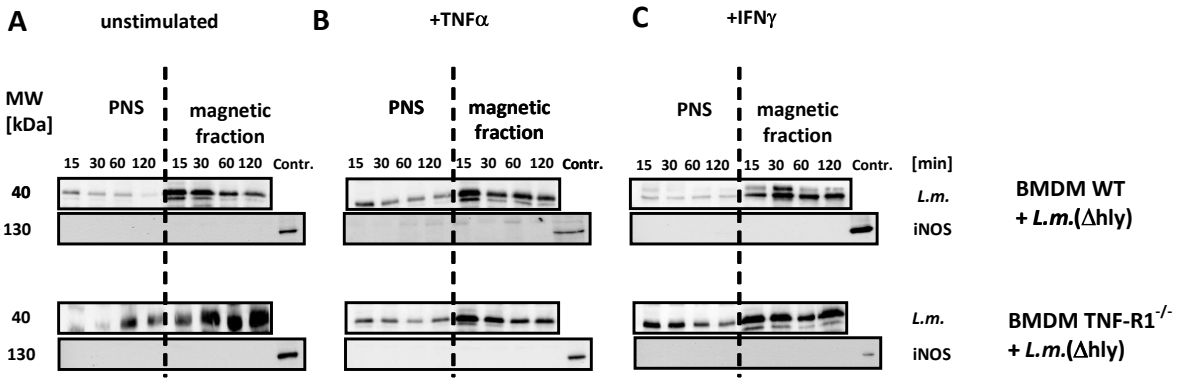

Figure 3.29 : Western Blot analysis of isolated phagosomes - detection of iNOS recruitment
Specific iNOS recruitment to L.m. - containing phagosomes was analysed by Western blot. Preparation of isolated phagosomes from figure 3.19 and 3.23 were used. (For preparation details see 3.3). ***A)*** *unstimulated* ***B)*** *TNFα stimulated and* ***C)*** *IFNγ stimulated cells show no iNOS recruitment at any time point. Contr. = positive control.*

A)

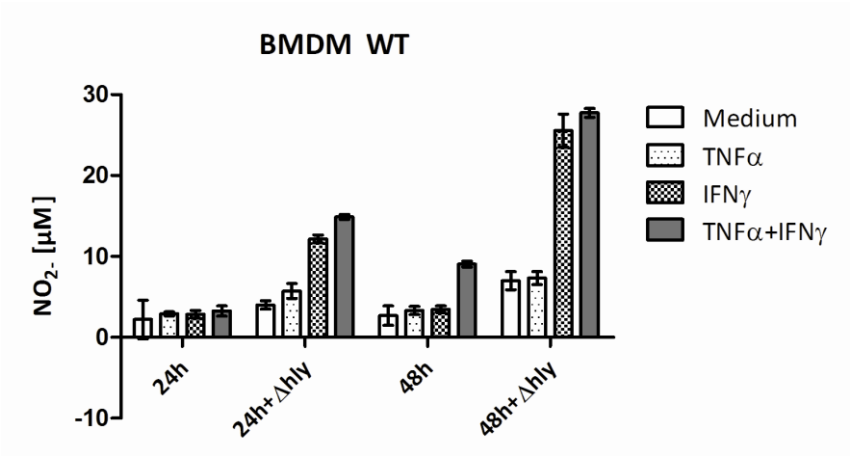

B)

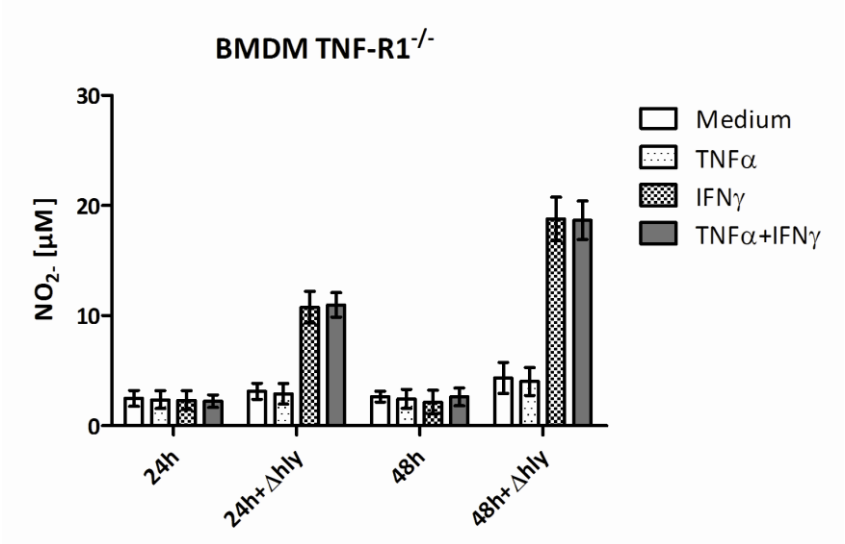

C)

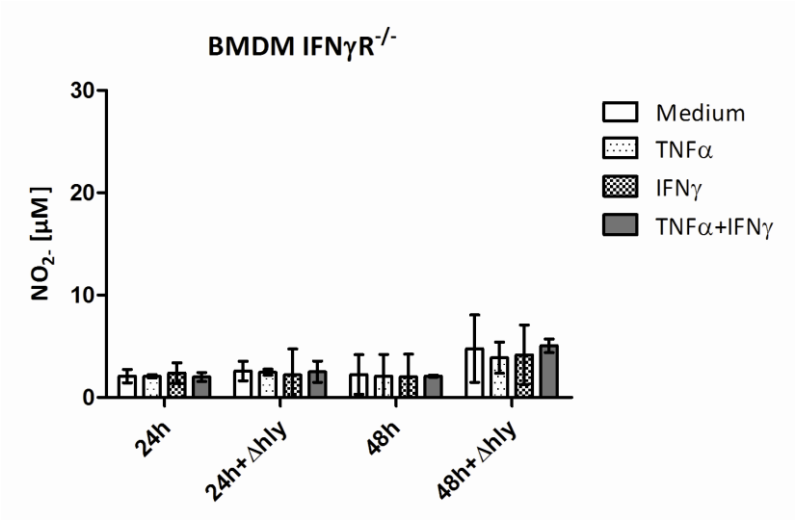

Figure 3.30: NO-Production of primary macrophages

In order analyse NO-production upon infection, macrophages were seeded on 96-Well plates in triplicates for each time point and stimulation pattern. Cells were stimulated with rmIFNγ (200 U/ml) overnight and supplemented with new medium 250 µl per well for infection. Cells were infected at a MOI 3 with the hemolyisn-mutant (Δhly). Cells were stimulated with 100 ng/ml rhTNFα during infection and TNFα was present at all times. After 24 and 48 hours of incubation supernatant were harvested for Nitrite (NO_2-) detection, respectively. NO-production was measured using Griess reagent: ***A)*** *shows NO-production of BMDM WT,* ***B)*** *of BMDM TNF-R1$^{-/-}$ and* ***C)*** *of BMDM IFNγR$^{-/-}$.* ***A)*** *One representative out of two independent experiments is shown. Data are given as mean±SD of triplicate assays.* ***B)*** *Data show means of three independent experiments ±SD.* ***C)*** *One representative out of two individual experiments is shown. Data are given as mean±SD of triplicate assays. BMDM = bone marrow derived macrophages.*

4. Discussion

The cytokine TNFα released by macrophages upon infection plays a pivotal role in innate immunity and eradication of intracellular bacteria such as *listeria monocytogenes (L.m.)*, *mycobacteria* and *legionella*. The work of Pfeffer *et al.* and Rothe *et al.* demonstrated that TNFα binding receptor TNF-R1 on hematopoietic cell surface is essential and sufficient for resistance against the intracellular bacterium *L.m.* (Endres *et al.*, 1997; Rothe *et al.*, 1993; Pfeffer *et al.*, 1993), whereas the second TNFα binding receptor TNF-R2 seems to play only a minor role (Erickson *et al.*, 1994). Mice treated with blocking antibody against TNFα or deficient in TNF-R1 lose their ability to kill bacteria and die upon infection (Nakane *et al.*, 1988). Therefore many pathogens and viruses have developed counterstrategies and produce modulatory proteins, which specifically target TNFα-related response elements in order to ensure their survival in the organism (Rahman and McFadden, 2006).

However, at this stage it is unclear how TNF-R1 contributes to these phenomenons. Schneider-Brachert *et al.* were able to show that the internalisation of TNF-R1 is an essential step in the recruitment of surface marker proteins for inducing TNFα-mediated apoptosis. Throughout this internalisation process, fusion events with *trans*-Golgi vesicles localise the proteins CTSD in its mature form and activated acid sphingomyelinase (ASMase) on the internalised TNF-receptosomes. Shortly afterwards, Cerro-Vadillo *et al.* linked CTSD to the eradication process of intracellular bacteria. They showed that mice deficient in CTSD are highly susceptible to infection with *L.m.* . Most recently, it was demonstrated that listeriolysin, the major virulence factor of *L.m.*, is a target of CTSD and was specifically cleaved by it (Carrasco-Marin *et al*., 2009). However, hints regarding this already arose in the work of Cerro-Vadillo *et al*. (Cerro-vadillo et al., 2006). In sum, these findings led to the main hypothesis that the generation of a "TNFα-activated phagolysosome" is a mechanism to eradicate intracellular bacteria. The biological relevance of TNF-R1-internalisation in principle is still not known and therefore was of special interest in this study. After ligand binding to TNF-R1, internalisation and fusion events with *trans*-Golgi vesicles, TNF-R1 composes a vesicle compartment that theoretically could direct mature CTSD towards the phagosome as a mechanism for fast eradication of *L.m*. This could occur before the pathogen leaves the phagosome, evading the degradative compartment of the phagolysosome.

4.1. Eradication of intracellular bacteria with the infection model of *Listeria monocytogenes* in macrophages

Some decades ago, Portnoy found that simulation with TNFα alone was insufficient to mediate bacterial killing. Mouse peritoneal macrophages stimulated with rTNFα showed no difference to unstimulated cells regarding bacterial load (Portnoy *et al.,* 1989*)*.

However, the priming of macrophages with IFNγ engendered a reduction of bacterial number and this was potentiated by additional stimulation with rTNFα. These findings provided an indication that a synergistic interplay of both cytokines might have taken place. Infection studies in this present work could partially confirm this data.

4.1.1. The synergy of IFNγ and TNFα is required for infection control of *Listeria monocytogenes* in macrophages

The bactericidal effects of TNFα and IFNγ were first tested with the macrophage cell-line J774. Replication of bacteria in response to TNFα and IFNγ was monitored over an eight-hour-long interval. However, the effects were not completely in accordance with Portnoy´s work. First, a reduction of bacterial number could not be achieved in any infection model and only an impairment of growth was observable upon IFNγ treatment. Also, additional stimulation with TNFα to IFNγ was unable to enhance bacterial killing. This may be due to the fact that the work of Portnoy and Langemans was performed with primary mouse peritoneal macrophages, which probably are more effective in bacterial killing then the above mentioned cell-line.

Another reason may be that bacterial infection always leads to involvement of the TLR-system in macrophages. Lipoteichoic acid and other bacteria components are ligands of TLRs, inducing gene transcription via NF-κB and finally leading into TNFα-production (see 1.3.1). Thus, this system was never free of TNFα during infection. Furthermore, stimulation with IFNγ enhances TNFα release during infection. Remarkably, many genes are synergistically inducible by TNFα and IFNγ. Some of these genes contain both an ISRE and a NF-κB site in their promoter region, demonstrating the strong relationship between those two cytokines (Boehm *et al.*, 1997).

A direct crosstalk between TNF-R1-signalling and IFNγ-signalling pathway was suggested in studies with the RAW264.7 macrophage cell line. TNFα and IFNγ synergise in the activation of macrophages and enhance NF-κB activation. The IFNγ-signalling component STAT-1α was found to interact with TNF-R1, resulting in an attenuation of TNFα mediated NF-κB activation. This complex appeared in lower extent when macrophages were stimulated with IFNγ because in consequence STAT-1α dimerises and translocates into the nucleus, decreasing the presence of available STAT-1α for the generation of the TNF-R1-STAT-1α complex (Wesemann and Benveniste, 2003). An enhanced NF-κB

activation by IFNγ was presumably detected in the present study because of the increasing release of TNFα observed during infection in IFNγ stimulated macrophages. This may be attributed to the above mentioned process (see 3.1 figure 3.2; 3.6.2 figure 3.17).

Murine macrophages were stimulated with recombinant human TNFα (rhTNFα) in order to ensure that only TNF-R1 is addressed for signalling, as human TNF specifically binds to mouse TNF-R1 and not to TNF-R2. However, the mouse-TNFα-ELISA data (figure 3.2) revealed that even infection with bacteria alone induced considerable amounts of mouse TNFα. This could be enhanced up to two-fold amounts through stimulation with IFNγ. Therefore, stimulation and involvement of TNF-R2 signalling can not be excluded from this infection system. On the other hand, TNF-R2 is mainly stimulated by membrane bound TNF, so an effect via TNF-R2 signalling is presumably negligible (Grell *et al.*, 1995). Nevertheless, the control was always under some sort of stimulation in this particular case. TNFα, and therefore signalling via TNF-R1, was invariably present due to autocrine stimulation. With the aid of confocal microscopy and phalloidin staining, Portnoy's observations regarding IFNγ could be confirmed. This cytokine sealed the phagosome in an unidentified way and kept *L.m*. trapped in the phagosome. To date, these effects had only be seen in primary peritoneal macrophages, but the present work could also evidence this observation in the macrophage cell-line J774 (figure 3.3).

Although it is known that TNFα and IFNγ are absolutely necessary for activation of macrophages and also for survival of mice during *L.m.* infection, the molecular mechanisms of listericidal activity of both cytokines is not fully understood (Buchmeier and Schreiber, 1985; Dalton *et al.*, 1993; Pfeffer *et al.*, 1993)). In particular, the uncertain contribution of TNF-R1 signalling in this process should be investigated in the present study. The model of a synergistical interplay between both cytokines and the participation of TNF-R1 in bacterial eradication seem to be likely and substantiate the hypothesis of this work. The momentousness of TNF-R1 signalling in IFNγ-primed macrophages for bacterial replication control was demonstrated with experiments which monitored the bactericidal properties of primary bone marrow derived macrophages upon cytokine stimulation. Macrophages deficient in TNF-R1 were not able to impede bacterial replication properly, even when primed with IFNγ. In comparison to medium control, no significant reduction of bacteria load was observable (figure 3.20). IFNγ still seemed to slow down the pathogen-escape out of the phagosome as no complete loss of bacterial replication occurred, but it could not restore full control either. Similar results were obtained from studies with TNF-R1 knockout macrophages and the intracellular bacterium *salmonella typhimurium*, implying a general impact of TNF-R1 on intracellular bacterial killing (Vazquez-Torres *et al.*, 2001). The missing TNF-R1 signalling events may render the maintenance of a controlled status, inconceivable in a longer-lasting infection (8 hours p.i.). Confocal microscopy evidenced this effect more precisely (see figure 3.22). Generally, *L.m.* can only be degraded by previously activated macrophages within the phagolysosomal compartment, but not after the escape

of the bacterium into the cytosol. IFNγ was shown to restrict the pathogen in the phagosomal compartment in all macrophages analysed in this work. Only in TNF-R1 deficient macrophages IFNγ stimulation failed to do so. Bacteria were able to break free from the phagosome and went forth into the cytoplasm at two hours p.i. This was not the case in WT macrophages upon IFNγ stimulation (see figure 3.18). Considering the effect of the IFNγ control experiments with macrophages of IFNγ-receptor deficient mice, substantial differences to WT macrophages also arose. The restriction of bacteria replication had completely vanished, irrespective of any added cytokine. Infection studies with TNF-R1$^{-/-}$ macrophages in this work demonstrate the contribution of TNF-R1 to infection control in IFNγ activated macrophages very clearly. The control of pathogen replication was only possible in the presence of TNF-R1, suggesting that IFNγ mediated effects in bacterial eradication have probably always been cooperative effects with TNFα and TNF-R1-signalling.

4.2. Biological function of TNF-R1 internalisation in macrophages

With the work of Schneider-Brachert *et al.*, TNF-R1 internalisation was shown to be an indispensible event for apoptotic signalling (Schneider-Brachert *et al.*, 2004). The subsequent recruitment of several adaptor proteins finally leads to DISC-formation and apoptosis. When working with macrophages, TNFα mediated apoptotic signalling undeniably plays only a minor role, as these cells are the primary producers of TNFα and do not proceed to apoptotic cell death upon stimulation. Monocyte derived macrophages express constitutively activated NF-κB and therefore are resistant to apoptotic stimuli (Kikuchi *et al.*, 1996). Little is known about the precise contribution of TNF-R1 to bacterial killing, but considering the results of this work it undoubtedly becomes a component of the *L.m*.-containing phagosome after ligand binding and internalisation (see 3.2 and 3.5).

The results of the present work showed that Internalisation of TNF-R1 takes also place in macrophages upon TNFα stimulation. This finding opened new insights into TNF-R1 signalling because internalisation seems to be involved in host defense, representing for the first time its participation in processes other then apoptosis. This is in accordance with earlier data, where complete truncation or selective inactivation of the TNF-R1 death domain (DD) led to loss of protection against *L.m.* infection in mice (Plitz *et al.*, 1999).Thus, signals emanated from TNF-R1 DD seems to be requisite for protection again *L.m*. infection *in vivo*.

Another component of TNF-R1-signalling pathway is the acid sphingomyelinase (ASMase) which is specifically activated upon TNFα stimulation and receptor internalisation (see 1.5.2). This TNFα and also IFNγ responsive enzyme is linked to the eradication process of intracellular bacteria. ASMase generates the signalling molecule ceramide, resulting in activation of CTSD within the phagolysosmal compartment. Mice deficient in ASMase were strongly impaired in their capacity to kill *L.m.* and died

upon infection even with low bacterial load of this pathogen (Utermöhlen *et al.*, 2003). Recent studies with ASMase deficient macrophages revealed the molecular and precise antibacterial effector mechanisms mediated by this enzyme. Defective phagosomal maturation and inefficient transfer of lysosomal hydrolases into the *L.m.*-containing phagosomes were observed. The lysosomal protease CTSD was found to be localised in equal amounts in phagosomes of ASMase deficient and wild-type macrophages, however the 43 kDa and 34 kDa mature form were increased only in wild-type cells (Schramm *et al.*, 2008; Utermöhlen *et al.*, 2008). These findings substantiate the earlier studies by Schneider-Brachert *et al.* and suggest an involvement of TNF-R1 in CTSD activation on the phagolysosomal compartment (Schneider-Brachert *el al.*, 2004). Therefore, it was asserted that TNF-R1 must interact with the bacteria-containing phagosome in a way that these findings can coherently occur. The conjunction of TNF-R1-receptosomes and phagosomes seemed to be likely and was to be proved with a variety of different experiments in the present study, as follows.

4.2.1. TNF-R1 is a component of *Listeria monocytogenes*-containing phagosomes

The first approach towards visualisation of the proximity of TNF-R1 after internalisation to phagocytosed bacteria was carried out with confocal microscopy. This method was used to illustrate whether TNF-R1 and *L.m.* colocalise in the same compartment. The ligand based staining of TNF-R1 allowed the specific labelling and internalisation of this receptor. Human biotin-TNFα interacts with streptavidin-FITC, resulting in the ligand complex which finally marked TNF-R1. Using this complex, confocal microscopy could demonstrate the presumptive colocalisation of bacteria and receptor (figure 3.4). These first hints were then supported by electron microscopy, which was used to contrast the localisation in higher detail. The acquisition of TNF-R1 to the *L.m.*-containing phagosome was corroborated with this method and therefore partially verified the hypothesis of this work. Gold-labelled TNF-R1 was demonstrated to be inside the bacteria-containing compartment surrounded by the phagosomal membrane and fortuitously even fusion events could be observed (figure 3.5D-F and 3.5C). The biochemical analysis of *L.m*.-containing phagosomes, isolated via the lipobiotin-based magnetic labelling of *L.m.* discussed in 4.4, was able to substantiate these findings on a protein level. The isolated bacteria-containing phagosomes showed an enhanced signal for mTNF-R1 on Western blot, indicating an enrichment of this protein in this compartment. Furthermore, time-dependent accumulation in J774 macrophages was additionally observed, reflecting the initiation of internalisation and fusion events with the phagosome. Accumulation of mTNF-R1 was also validated for phagosomes from wild-type and IFNγR deficient macrophages, demonstrating the general fusion of these two compartments in different macrophage populations. In previous works from our group, TNF-R1-containing compartments were separated with the analogue technique of vesicle isolation by

magnetic labelling of the receptor. Contrariwise, isolation of TNF-R1-receptosomes from *L.m.*-infected macrophages could demonstrate that *L.m.* specific protein was detectable in these vesicles, confirming the previous results. In sum, this work led to an initial conclusion that TNF-R1 fuses with *L.m.*-containing phagosomes after TNFα stimulation and receptor-internalisation. The initial hypothesis was now verified by providing evidence from two independent Macrophage populations: The macrophage cell-line J774 and bone marrow derived macrophages, suggesting that TNF-R1 recruitment to bacterial phagosomes might be a general event during infection with intracellular bacteria. As a result, the specific contribution of TNF-R1 signalling to phagosomal bactericidal mechanisms was to be investigated with the use of the new phagosome-isolation protocol. Results obtained from J774 macrophages are displayed in the following chapter, and are discussed separately to those obtained from primary bone marrow derived macrophages to facilitate discussion of the distinct findings regarding CTSD.

4.2.2. Activation of CTSD in the phagosome - receptosome compartment in J774 macrophages is induced by TNF-R1

In recent years, lysosomal proteases were suggested to contribute considerably to microbicidal activity besides the general effector mechanism, such as RNI and ROS generation (Reeves *et al.*, 2002 Cerro-Vadillo *et al.*, 2006; Utermöhlen *et al.*, 2008). The experiments in the present study were predominantly focused on the protease CTSD as an effector molecule for bacterial eradication. It was shown to be part of internalised receptosomes in late stage and linked TNF-R1 signalling to bactericidal components (see 1.5.1). The found conjunction of TNF-R1-receptosome and bacteria-containing phagosome (see 3.2) was thought to be a mechanism which could route activated CTSD as a bactericidal molecule towards the phagosome. The new phagosome-isolation protocol allowed the specific purification of *L.m.*-containing phagosomes in order to study molecular changes occurring on the phagosomal compartment upon cytokine treatment. Under different stimulation conditions, selective activation of CTSD was observed. The most striking result was that besides IFNγ, TNFα stimulation alone induced CTSD activation in the phagosome, indicated by the early appearance of the active 34 kD form. By contrast, unstimulated macrophages failed to recruit activated lysosomal protease CTSD to the phagosome and merely the intermediate form (43 KDa) appeared. This indicated that activated CTSD was not delivered by TNF-R1 or fusion of phagosome and *trans*-Golgi-vesicles containing CTSD must have occurred, but protease activation was not ultimately induced. This finding can be the consequence of various reasons, which could act in a combined manner. One explanation could be missing ceramide which is generated by activated SMase and is known to activate CTSD (Heinrich *et al.*, 2000). As mentioned previously, TNF-R1 induces ASMase activation upon TNFα stimulation and receptor internalisation (see 1.5.2). Since ASMase deficient macrophages

showed impaired fusion of late phagosomes with lysosomes and reduced acidification, this might result from missing TNF-R1 signalling also. Another reason could be the lack of cathepsin L and/or cathepsin B, which have been reported to be involved in CTSD activation . Perhaps these and other proteases might not have been recruited to the phagosome and therefore activation of CTSD was not induced.

The observation of CTSD activation upon TNFα treatment was challenging and one important question arose from this finding: While activated CTSD is present in the bacteria-containing phagosome, why does TNFα alone seems to be insufficient to control bacteria infection? This leads consequently to the assumption that CTSD is probably not the essential molecule in bacterial eradication mechanisms, as generally supposed to date.

However, one important fact must be noted at this point: experiments regarding phagosome isolation were all performed with the hemolytic negative mutant of *L.m.* (Δhly), which stays in the phagosomes and does not translocate into the cytoplasm for replication. The selection of this mutant *L.m.* facilitated a localised and specific study of peri-phagosomal phenomena, but at the same time we were conscious of a possible *in vitro* bias due to a not limited, non physiological cytokine impact on the phagosome. If the major mechanism of IFNγ is to mediate the retention of *L.m.* in the phagosome, we might have created an environment similar to IFNγ stimulation with the use of this mutant of *L.m.* This might allow recruitment of proteins and effector molecules to the phagosomal compartment at later time points. Infection with the wild-type strain of *L.m.*, this recruitment might not have normally taken place due to fast escape of the pathogen out of the phagosome. However, early time points should reflect physiological TNFα mediated effects, as *L.m.*-escape into the cytoplasm is reported to start at about 30 min after infection (Myers *et al.*, 2003). Thus, the activation of CTSD is likely to be induced upon TNFα stimulation and due to fusion of TNF-R1-receptosomes with bacteria-containing phagosomes. The later time points p.i. show stages where recruitment might not occur in the normal physiological response to virulent *L.m.* infection. However, in early time points (15 min and 30 min p.i.) it should reliably indicate cytokine driven effects on the phagosomal compartment. The same effects might be seen in the IFNγ treated macrophages. INFγ mediated activities are always occurring in cooperation with TNFα (compare 4.1.1). The CTSD activation observed on IFNγ stimulated phagosomes might be one of these TNFα mediated effects, as TNFα alone was sufficient to induce CTSD activation also.

Taken together, this work could prove for the first time that TNFα stimulation results in activation of the protease CTSD on the phagosomal compartment. This is accompanied by specific recruitment of TNF-R1 to the phagosome, evoking a new molecular contribution of TNF-R1 internalisation and signalling to the fate of phagocytosed bacteria. Furthermore, the isolation of magnetic labelled TNF-R1-containing compartments substantiated these findings. Activated CTSD appeared in these

isolated receptosomes together with *L.m.*-specific protein, demonstrating the association of all components of the "TNFα-activated phagolysosome" (see figure 3.16). However, whether these effects of missing CTSD activation are due to impaired acidification of the phagsosome or caused by the absence of other essential components can not be discerned at this stage of the work and implies further investigations.

Paradoxically, the marker of the lysosomal compartment LAMP1 seemed to appear rather early and time-dependent recruitment was not observed. The unstimulated cells behaved similar to the stimulated macrophages, which was unexpected considering the differences observed in CTSD activation. Similar results were obtained from work with IgG-beads-containing phagosomes, where the protein LAMP1 appeared within the first three minutes after phagocytosis (Sturgill-Koszycki *et al.*, 1996). Moreover, recent studies revealed that proteolytic activity of lysosomal proteases can be detected within phagosomes early in the phagosomal maturation process, demonstrating that characteristical components of a phagolysosome may appear sooner than excpected (Yates *et al.*, 2005).

Not only the host reacts to phagocytosed bacteria, but also the pathogen itself releases factors that interfere and counter host bacterial killing mechanisms. The protein LLO is one of the major determinants of *L.m*. virulence. This protein is responsible for phagosomal membrane lysis and allows the pathogen to translocate into the cytoplasm for replication (see 1.2.1). LLO was suggested to prevent the fusion of phagosomes with lysosomes in order to save the pathogen from the degradative environment of the phagoso-lysosome (Shaughnessy *et al.*, 2006). Recently this protein was demonstrated to be specifically cleaved by CTSD, substantiating the role of this above discussed hydrolase in innate immunity against *L.m.* (Carrasco-Marin *et al.*, 2009). The pathogen in turn uses the host factor γ-Interferon inducible lysosomal reductase (GILT) for its own benefit, as it activates the lytic enzyme LLO. GILT was shown to be critical for activation of LLO and mice deficient in this host derived protein are well-protected against *L.m.* infection.

4.2.3. Activation of CTSD in the phagosome - receptosome compartment in primary macrophages is independent of TNF-R1

The precise mechanism of bacterial killing mediated by the protease CTSD in the *L.m.*-containing phagosome still seems to be uncertain considering the results of this work. TNFα stimulated J774 macrophages revealed activated CTSD in the phagosome rather early but showed no bacterial replication control during infection with *L.m*. (see figure 3.15B and 3.1 respectively). These findings correspond to the data elicited from isolated phagosomes of primary macrophages.

Wild-type macrophages showed processed and mature CTSD on isolated phagosomes, very early and irrespective of any cytokine stimulation. Similar observations were made from TNF-R1 and IFNγR

deficient macrophages. This outcome was puzzling at a first glance. Wild-type macrophages were able to control bacterial replication only upon IFNγ treatment (see 3.6.1) and TNF-R1 deficient macrophages were not able to restrict bacterial propagation under any cytokine conditions (see 3.6.3) likewise, IFNγR deficient macrophages. These cells could also not control bacterial propagation when treated with IFNγ or TNFα. Paradoxically, the activated form of CTSD was detectable in similar amounts in isolated phagosome of all of these primary macrophages, irrespective of TNF-R1 or IFNγR knockout condition or of any cytokine treatment. These data seem to persist in contrast to current publications. $CTSD^{-/-}$ mice showed increased susceptibility to *L.m.* infection and *in vitro* infection of bone marrow macrophages from these mice were able to confirm the loss of bacterial growth control (Cerro-Vadillo *et al.*, 2006). Noteworthy, these mice expressed only a non functional CTSD which was called for simplicity $CTSD^{-/-}$. Saftig and co-workers generated this mouse model of CTSD deficiency, in which the open reading frame (ORF) of the *CTSD* gene is interrupted at exon 4 and the truncated ORF only encodes the N-terminal quarter of mature CTSD (Saftig *et al.*, 1995). The affected mice appear to develop normally for the first two weeks of life, suffering from anorexia and seizures and leading to death at postnatal day 26±1. These mice are impaired in viability in general and only heterozygous mice can carry and breed homozygous embryos. However, this study suggested that *in vivo* functions of CTSD may concern rather activation−or inactivation−of signalling proteins by limited proteolysis in the endosomal and/or lysosomal compartment. Severe deficiencies in proteolytic degradation of intermediates can be compensated by the activities of the remaining endopeptidases according to the authors' view. In their opinion, CTSD did not seem to be essential for bulk degradation of proteins in the lysosomal compartment. CTSD may have a particular function as an effector molecule which targets bacteria and/or bacterial virulence factors, in order to mediate bacterial killing in the phagosomes. So it is reasonable to question whether deficiency in bacterial replication control in these genetically modified mice is due to this particular activity of CTSD or, on the other hand, if it results from a general systemic defect in activation or inactivation of signalling proteins. This offers yet another possible reason for the observed *L.m*. susceptibility in macrophages. The cytolysin LLO was suggested to be the direct target of CTSD, resulting in its degradation and in eventual control of *L.m.* infection (Cerro-Vadillo *et al.*, 2006; Carrasco-Marin *et al.*, 2009). Reasonably, there might also be other host cell proteins affected by CTSD which would result in less efficient bacterial killing in its absence.

Considering the new findings presented in this current study, it seems more likely that CTSD contributes to bacterial killing in a collateral way, rather than acting directly on *L.m.* factors within the phagosome. Obviously, fusion events with *trans*-golgi-vesicles containing CTSD take place, demonstrated by the appearance of intermediate CTSD (43kDa) in all monitored phagosomes. Activation and processing of CTSD seems to occur in macrophages, independent of impairmed

bacterial propagation control. For instance, the most prominent CTSD activation on the phagosome was detected in IFNγR$^{-/-}$ macrophages, but these were unable to control bacterial replication and this was demonstrated by the bacterial growth assays (figures 3.28 and 3.25, respectively). The same observation can be made in TNF-R1 deficient macrophages, as mentioned above. These results imply that CTSD might affect signalling components of the TNF-R1 pathway which are missing in the knockout system and absent on the phagosome in unstimulated macrophages. Therefore, internalisation and fusion of TNF-R1-receptosomes with the phagosome might bring the important components to the phagosomal compartment, mediating their bactericidal effects. Direct routing of CTSD to the phagosome by TNF-R1 seems unlikely, considering the observed CTSD activation in isolated pagosomes of TNF-R1 defeicient macrophages. However, an indirect role of CTSD related to TNF-R1 signalling in bacterial killing is still conceivable.

4.2.4. The role of the IFNγ induced proteins Rab5a and LRG-47 on the phagosome

A significant number of proteins, synthesised in response to a phagocytic signal, play a general role in phagosome maturation and functions. The most obvious class of proteins which can influence these processes are those that are inserted into the membrane or delivered within the lumen of the phagosome, such as Rab GTPases or CTSD, respectively. In particular, intracellular bacteria are able to interfere with vesicle trafficking regulators to their advantage while still residing in the vacuole. They achieve this with modifying and adapting the given vacuolar environmental conditions into those of their particular needs. One protein which interferes with virulence factors of the intracellular pathogen *L.m*. is Rab5, which was suggested to influence the pathogen's life cycle. Infected macrophages showed up-regulation of Rab5 on *L.m.*-containing phagosomes in order to prevent phagosome maturation by blocking the GTPase´s activity (Alvarez-Dominguez *et al.*, 1996). Later investigations demonstrated that in particular the isoform Rab5a is essential for *L.m.* destruction and IFNγ signalling regulates the GTPase`s expression. The activation of Rab5a was suggested to be one of the IFNγ driven mechanisms which lead to eradication of the pathogen *L.m.* in the phagolysosome. Stimulation with IFNγ specifically enhances Rab5a synthesis and processing, including translocation of newly synthesised Rab5a to intracellular membranes. Similar to most low molecular weight GTPases, Rab5a is active in the GTP bound form (Rybin *et al.*, 1996 Alvarez Dominguez *et al.*, 1996). The guanine nucleotide exchange from GDP to GTP as well as GTP hydrolysis was shown to be induced by IFNγ, also on the GTPase Rab5a (Alvarez-Dominguez and Stahl, 1998).
Further studies proposed that activated Rab5a controls the recruitment of active Rac2 (**Ra**s-related **C**3 botulinum toxin substrate **2**) and the assembly of phagocyte NADPH oxidase to the phagosome, which leads to production of toxic radicals for elimination of the intracellular pathogen. These Rab5a

mediated actions compromised *L.m*. viability and survival in the phagolysosome. Interestingly, recent studies have shown that the pathogen itself produces a virulence factor, **g**lycer**a**ldehyde-3-**p**hosphate **d**e**h**ydrogenase (GAPDH or p40 protein), which specifically interferes with Rab5a by inhibition of its GDP/GTP exchange activity and additionally halts its recruitment to the phagosome (Alvarez-Dominguez *et al.*, 2008). The pathogen's specific response to this GTPase emphasises and confirms the importance of this protein in the bacterial eradication process, because of its particular status as a target for a specific bacterial virulence factor.

In this study, isolated *L.m*.-containing phagosomes of J774 macrophages and BMDM WT showed similar amounts of Rab5, irrespective of any given stimulation conditions. However, TNF-R1$^{-/-}$ macrophages failed to recruit Rab5 to phagosomes in both unstimulated and TNFα stimulated cells (figure 3.24). Additionally, in BMDM of IFNγR deficient mice hardly any Rab5 was detectable on the phagosomal compartment (see figure 3.28). These listed cells were all impaired in their capability to restrict bacterial replication. In the current study, it is not clear which particular isoform of Rab5 is recruited to the phagosome as the antibody used in these assays detected all isoforms: Rab5a, Rab5b and Rab5c, therefore an exact differentiation is not possible. Only through IFNγ stimulation Rab5 appeared on isolated phagosomes in TNF-R1$^{-/-}$ macrophages. Therefore, it might be the isoform Rab5a which was detected here, as expression and activation was described to be induced by IFNγ stimulation (Alvarez-Dominguez *et al.,* 1998), but was not yet determined in this work. Nevertheless, these results strongly suggest that bacterial replication control is closely related to the routing of Rab5 or Rab5a to the phagosomal membrane. This could be a conceivable reason for the impaired infection control in TNF-R1 deficient and also in IFNγR$^{-/-}$ macrophages. However, the stimulation with IFNγ induced phagosomal Rab5 recruitment, yet IFNγ stimulation was incapable of restoring replication control in TNF-R1 knockout macrophages (see figure 3.21). This suggests that IFNγ induced Rab5 or in particular Rab5a expression is sufficient to recruit this GTPase to the phagosome, independent of TNF-R1, but it is insufficient for bacterial growth restriction. TNF-R1 might be important for activation of Rab5, demonstrating another conceivable mechanism driven by a synergistic interplay of both cytokines, TNFα and IFNγ.

Another recently found and characterised GTPase is LRG-47, which was also proposed to play a crucial role in intracellular bacteria killing. Collazo and his co-workers investigated the importance of this GTPase which belongs to the 48kDa GTP binding proteins family. These are encoded by IFNγ induced genes and expressed after infections with many different pathogens (Collazo *et al.*, 2001). LRG-47 was shown to serve as a critical vacuolar trafficking component, used to dispose of intracellular pathogens such as *mycobacterium tuberculosis*. Phagosomes in LRG-47 deficient macrophages were selectively impaired in their fusion with lysosmes, leading to ineffective eradication of the pathogen (MacMicking *et al.*, 2003). Loss of LRG-47 in macrophages yielded

specific defects in phagosome trafficking throughout the endolysosomal pathway and does not affect IFNγ induced macrophages effector mechanisms such as RNI and ROS generation. On this issue, it was ascertained whether LRG-47 recruitment on phagosomes might be altered or induced by TNF-R1. It was found here that this GTPase is only detectable on IFNγ stimulated phagosomes, independent of TNF-R1 knockout condition. This generally excludes LRG-47 as a valid candidate, implicated in TNF-R1 mediated bacterial killing. In sum, Rab5 seems to be involved in TNF-R1 related mechanisms against *L.m.*, whereas the other monitored GTPase, LRG-47, was ascertained to be dispensable in this particular context.

4.3. Oxidative burst formation and RNI generation in context with TNF-R1 signalling

TNF-R1 deficient mice are highly susceptible to *L.m*. infection despite of functional nitric oxide synthesis, oxidative burst formation and production of inflammatory cytokines (including IFNγ). These findings are in correspondence to data of mice deficient in an essential subunit of phagocyte NADPH oxidase ($p47^{phox}$). These animals were not able to generate ROS, but still showed resistance to listeriosis (Endres *et al.*, 1997). This implicates that there must exist other molecular components than ROS for bacterial eradication. Remarkably in this context, TNF-R1 was recently shown to activate NADPH oxidase 1 (Nox1), another member of NADPH oxidases, resulting in ROS production and necrotic cell death (Kim *et al.*, 2007). Further investigations to the precise molecular mechanism of TNF-R1 mediated ROS production revealed that riboflavin kinase (RFK) is the protein which connects TNF-R1 and Nox1. RFK binds to the DD of TNF-R1 and $p22^{phox}$, a common subunit of NADPH oxidases, bridging both components for TNFα induced ROS production (Yazdanpanah *et al.*, 2009). Infection studies with the intracellular pathogen *Salmonella* suggested a TNF-R1 dependent recruitment of NADPH phagocyte oxidase to the bacteria-containing phagosomes. Macrophages derived from TNF-R1-knockout mice failed to localise the $p22^{phox}$-harbouring vesicles close to *Salmonella*-containing phagosomes, in contrast to infected wild-type macrophages. Even IFNγ stimulation could not change these findings (Vazquez-Torres *et al.*, 2001). This strongly suggests a prerequisite presence of TNF-R1 on the phagosome for generating bactericidal ROS in the bacterial killing process. Similar amounts of ROS and RNI were also generated in ASMase deficient macrophages, implicating the existence of other non-oxidative listericidal mechanisms (McCollister *et al.*, 2007; Uthermölen *et al.*, 2003). However, phagosomes of these cells showed subsequent increasing amounts of $p22^{phox}$, indicating fusion events with vesicles carrying this subunit of phagocyte NADPH oxidase. These cells lack an important TNF-R1 signalling downstream element, but the receptor itself internalises and can recruit other essential molecules which induce ROS and RNI generation on the phagosome. Müller and co-workers showed that wild-type and TNFα deficient

macrophages produce similar amounts of NO, but inhibition of its production led to a remarkable loss of antilisterial activity in these macrophages. This suggests that the presence of NO is necessary but not sufficient for *L.m.* elimination (Muller *et al.*, 1999).

RNI in general are known to be potent antimicrobial agents in murine macrophages (MacMicking *et al.,* 1997). RNI might represent molecules which contribute to the bacterial eradication process in a TNF-R1 dependent manner. Since iNOS is the key enzyme in RNI production (see 1.3.4), it was investigated whether TNF-R1 is linked to phagosomal iNOS recruitment with the aim of routing bactericidal molecules to this compartment. This work demonstrated that iNOS was not localised on the phagosome in the early phase of infection (two hours p.i.). This was also independent of TNFα or IFNγ stimulation, although iNOS expression is known to be induced by these cytokines (Stuehr and Marletta, 1987a; Stuehr and Marletta, 1987b; Xie *et al.*, 1992). Furthermore, this enzyme was reported to colocalise with bacteria-containing phagosomes. However, microorganisms such as *mycobacterium tuberculosis* specifically prevent the recruitment of iNOS in order to evade its microbicidal action (Miller *et al.*, 2004). The absence of iNOS observed in *L.m.*-containing phagosomes might also constitute a pathogen driven mechanism, but this was not investigated in detail in this work (figure 3.29). In order to exclude a general impairment in RNI production in these cells, NO production was monitored systematically 24 and 48 hours after infection using Griess reagent (figure 3.30). Production of NO seemed to occur in all macrophages independent of TNF-R1 presence. Therefore, an iNOS delivering mechanism carried out by TNF-R1 to the phagosome did not seem very likely either. Monitoring recruitment of components of ROS production system, such as $p22^{phox}$, might be interesting in context with TNF-R1 signalling. Experiments regarding this aspect could be an element of further investigations.

4.4. Magnetic isolation of *Listeria monocytogenes*-containing phagosomes

An essential objective of this work was to adjust the new phagosomal isolation protocol to *L.m.*-infected J774 macrophages. This new method was developed by C. Steinhäuser from the laboratory of Dr. N. Reiling in Borstel, Germany. It has been originally used for the isolation of *mycobacteria*-containing phagosomes from BMDM. This novel protocol allows the detailed analysis of the physical and biochemical nature of pathogen-containing vacuoles in host cells. For the magnetic labelling of bacteria, a strategy based on exploiting the intercalation of lipids into biological membrane systems was used. In particular, lipopeptides have been previously reported to rapidly integrate into membrane model systems (Schromm *et al.*, 2007). Synthetic biotinylated lipopeptides were used to label microbial surface in this work. The interaction of biotin with streptavidin was used to couple magnetic beads to the bacterial surface. The specific intercalation of Lipobiotin (LB) into bacterial

membrane of *L.m.* was validated by flow cytometric analysis and subsequently prepared the pathogen for magnetic labelling (figure 3.8). Eventual influence on bacterial fate due to pathogen surface modification was considered to be negligible, as only a slight activation of macrophages was observed upon infection with labelled bacteria (see 3.3.2). Bacterial uptake and replication ability was also shown to be unimpaired for *L.m.* upon magnetic labelling (see 3.3.3). One of the essential steps in this protocol is the controlled disruption of the macrophages' plasma membrane without causing harm to the phagosomal membranes. Sonication of these cells with short-intervalled, low-intensity pulses permitted fulfilment of these requirements. Transmission electron microscopy (TEM) revealed the intact shape of the phagosomal membrane after this procedure, demonstrating the applicability of disruption by ultrasonics (figure 3.12, G and H and 7.2). Magnetism has been a common tool for magnetic cell separation in cell biology for many years. In recent studies phagosomes have also been isolated with the use of this separation principle (Lonnbro *et al.*, 2008; Pethe *et al.*, 2004). The magnetic isolation of labelled bacterial phagosomes in this work was carried out in a custom built chamber with a novel matrix free flow column. The system generates a high gradient magnetic field focussing on the inner wall of the column, allowing attachment of the phagosomal compartments which contain magnetic labelled bacteria. Therein, these samples are completely protected from any contact to ferromagnetic materials and can easily be rinsed by vertical flow-through. In contrast to elaborate phagosome-isolation protocols which are based on density centrifugation, this new protocol works effectively and is carried out relatively fast, lasting less than two hours. This was demonstrated with the specific enrichment of *L.m.*-containing phagosomes shown by TEM (figure 3.12F) and by Western blot (figure 3.13; 3.20; 3.24 and 3.28). In sum, this novel labelling technique combined with the unique isolation procedure provided an efficient protocol for isolation of *L.m*.-containing phagosomes. Based on the small amounts of cells which are needed ($2x10^7$) and the easy handling of this protocol, it permits molecular snapshots with short kinetics. This work was able to validate this isolation protocol as a convenient method for the investigation of specific changes induced by the cytokines TNFα and IFNγ on the *L.m.*-containing phagosomes and will consequently be employed for further studies.

4.5. Conclusion and Perspective

TNF-R1 and the related signalling component CTSD have been shown to be instrumental in the eradication process of intracellular pathogens such as *L.m*. (Pfeffer *et al.,* 1993; Cerro-Vadillo *et al.*, 2006; Carrasco-Marin *et al.*, 2009). The hypothesis of this work was that the generation of a "TNFα-activated phagolysosome" after internalisation of TNF-R1 and fusion with the bacteria-containing phagosome could be a mechanism which creates an antimicrobial environment against intracellular bacteria. This hypothetical compartment was shown to exist through various methods. The evidence of fusion events comprising TNF-R1-receptosomes and *L.m.*-containing phagosomes was the most striking result of this work. Further investigations revealed the existence of other molecules that are involved in listerial eradication, in context with TNF-R1 signalling.

The findings of this study showed that CTSD is activated by TNFα on the *L.m*.-containing phagosomes in J774 macrophages. In addition, infection of primary cells could not demonstrate any alterations in CTSD activation on the phagosomes, challenging the indispensability of CTSD for the bacterial eradication process in general.

Furthermore, the newly protocol of phagosome isolation allows a detailed analysis of a variety of proteins recruited to phagosomes, which may contribute to the effective killing of intracellular bacteria. The specific role of cytokines, such as IFNγ and TNFα, in this eradication process are still not fully understood and will certainly be a matter of interest in future work. The data presented in this study demonstrated that the underlying molecular mechanisms of bacterial killing are very complex and can not be addressed to one key molecule. The experiments of this study shed light on some molecules which might be involved in TNF-R1 mediated listericidal mechanisms. Not only Rab5 seemed to be an interesting candidate in this particular context (see 4.2.4), but also well-known molecular bactericidal components such as ROS seemed to be strongly related to TNF-R1 dependent mechanisms (see 4.3). Therefore, it is of further interest to have a closer look at components of ROS generation, such as $p22^{phox}$, and their influence on bacterial fate in phagosomes. Furthermore, for effective bacterial killing, cytokine driven mechanisms must be rapid enough to reach the virulent pathogen *L.m*. before it escapes from the phagosomal compartment. The characterisation of phagosomes containing the *L.m*. virulent strain (EGDe), as well as the analysis of shorter kinetics (3-10 min), will presumably provide more detailed insights into the macrophage-pathogen interaction and the influence of cytokines on this biological relationship.

To analyse the precise listericidal mechanisms dependent on TNF-R1-internalisation, infection studies with macrophages carrying an internalisation deficient TNF-R1 (TNF-R1 Δ TRID) should render further knowledge about this intricate process. TNF-R1 seems to be a key player in bactericidal mechanisms

and its now confirmed presence in bacteria-containing phagosomes has opened new prospects in the involvement of molecules that are related to this specific receptor.

5. References

Aaronson DS and Horvath CM (2002). A road map for those who don't know JAK-STAT. Science 296. 1653-1655.

Adam D, Wiegmann K, Adam-Klages S, Ruff A, Kronke M (1996). A novel cytoplasmic domain of the p55 tumor necrosis factor receptor initiates the neutral sphingomyelinase pathway. J Biol Chem 271. 14617-14622.

Adam-Klages S, Adam D, Wiegmann K, Struve S, Kolanus W, Schneider-Mergener J, Kronke M (1996). FAN, a novel WD-repeat protein, couples the p55 TNF-receptor to neutral sphingomyelinase. Cell 86. 937-947.

Aktan F (2004). iNOS-mediated nitric oxide production and its regulation Life Sci 75. 639-653.

Alvarez-Dominguez C, Barbieri AM, Beron W, Wandinger-Ness A, Stahl PD (1996). Phagocytosed live Listeria monocytogenes influences Rab5-regulated in vitro phagosome-endosome fusion. J Biol Chem 271.13834-13843.

Alvarez-Dominguez C, Madrazo-Toca F, Fernandez-Prieto L, Vandekerckhove J, Pareja E, Tobes R, Gomez-Lopez MT, Cerro-Vadillo E, Fresno M, Leyva-Cobian F, Carrasco-Marin E (2008). Characterization of a Listeria monocytogenes protein interfering with Rab5a. Traffic 9. 325-337.

Alvarez-Dominguez C and Stahl PD (1998). Interferon-gamma selectively induces Rab5a synthesis and processing in mononuclear cells. J Biol Chem 273. 33901-33904.

Alvarez-Dominguez C and Stahl PD (1999). Increased expression of Rab5a correlates directly with accelerated maturation of Listeria monocytogenes phagosomes. J Biol Chem 274. 11459-11462.

Baeuerle PA and Baltimore D (1996). NF-kappa B: ten years after. Cell 87. 13-20.

Beutler B, Greenwald D, Hulmes JD, Chang M, Pan YC, Mathison J, Ulevitch R, Cerami A (1985). Identity of tumour necrosis factor and the macrophage-secreted factor cachectin. Nature 316. 552-554.

Black RA, Rauch CT, Kozlosky CJ, Peschon JJ, Slack JL, Wolfson MF, Castner BJ, Stocking KL, Reddy P, Srinivasan S, Nelson N, Boiani N, Schooley KA, Gerhart M, Davis R, Fitzner JN, Johnson RS, Paxton RJ, March CJ, Cerretti DP (1997). A metalloproteinase disintegrin that releases tumour-necrosis factor-alpha from cells. Nature 385. 729-733.

Boehm U, Klamp T, Groot M, Howard JC (1997). Cellular responses to interferon-gamma. Annu Rev Immunol 15. 749-795.

Bonazzi M, Lecuit M, Cossart P (2009). Listeria monocytogenes internalin and E-cadherin: from bench to bedside. Cold Spring Harb Perspect Biol 1. a003087.

Bonifacino JS and Traub LM (2003). Signals for sorting of transmembrane proteins to endosomes and lysosomes. Annu Rev Biochem 72. 395-447.

Buchmeier NA and Schreiber RD (1985). Requirement of endogenous interferon-gamma production for resolution of Listeria monocytogenes infection. Proc Natl Acad Sci U S A 82. 7404-7408.

Carrasco-Marin E, Madrazo-Toca F, de lT, Jr., Cacho-Alonso E, Tobes R, Pareja E, Paradela A, Albar JP, Chen W, Gomez-Lopez MT, Alvarez-Dominguez C (2009a). The innate immunity role of cathepsin-D is linked to Trp-491 and Trp-492 residues of listeriolysin O. Mol Microbiol 72. 668-682.

Carrasco-Marin E, Madrazo-Toca F, de lT, Jr., Cacho-Alonso E, Tobes R, Pareja E, Paradela A, Albar JP, Chen W, Gomez-Lopez MT, Alvarez-Dominguez C (2009b). The innate immunity role of cathepsin-D is linked to Trp-491 and Trp-492 residues of listeriolysin O. Mol Microbiol 72. 668-682.

Carrero JA, Calderon B, Unanue ER (2004). Type I interferon sensitizes lymphocytes to apoptosis and reduces resistance to Listeria infection. J Exp Med 200. 535-540.

Carswell EA, Old LJ, Kassel RL, Green S, Fiore N, Williamson B (1975). An endotoxin-induced serum factor that causes necrosis of tumors. Proc Natl Acad Sci U S A 72. 3666-3670.

Cerro-Vadillo E, Madrazo-Toca F, Carrasco-Marin E, Fernandez-Prieto L, Beck C, Leyva-Cobian F, Saftig P,Alvarez-Dominguez C (2006). Cutting edge: a novel nonoxidative phagosomal mechanism exerted by cathepsin-D controls Listeria monocytogenes intracellular growth. J Immunol 176. 1321-1325.

Chan FK, Chun HJ, Zheng L, Siegel RM, Bui KL, Lenardo MJ (2000). A domain in TNF receptors that mediates ligand-independent receptor assembly and signaling. Science 288. 2351-2354.

Chang L and Karin M (2001). Mammalian MAP kinase signalling cascades. Nature 410. 37-40.

Chen G and Goeddel DV (2002). TNF-R1 signaling: a beautiful pathway. Science 296. 1634-1635.

Chico-Calero I, Suarez M, Gonzalez-Zorn B, Scortti M, Slaghuis J, Goebel W, Vazquez-Boland JA (2002). Hpt, a bacterial homolog of the microsomal glucose- 6-phosphate translocase, mediates rapid intracellular proliferation in Listeria.Proc Natl Acad Sci U S A 99. 431-436.

Coley WB (1893). *The Treatment of Malignant Tumors by Repeated Innoculations of Erysipelas: With a Report of Ten Original Cases*. American Journal of the Medical Sciences 10. 487-511.

Collazo CM, Yap GS, Sempowski GD, Lusby KC, Tessarollo L, Woude GF, Sher A, Taylor GA (2001). Inactivation of LRG-47 and IRG-47 reveals a family of interferon gamma-inducible genes with essential, pathogen-specific roles in resistance to infection. J Exp Med 194. 181-188.

Cossart P, Vicente MF, Mengaud J, Baquero F, Perez-Diaz JC, Berche P (1989). Listeriolysin O is essential for virulence of Listeria monocytogenes: direct evidence obtained by gene complementation Infect Immun 57. 3629-3636.

Dalton DK, Pitts-Meek S, Keshav S, Figari IS, Bradley A, Stewart TA (1993). Multiple defects of immune cell function in mice with disrupted interferon-gamma genes. Science 259. 1739-1742.

Desjardins M, Huber LA, Parton RG, Griffiths G (1994). Biogenesis of phagolysosomes proceeds through a sequential series of interactions with the endocytic apparatus. J Cell Biol 124. 677-688.

Devin A, Cook A, Lin Y, Rodriguez Y, Kelliher M, Liu Z (2000). The distinct roles of TRAF2 and RIP in IKK activation by TNF-R1: TRAF2 recruits IKK to TNF-R1 while RIP mediates IKK activation. Immunity 12. 419-429.

DiDonato JA, Hayakawa M, Rothwarf DM, Zandi E, Karin M (1997). A cytokine-responsive IkappaB kinase that activates the transcription factor NF-kappaB. Nature 388. 548-554.

Dong C, Davis RJ, Flavell RA (2002). MAP kinases in the immune response. Annu Rev Immunol 20. 55-72.

Duclos S, Diez R, Garin J, Papadopoulou B, Descoteaux A, Stenmark H, Desjardins M (2000). Rab5 regulates the kiss and run fusion between phagosomes and endosomes and the acquisition of phagosome leishmanicidal properties in RAW 264.7 macrophages. J Cell Sci 113 Pt 19. 3531-3541.

Ea CK, Deng L, Xia ZP, Pineda G, Chen ZJ (2006). Activation of IKK by TNFalpha requires site-specific ubiquitination of RIP1 and polyubiquitin binding by NEMO. Mol Cell 22. 245-257.

Eck MJ and Sprang SR (1989). The structure of tumor necrosis factor-alpha at 2.6 A resolution. Implications for receptor binding. J Biol Chem 264. 17595-17605.

Edelson BT and Unanue ER (2001). Intracellular antibody neutralizes Listeria growth. Immunity 14. 503-512.

Endres R, Luz A, Schulze H, Neubauer H, Futterer A, Holland SM, Wagner H, Pfeffer K (1997). Listeriosis in p47(phox-/-) and TRp55-/- mice: protection despite absence of ROI and susceptibility despite presence of RNI. Immunity 7. 419-432.

Erickson SL, de Sauvage FJ, Kikly K, Carver-Moore K, Pitts-Meek S, Gillett N, Sheehan KC, Schreiber RD, Goeddel DV, Moore MW (1994). Decreased sensitivity to tumour-necrosis factor but normal T-cell development in TNF receptor-2-deficient mice. Nature 372. 560-563.

Fadok VA, Bratton DL, Konowal A, Freed PW, Westcott JY, Henson PM (1998). Macrophages that have ingested apoptotic cells in vitro inhibit proinflammatory cytokine production through autocrine/paracrine mechanisms involving TGF-beta, PGE2, and PAF. J Clin Invest 101. 890-898.

Fruh K and Yang Y (1999). Antigen presentation by MHC class I and its regulation by interferon gamma. Curr Opin Immunol 11. 76-81.

Funato K, Beron W, Yang CZ, Mukhopadhyay A, Stahl PD (1997). Reconstitution of phagosome-lysosome fusion in streptolysin O-permeabilized cells. J Biol Chem 272. 16147-16151.

Gaillard JL, Berche P, Mounier J, Richard S, Sansonetti P (1987). In vitro model of penetration and intracellular growth of Listeria monocytogenes in the human enterocyte-like cell line Caco-2. Infect Immun 55. 2822-2829.

Gaillard JL, Jaubert F, Berche P (1996). The inlAB locus mediates the entry of Listeria monocytogenes into hepatocytes in vivo. J Exp Med 183. 359-369.

Gearing AJ, Beckett P, Christodoulou M, Churchill M, Clements J, Davidson AH, Drummond AH, Galloway WA, Gilbert R, Gordon JL, . (1994). Processing of tumour necrosis factor-alpha precursor by metalloproteinases. Nature 370. 555-557.

Geissmann F, Jung S, Littman DR (2003). Blood monocytes consist of two principal subsets with distinct migratory properties. Immunity 19. 71-82.

Gilbert RJ (2010). Cholesterol-dependent cytolysins. Adv Exp Med Biol 677. 56-66.

Gordon S and Martinez FO (2010). Alternative activation of macrophages: mechanism and functions. Immunity 32. 593-604.

Gregory SH and Wing EJ (1998). Neutrophil-Kupffer-cell interaction in host defenses to systemic infections. Immunol Today 19. 507-510.

Grell M, Douni E, Wajant H, Lohden M, Clauss M, Maxeiner B, Georgopoulos S, Lesslauer W, Kollias G, Pfizenmaier K, Scheurich P (1995). The transmembrane form of tumor necrosis factor is the prime activating ligand of the 80 kDa tumor necrosis factor receptor. Cell 83. 793-802.

Grell M, Wajant H, Zimmermann G, Scheurich P (1998). The type 1 receptor (CD120a) is the high-affinity receptor for soluble tumor necrosis factor. Proc Natl Acad Sci U S A 95. 570-575.

Grivennikov SI, Kuprash DV, Liu ZG, Nedospasov SA (2006). Intracellular signals and events activated by cytokines of the tumor necrosis factor superfamily: From simple paradigms to complex mechanisms. Int Rev Cytol 252. 129-161.

Haas A (2007). The phagosome: compartment with a license to kill. Traffic 8. 311-330.

Hamon M, Bierne H, Cossart P (2006). Listeria monocytogenes: a multifaceted model. Nat Rev Microbiol 4. 423-434.

Harrison RE, Bucci C, Vieira OV, Schroer TA, Grinstein S (2003). Phagosomes fuse with late endosomes and/or lysosomes by extension of membrane protrusions along microtubules: role of Rab7 and RILP. Mol Cell Biol 23. 6494-6506.

Hasilik A, von Figura K, Conzelmann E, Nehrkorn H, Sandhoff K (1982). Lysosomal enzyme precursors in human fibroblasts. Activation of cathepsin D precursor in vitro and activity of beta-hexosaminidase A precursor towards ganglioside GM2. Eur J Biochem 125. 317-321.

Havell EA (1987). Production of tumor necrosis factor during murine listeriosis. J Immunol 139. 4225-4231.

Hayashi F, Smith KD, Ozinsky A, Hawn TR, Yi EC, Goodlett DR, Eng JK, Akira S, Underhill DM, Aderem A (2001). The innate immune response to bacterial flagellin is mediated by Toll-like receptor 5. Nature 410. 1099-1103.

Hayden MS and Ghosh S (2008). Shared principles in NF-kappaB signaling. Cell 132. 344-362.

Hehlgans T and Pfeffer K (2005). The intriguing biology of the tumour necrosis factor/tumour necrosis factor receptor superfamily: players, rules and the games. Immunology 115. 1-20.

Heinrich M, Neumeyer J, Jakob M, Hallas C, Tchikov V, Winoto-Morbach S, Wickel M, Schneider-Brachert W, Trauzold A, Hethke A, Schutze S (2004). Cathepsin D links TNF-induced acid sphingomyelinase to Bid-mediated caspase-9 and -3 activation. Cell Death Differ 11. 550-563.

Heinrich M, Wickel M, Schneider-Brachert W, Sandberg C, Gahr J, Schwandner R, Weber T, Saftig P, Peters C, Brunner J, Kronke M, Schutze S (1999). Cathepsin D targeted by acid sphingomyelinase-derived ceramide. EMBO J 18. 5252-5263.

Heinrich M, Wickel M, Winoto-Morbach S, Schneider-Brachert W, Weber T, Brunner J, Saftig P, Peters C, Kronke M, Schutze S (2000). Ceramide as an activator lipid of cathepsin D. Adv Exp Med Biol 477. 305-315.

Hesse M, Modolell M, La Flamme AC, Schito M, Fuentes JM, Cheever AW, Pearce EJ, Wynn TA (2001). Differential regulation of nitric oxide synthase-2 and arginase-1 by type 1/type 2 cytokines in vivo: granulomatous pathology is shaped by the pattern of L-arginine metabolism. J Immunol 167. 6533-6544.

Hibbs JB, Jr. (2002). Infection and nitric oxide. J Infect Dis 185 Suppl 1. S9-17.

Hoff A, Andre T, Schaffer TE, Jung G, Wiesmuller KH, Brock R (2002). Lipoconjugates for the noncovalent generation of microarrays in biochemical and cellular assays. Chembiochem 3. 1183-1191.

Hsu H, Huang J, Shu HB, Baichwal V, Goeddel DV (1996a). TNF-dependent recruitment of the protein kinase RIP to the TNF receptor-1 signaling complex. Immunity 4. 387-396.

Hsu H, Shu HB, Pan MG, Goeddel DV (1996b). TRADD-TRAF2 and TRADD-FADD interactions define two distinct TNF receptor 1 signal transduction pathways. Cell 84. 299-308.

Hsu H, Xiong J, Goeddel DV (1995). The TNF receptor 1-associated protein TRADD signals cell death and NF-kappa B activation. Cell 81. 495-504.

Hu Y, Baud V, Delhase M, Zhang P, Deerinck T, Ellisman M, Johnson R, Karin M (1999). Abnormal morphogenesis but intact IKK activation in mice lacking the IKKalpha subunit of IkappaB kinase. Science 284. 316-320.

Huang S, Hendriks W, Althage A, Hemmi S, Bluethmann H, Kamijo R, Vilcek J, Zinkernagel RM, Aguet M (1993). Immune response in mice that lack the interferon-gamma receptor. Science 259. 1742-1745.

James MN and Sielecki AR (1986). Molecular structure of an aspartic proteinase zymogen, porcine pepsinogen, at 1.8 A resolution. Nature 319. 33-38.

Jiang J, Zenewicz LA, San Mateo LR, Lau LL, Shen H (2003). Activation of antigen-specific CD8 T cells results in minimal killing of bystander bacteria. J Immunol 171. 6032-6038.

Jin MS and Lee JO (2008). Structures of the toll-like receptor family and its ligand complexes. Immunity 29. 182-191.

Jin Z and El Deiry WS (2006). Distinct signaling pathways in T. Mol Cell Biol 26. 8136-8148.

Jones EY, Stuart DI, Walker NP (1989). Structure of tumour necrosis factor. Nature 338. 225-228.

Jordens I, Marsman M, Kuijl C, Neefjes J (2005). Rab proteins, connecting transport and vesicle fusion. Traffic 6. 1070-1077.

Kagi D, Ledermann B, Burki K, Hengartner H, Zinkernagel RM (1994). CD8+ T cell-mediated protection against an intracellular bacterium by perforin-dependent cytotoxicity. Eur J Immunol 24. 3068-3072.

Karin M and Lin A (2002). NF-kappaB at the crossroads of life and death. Nat Immunol 3. 221-227.

Karunasagar I, Senghaas B, Krohne G, Goebel W (1994). Ultrastructural study of Listeria monocytogenes entry into cultured human colonic epithelial cells. Infect Immun 62. 3554-3558.

Kikuchi H, Iizuka R, Sugiyama S, Gon G, Mori H, Arai M, Mizumoto K, Imajoh-Ohmi S (1996). Monocytic differentiation modulates apoptotic response to cytotoxic anti-Fas antibody and tumor necrosis factor alpha in human monoblast U937 cells. J Leukoc Biol 60. 778-783.

Kim YS, Morgan MJ, Choksi S, Liu ZG (2007). TNF-induced activation of the Nox1 NADPH oxidase and its role in the induction of necrotic cell death. Mol Cell 26. 675-687.

Kotlyarov A, Neininger A, Schubert C, Eckert R, Birchmeier C, Volk HD, Gaestel M (1999). MAPKAP kinase 2 is essential for LPS-induced TNF-alpha biosynthesis. Nat Cell Biol 1. 94-97.

Kreider T, Anthony RM, Urban JF, Jr., Gause WC (2007). Alternatively activated macrophages in helminth infections. Curr Opin Immunol 19. 448-453.

Laemmli UK (1970). Cleavage of structural proteins during the assembly of the head of bacteriophage T4. Nature 227. 680-685.

Langermans JA, van der Hulst ME, Nibbering PH, Hiemstra PS, Fransen L, Van Furth R (1992). IFN-gamma-induced L-arginine-dependent toxoplasmastatic activity in murine peritoneal macrophages is mediated by endogenous tumor necrosis factor-alpha. J Immunol 148. 568-574.

Laurent-Matha V, Derocq D, Prebois C, Katunuma N, Liaudet-Coopman E (2006). Processing of human cathepsin D is independent of its catalytic function and auto-activation: involvement of cathepsins L and B. J Biochem 139. 363-371.

Lecuit M (2005). Understanding how Listeria monocytogenes targets and crosses host barriers. Clin Microbiol Infect 11. 430-436.

Lehner MD, Schwoebel F, Kotlyarov A, Leist M, Gaestel M, Hartung T (2002). Mitogen-activated protein kinase-activated protein kinase 2-deficient mice show increased susceptibility to Listeria monocytogenes infection. J Immunol 168. 4667-4673.

Li H, Kobayashi M, Blonska M, You Y, Lin X (2006). Ubiquitination of RIP is required for tumor necrosis factor alpha-induced NF-kappaB activation. J Biol Chem 281. 13636-13643.

Li H, Zhu H, Xu CJ, Yuan J (1998). Cleavage of BID by caspase 8 mediates the mitochondrial damage in the Fas pathway of apoptosis. Cell 94. 491-501.

Li Q, Van Antwerp D, Mercurio F, Lee KF, Verma IM (1999). Severe liver degeneration in mice lacking the IkappaB kinase 2 gene. Science 284. 321-325.

Li Q and Verma IM (2002). NF-kappaB regulation in the immune system. Nat Rev Immunol 2. 725-734.

Liao W, Xiao Q, Tchikov V, Fujita K, Yang W, Wincovitch S, Garfield S, Conze D, El Deiry WS, Schutze S, Srinivasula SM (2008). CARP-2 is an endosome-associated ubiquitin ligase for RIP and regulates TNF-induced NF-kappaB activation. Curr Biol 18. 641-649.

Locksley RM, Killeen N, Lenardo MJ (2001). The TNF and TNF receptor superfamilies: integrating mammalian biology. Cell 104. 487-501.

Lonnbro P, Nordenfelt P, Tapper H (2008). Isolation of bacteria-containing phagosomes by magnetic selection. BMC Cell Biol 9. 35.

Lukacs GL, Rotstein OD, Grinstein S (1990). Phagosomal acidification is mediated by a vacuolar-type H(+)-ATPase in murine macrophages. J Biol Chem 265. 21099-21107.

Luo X, Budihardjo I, Zou H, Slaughter C, Wang X (1998). Bid, a Bcl2 interacting protein, mediates cytochrome c release from mitochondria in response to activation of cell surface death receptors. Cell 94. 481-490.

Luzio JP, Pryor PR, Gray SR, Gratian MJ, Piper RC, Bright NA (2005). Membrane traffic to and from lysosomes. Biochem Soc Symp 77-86.

Mackaness GB (1962). Cellular resistance to infection. J Exp Med 116. 381-406.

MacMicking J, Xie QW, Nathan C (1997). Nitric oxide and macrophage function. Annu Rev Immunol 15. 323-350.

MacMicking JD, Taylor GA, McKinney JD (2003). Immune control of tuberculosis by IFN-gamma-inducible LRG-47. Science 302. 654-659.

McCollister BD, Myers JT, Jones-Carson J, Voelker DR, Vazquez-Torres A (2007). Constitutive acid sphingomyelinase enhances early and late macrophage killing of Salmonella enterica serovar Typhimurium. Infect Immun 75. 5346-5352.

Mengaud J, Chenevert J, Geoffroy C, Gaillard JL, Cossart P (1987). Identification of the structural gene encoding the SH-activated hemolysin of Listeria monocytogenes: listeriolysin O is homologous to streptolysin O and pneumolysin. Infect Immun 55. 3225-3227.

Micheau O and Tschopp J (2003). Induction of TNF receptor I-mediated apoptosis via two sequential signaling complexes. Cell 114. 181-190.

Miller BH, Fratti RA, Poschet JF, Timmins GS, Master SS, Burgos M, Marletta MA, Deretic V (2004). Mycobacteria inhibit nitric oxide synthase recruitment to phagosomes during macrophage infection. Infect Immun 72. 2872-2878.

Moller W, Nemoto I, Matsuzaki T, Hofer T, Heyder J (2000). Magnetic phagosome motion in J774A.1 macrophages: influence of cytoskeletal drugs. Biophys J 79. 720-730.

Mosser DM (2003). The many faces of macrophage activation. J Leukoc Biol 73. 209-212.

Mosser DM and Edwards JP (2008). Exploring the full spectrum of macrophage activation. Nat Rev Immunol 8. 958-969.

Mu FT, Callaghan JM, Steele-Mortimer O, Stenmark H, Parton RG, Campbell PL, McCluskey J, Yeo JP, Tock EP, Toh BH (1995). EEA1, an early endosome-associated protein. EEA1 is a conserved alpha-helical peripheral membrane protein flanked by cysteine "fingers" and contains a calmodulin-binding IQ motif. J Biol Chem 270. 13503-13511.

Muller M, Althaus R, Frohlich D, Frei K, Eugster HP (1999). Reduced antilisterial activity of TNF-deficient bone marrow-derived macrophages is due to impaired superoxide production. Eur J Immunol 29. 3089-3097.

Munro JM, Pober JS, Cotran RS (1989). Tumor necrosis factor and interferon-gamma induce distinct patterns of endothelial activation and associated leukocyte accumulation in skin of Papio anubis. Am J Pathol 135. 121-133.

Murray HW (1988). Interferon-gamma, the activated macrophage, and host defense against microbial challenge. Ann Intern Med 108. 595-608.

Myers JT, Tsang AW, Swanson JA (2003). Localized reactive oxygen and nitrogen intermediates inhibit escape of Listeria monocytogenes from vacuoles in activated macrophages. J Immunol 171. 5447-5453.

Nakane A and Minagawa T (1984). The significance of alpha/beta interferons and gamma interferon producedin mice infected with Listeria monocytogenes. Cell Immunol 88. 29-40.

Nakane A, Minagawa T, Kato K (1988). Endogenous tumor necrosis factor (cachectin) is essential to host resistance against Listeria monocytogenes infection. Infect Immun 56. 2563-2569.

Nathan C (1991). Mechanisms and modulation of macrophage activation. Behring Inst Mitt 200-207.

Nathan C (2008). Metchnikoff's Legacy in 2008. Nat Immunol 9. 695-698.

Nathan CF (1987). Secretory products of macrophages. J Clin Invest 79. 319-326.

Nauseef WM (2004). Assembly of the phagocyte NADPH oxidase. Histochem Cell Biol 122. 277-291.

Nedwin GE, Svedersky LP, Bringman TS, Palladino MA, Jr., Goeddel DV (1985). Effect of interleukin 2, interferon-gamma, and mitogens on the production of tumor necrosis factors alpha and beta. J Immunol 135. 2492-2497.

Neumeyer J, Hallas C, Merkel O, Winoto-Morbach S, Jakob M, Thon L, Adam D, Schneider-Brachert W, Schutze S (2006). TNF-receptor I defective in internalization allows for cell death through activation of neutralsphingomyelinase. Exp Cell Res 312. 2142-2153.

Bruns P. (1888). *Die Heilwirkung des Erysipels auf Geschwülste*. Beitr Klin Chir 3 443-466.

Pamer EG (2004). Immune responses to Listeria monocytogenes. Nat Rev Immunol 4. 812-823.

Park SF and Stewart GS (1990). High-efficiency transformation of Listeria monocytogenes by electroporation of penicillin-treated cells. Gene 94. 129-132.

Pestka S, Krause CD, Walter MR (2004). Interferons, interferon-like cytokines, and their receptors. Immunol Rev 202. 8-32.

Pethe K, Swenson DL, Alonso S, Anderson J, Wang C, Russell DG (2004). Isolation of Mycobacterium tuberculosis mutants defective in the arrest of phagosome maturation. Proc Natl Acad Sci U S A 101. 13642-13647.

Pfeffer K, Matsuyama T, Kundig TM, Wakeham A, Kishihara K, Shahinian A, Wiegmann K, Ohashi PS, Kronke M, Mak TW (1993). Mice deficient for the 55 kd tumor necrosis factor receptor are resistant to endotoxic shock, yet succumb to L. monocytogenes infection. Cell 73. 457-467.

Platanias LC (2003). The p38 mitogen-activated protein kinase pathway and its role in interferon signaling. Pharmacol Ther 98. 129-142.

Platanias LC (2005). Mechanisms of type-I- and type-II-interferon-mediated signalling. Nat Rev Immunol 5. 375-386.

Platanias LC and Fish EN (1999). Signaling pathways activated by interferons. Exp Hematol 27. 1583-1592.

Plitz T, Huffstadt U, Endres R, Schaller E, Mak TW, Wagner H, Pfeffer K (1999). The resistance against Listeria monocytogenes and the formation of germinal centers depend on a functional death domain of the 55 kDa tumor necrosisfactor receptor. Eur J Immunol 29. 581-591.

Pluddemann A, Mukhopadhyay S, Gordon S (2011). Innate immunity to intracellular pathogens: macrophage receptors and responses to microbial entry. Immunol Rev 240. 11-24.

Portnoy DA, Schreiber RD, Connelly P, Tilney LG (1989). Gamma interferon limits access of Listeria monocytogenes to the macrophage cytoplasm. J Exp Med 170. 2141-2146.

Prada-Delgado A, Carrasco-Marin E, Bokoch GM, Alvarez-Dominguez C (2001). Interferon-gamma listericidal action is mediated by novel Rab5a functions at the phagosomal environment. J Biol Chem 276. 19059-19065.

Prada-Delgado A, Carrasco-Marin E, Pena-Macarro C, Cerro-Vadillo E, Fresno-Escudero M, Leyva-Cobian F, Alvarez-Dominguez C (2005). Inhibition of Rab5a exchange activity is a key step for Listeria monocytogenes survival. Traffic 6. 252-265.

Rahman MM and McFadden G (2006). Modulation of tumor necrosis factor by microbial pathogens. PLoS Pathog 2. e4.

Ralph P, Moore MA, Nilsson K (1976). Lysozyme synthesis by established human and murine histiocytic lymphoma cell lines. J Exp Med 143. 1528-1533.

Reeves EP, Lu H, Jacobs HL, Messina CG, Bolsover S, Gabella G, Potma EO, Warley A, Roes J, Segal AW (2002). Killing activity of neutrophils is mediated through activation of proteases by K+ flux. Nature 416. 291-297.

Rodriguez J and Lazebnik Y (1999). Caspase-9 and APAF-1 form an active holoenzyme. Genes Dev 13. 3179-3184.

Rollins BJ, Yoshimura T, Leonard EJ, Pober JS (1990). Cytokine-activated human endothelial cells synthesize and secrete a monocyte chemoattractant, MCP-1/JE. Am J Pathol 136. 1229-1233.

Rothe J, Lesslauer W, Lotscher H, Lang Y, Koebel P, Kontgen F, Althage A, Zinkernagel R, Steinmetz M, Bluethmann H (1993). Mice lacking the tumour necrosis factor receptor 1 are resistant to TNF-mediated toxicity but highly susceptible to infection by Listeria monocytogenes. Nature 364. 798-802.

Russell DG (2001). Mycobacterium tuberculosis: here today, and here tomorrow. Nat Rev Mol Cell Biol 2. 569-577.

Rutschman R, Lang R, Hesse M, Ihle JN, Wynn TA, Murray PJ (2001). Cutting edge: Stat6-dependent substrate depletion regulates nitric oxide production. J Immunol 166. 2173-2177.

Rybin V, Ullrich O, Rubino M, Alexandrov K, Simon I, Seabra MC, Goody R, Zerial M (1996). GTPase activity of Rab5 acts as a timer for endocytic membrane fusion. Nature 383. 266-269.

Safley SA, Jensen PE, Reay PA, Ziegler HK (1995). Mechanisms of T cell epitope immunodominance analyzed in murine listeriosis. J Immunol 155. 4355-4366.

Saftig P, Hetman M, Schmahl W, Weber K, Heine L, Mossmann H, Koster A, Hess B, Evers M, von Figura K, . (1995). Mice deficient for the lysosomal proteinase cathepsin D exhibit progressive atrophy of the intestinal mucosa and profound destruction of lymphoid cells. EMBO J 14. 3599-3608.

Scaffidi C, Krammer PH, Peter ME (1999). Isolation and analysis of components of CD95 (APO-1/Fas) death-inducing signaling complex. Methods 17. 287-291.

Schneider-Brachert W, Tchikov V, Neumeyer J, Jakob M, Winoto-Morbach S, Held-Feindt J, Heinrich M, Merkel O, Ehrenschwender M, Adam D, Mentlein R, Kabelitz D, Schutze S (2004). Compartmentalization of TNF receptor 1 signaling: internalized TNF receptosomes as death signaling vesicles. Immunity 21. 415-428.

Schnupf P, Portnoy DA, Decatur AL (2006). Phosphorylation, ubiquitination and degradation of listeriolysin O in mammalian cells: role of the PEST-like sequence. Cell Microbiol 8. 353-364.

Schramm M, Herz J, Haas A, Kronke M, Utermohlen O (2008). Acid sphingomyelinase is required for efficient phago-lysosomal fusion. Cell Microbiol 10. 1839-1853.

Schromm AB, Howe J, Ulmer AJ, Wiesmuller KH, Seyberth T, Jung G, Rossle M, Koch MH, Gutsmann T, Brandenburg K (2007). Physicochemical and biological analysis of synthetic bacterial lipopeptides: validity of the concept of endotoxic conformation. J Biol Chem 282. 11030-11037.

Schuerch DW, Wilson-Kubalek EM, Tweten RK (2005). Molecular basis of listeriolysin O pH dependence. Proc Natl Acad Sci U S A 102. 12537-12542.

Schutze S, Tchikov V, Schneider-Brachert W (2008). Regulation of TNFR1 and CD95 signalling by receptor compartmentalization. Nat Rev Mol Cell Biol 9. 655-662.

Segal AW (2005). How neutrophils kill microbes. Annu Rev Immunol 23. 197-223.

Seki E, Tsutsui H, Tsuji NM, Hayashi N, Adachi K, Nakano H, Futatsugi-Yumikura S, Takeuchi O, Hoshino K, Akira S, Fujimoto J, Nakanishi K (2002). Critical roles of myeloid differentiation factor 88-dependent proinflammatory cytokine release in early phase clearance of Listeria monocytogenes in mice. J Immunol 169. 3863-3868.

Shaughnessy LM, Hoppe AD, Christensen KA, Swanson JA (2006). Membrane perforations inhibit lysosome fusion by altering pH and calcium in Listeria monocytogenes vacuoles. Cell Microbiol 8. 781-792.

Shen Y, Naujokas M, Park M, Ireton K (2000). InIB-dependent internalization of Listeria is mediated by the Met receptor tyrosine kinase. Cell 103. 501-510.

Shi Y (2006). Mechanical aspects of apoptosome assembly. Curr Opin Cell Biol 18. 677-684.

Shiloh MU, MacMicking JD, Nicholson S, Brause JE, Potter S, Marino M, Fang F, Dinauer M, Nathan C (1999). Phenotype of mice and macrophages deficient in both phagocyte oxidase and inducible nitric oxide synthase. Immunity 10. 29-38.

Shtrichman R and Samuel CE (2001). The role of gamma interferon in antimicrobial immunity. Curr Opin Microbiol 4. 251-259.

Siebenlist U, Franzoso G, Brown K (1994). Structure, regulation and function of NF-kappa B. Annu Rev Cell Biol 10. 405-455.

Siegel RM, Chan FK, Chun HJ, Lenardo MJ (2000). The multifaceted role of Fas signaling in immune cell homeostasis and autoimmunity. Nat Immunol 1. 469-474.

Singh R, Jamieson A, Cresswell P (2008). GILT is a critical host factor for Listeria monocytogenes infection. Nature 455. 1244-1247.

Sirard JC, Fayolle C, de Chastellier C, Mock M, Leclerc C, Berche P (1997). Intracytoplasmic delivery of listeriolysin O by a vaccinal strain of Bacillus anthracis induces CD8-mediated protection against Listeria monocytogenes. J Immunol 159. 4435-4443.

Smith CA, Farrah T, Goodwin RG (1994). The TNF receptor superfamily of cellular and viral proteins: activation, costimulation, and death. Cell 76. 959-962.

Smith GA, Marquis H, Jones S, Johnston NC, Portnoy DA, Goldfine H (1995). The two distinct phospholipases C of Listeria monocytogenes have overlapping roles in escape from a vacuole and cell-to-cell spread. Infect Immun 63. 4231-4237.

Sousa S, Lecuit M, Cossart P (2005). Microbial strategies to target, cross or disrupt epithelia. Curr Opin Cell Biol 17. 489-498.

Stanger BZ, Leder P, Lee TH, Kim E, Seed B (1995). RIP: a novel protein containing a death domain that interacts with Fas/APO-1 (CD95) in yeast and causes cell death. Cell 81. 513-523.

Stenmark H, Parton RG, Steele-Mortimer O, Lutcke A, Gruenberg J, Zerial M (1994). Inhibition of rab5 GTPase activity stimulates membrane fusion in endocytosis. EMBO J 13. 1287-1296.

Strassmann G, Patil-Koota V, Finkelman F, Fong M, Kambayashi T (1994). Evidence for the involvement of interleukin 10 in the differential deactivation of murine peritoneal macrophages by prostaglandin E2. J Exp Med 180. 2365-2370.

Stritzker J and Goebel W (2004). Listeria monocytogenes infection-dependent transfer of exogenously added DNA to fibroblast COS-1 cells. Mol Genet Genomics 272. 497-503.

Stuehr DJ and Marletta MA (1987a). Induction of nitrite/nitrate synthesis in murine macrophages by BCG infection, lymphokines, or interferon-gamma. J Immunol 139. 518-525.

Stuehr DJ and Marletta MA (1987b). Synthesis of nitrite and nitrate in murine macrophage cell lines. Cancer Res 47. 5590-5594.

Sturgill-Koszycki S, Schaible UE, Russell DG (1996). Mycobacterium-containing phagosomes are accessible to early endosomes and reflect a transitional state in normal phagosome biogenesis. EMBO J 15. 6960-6968.

Takeshima H, Sakaguchi M, Mihara K, Murakami K, Omura T (1995). Intracellular targeting of lysosomal cathepsin D in COS cells. J Biochem 118. 981-988.

Tartaglia LA, Pennica D, Goeddel DV (1993). Ligand passing: the 75-kDa tumor necrosis factor (TNF) receptor recruits TNF for signaling by the 55-kDa TNF receptor. J Biol Chem 268. 18542-18548.

Tartaglia LA, Weber RF, Figari IS, Reynolds C, Palladino MA, Jr., Goeddel DV (1991). The two different receptors for tumor necrosis factor mediate distinct cellular responses. Proc Natl Acad Sci U S A 88. 9292-9296.

Tchikov V and Schutze S (2008). Immunomagnetic isolation of tumor necrosis factor receptosomes. Methods Enzymol 442. 101-123.

Tilney LG and Portnoy DA (1989). Actin filaments and the growth, movement, and spread of the intracellular bacterial parasite, Listeria monocytogenes. J Cell Biol 109. 1597-1608.

Tiwari S, Choi HP, Matsuzawa T, Pypaert M, MacMicking JD (2009). Targeting of the GTPase Irgm1 to the phagosomal membrane via PtdIns(3,4)P(2) and PtdIns(3,4,5)P(3) promotes immunity to mycobacteria. Nat Immunol 10. 907-917.

Towbin H, Staehelin T, Gordon J (1979). Electrophoretic transfer of proteins from polyacrylamide gels to nitrocellulose sheets: procedure and some applications. Proc Natl Acad Sci U S A 76. 4350-4354.

Toyohara A and Inaba K (1989). Transport of phagosomes in mouse peritoneal macrophages. J Cell Sci 94 (Pt 1). 143-153.

Tripp CS, Wolf SF, Unanue ER (1993). Interleukin 12 and tumor necrosis factor alpha are costimulators of interferon gamma production by natural killer cells in severe combined immunodeficiency mice with listeriosis, and interleukin 10 is a physiologic antagonist. Proc Natl Acad Sci U S A 90. 3725-3729.

Turrens JF and Boveris A (1980). Generation of superoxide anion by the NADH dehydrogenase of bovine heart mitochondria. Biochem J 191. 421-427.

Unanue ER (1997). Studies in listeriosis show the strong symbiosis between the innate cellular system and the T-cell response. Immunol Rev 158. 11-25.

Utermohlen O, Herz J, Schramm M, Kronke M (2008). Fusogenicity of membranes: the impact of acid sphingomyelinase on innate immune responses. Immunobiology 213. 307-314.

Utermohlen O, Karow U, Lohler J, Kronke M (2003). Severe impairment in early host defense against Listeria monocytogenes in mice deficient in acid sphingomyelinase. J Immunol 170. 2621-2628.

Varinou L, Ramsauer K, Karaghiosoff M, Kolbe T, Pfeffer K, Muller M, Decker T (2003). Phosphorylation of the Stat1 transactivation domain is required for full-fledged IFN-gamma-dependent innate immunity. Immunity 19. 793-802.

Vazquez-Boland JA, Kuhn M, Berche P, Chakraborty T, Dominguez-Bernal G, Goebel W, Gonzalez-Zorn B, Wehland J, Kreft J (2001). Listeria pathogenesis and molecular virulence determinants. Clin Microbiol Rev 14. 584-640.

Vazquez-Torres A, Fantuzzi G, Edwards CK, III, Dinarello CA, Fang FC (2001). Defective localization of the NADPH phagocyte oxidase to Salmonella-containing phagosomes in tumor necrosis factor p55 receptor-deficient macrophages. Proc Natl Acad Sci U S A 98. 2561-2565.

Vieira OV, Botelho RJ, Grinstein S (2002). Phagosome maturation: aging gracefully. Biochem J 366. 689-704.

Wajant H (2003). Death receptors. Essays Biochem 39. 53-71.

Wang CY, Mayo MW, Korneluk RG, Goeddel DV, Baldwin AS, Jr. (1998). NF-kappaB antiapoptosis: induction of TRAF1 and TRAF2 and c-IAP1 and c-IAP2 to suppress caspase-8 activation. Science 281. 1680-1683.

Wang X (2001). The expanding role of mitochondria in apoptosis. Genes Dev 15. 2922-2933.

Wertz IE, O'Rourke KM, Zhou H, Eby M, Aravind L, Seshagiri S, Wu P, Wiesmann C, Baker R, Boone DL, Ma A, Koonin EV, Dixit VM (2004). De-ubiquitination and ubiquitin ligase domains of A20 downregulate NF-kappaB signalling. Nature 430. 694-699.

Wesemann DR and Benveniste EN (2003). STAT-1 alpha and IFN-gamma as modulators of TNF-alpha signaling in macrophages: regulation and functional implications of the TNF receptor 1:STAT-1 alpha complex. J Immunol 171. 5313-5319.

White DW and Harty JT (1998). Perforin-deficient CD8+ T cells provide immunity to Listeria monocytogenes by a mechanism that is independent of CD95 and IFN-gamma but requires TNF-alpha. J Immunol 160. 898-905.

Xie QW, Cho HJ, Calaycay J, Mumford RA, Swiderek KM, Lee TD, Ding A, Troso T, Nathan C (1992). Cloning and characterization of inducible nitric oxide synthase from mouse macrophages. Science 256. 225-228.

Yates RM, Hermetter A, Russell DG (2005). The kinetics of phagosome maturation as a function of phagosome/lysosome fusion and acquisition of hydrolytic activity. Traffic 6. 413-420.

Yazdanpanah B, Wiegmann K, Tchikov V, Krut O, Pongratz C, Schramm M, Kleinridders A, Wunderlich T, Kashkar H, Utermohlen O, Bruning JC, Schutze S, Kronke M (2009). Riboflavin kinase couples TNF receptor 1 to NADPH oxidase. Nature 460. 1159-1163.

Youle RJ and Strasser A (2008). The BCL-2 protein family: opposing activities that mediate cell death. Nat Rev Mol Cell Biol 9. 47-59.

Zaidi N, Maurer A, Nieke S, Kalbacher H (2008). Cathepsin D: a cellular roadmap. Biochem Biophys Res Commun 376. 5-9.

Zheng L, Bidere N, Staudt D, Cubre A, Orenstein J, Chan FK, Lenardo M (2006). Competitive control of independent programs of tumor necrosis factor receptor-induced cell death by TRADD and RIP1. Mol Cell Biol 26. 3505-3513.

Zou H, Li Y, Liu X, Wang X (1999). An APAF-1.cytochrome c multimeric complex is a functional apoptosome that activates procaspase-9. J Biol Chem 274. 11549-11556.

6. List of figures and tables

Figures

Tables

7. Appendix

7.1. TEM of magnetic labelled *Listeria monocytogenes* in J774 macrophages

Unstimulated J774 macrophages

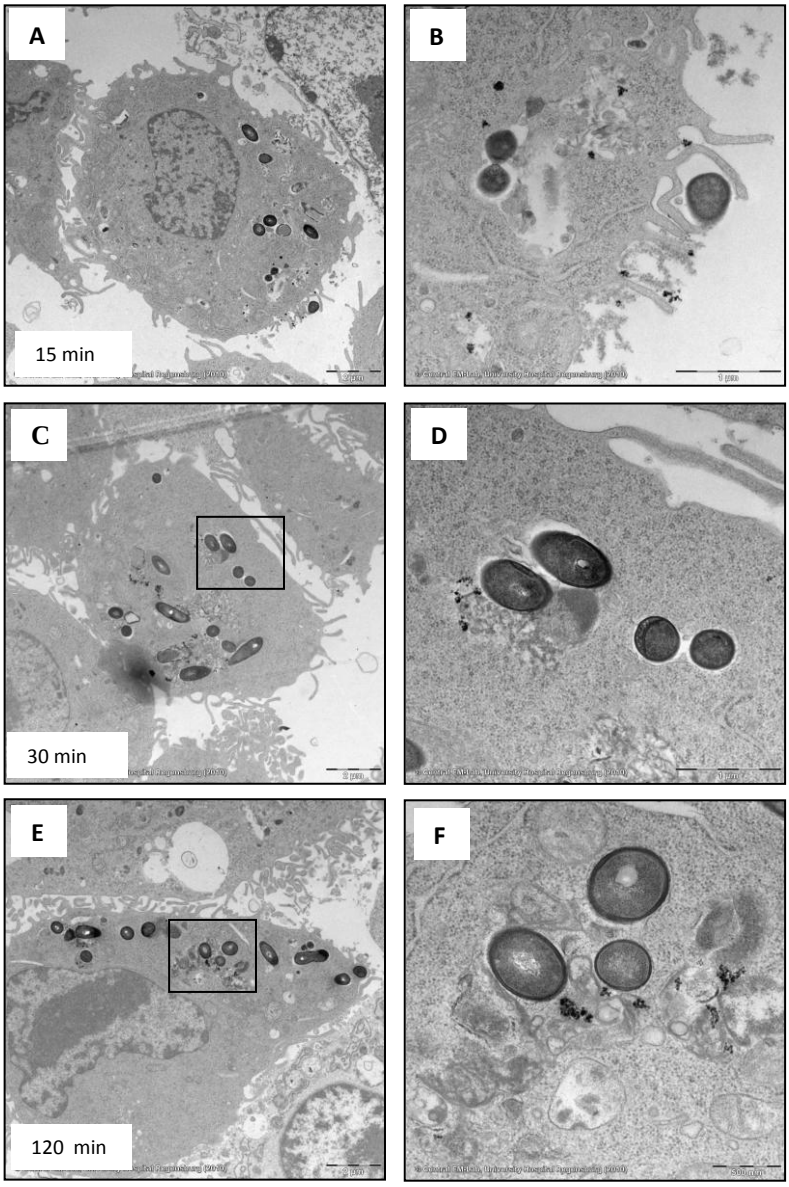

TNFα stimulated J774 macrophages

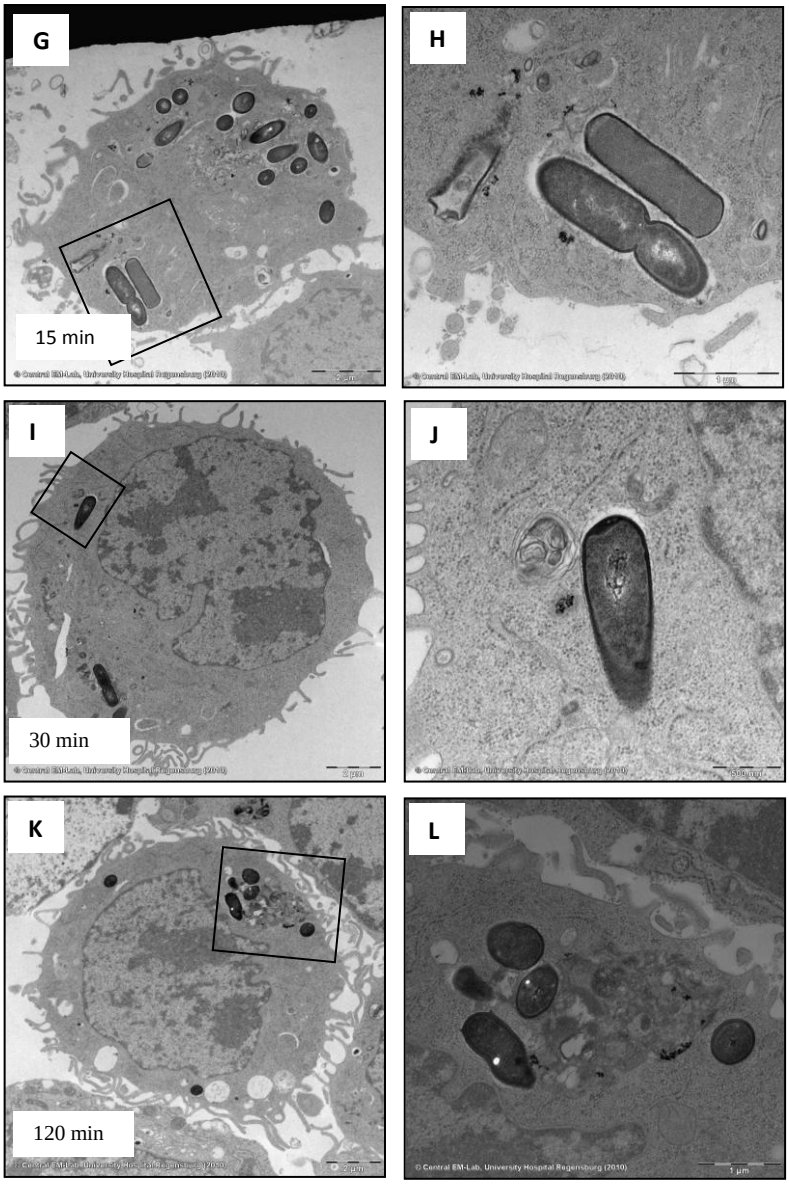

IFNγ stimulated J774 macrophages

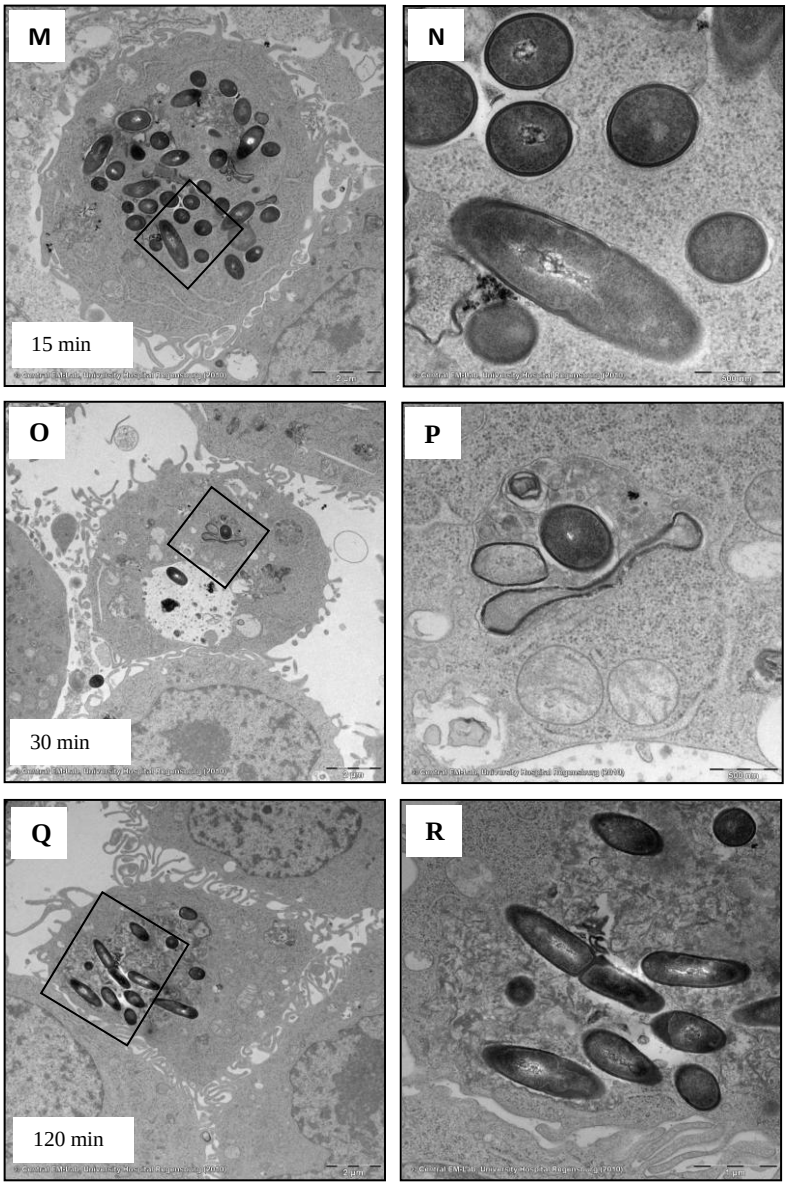

TNFα+IFNγ stimulated J774 macrophages

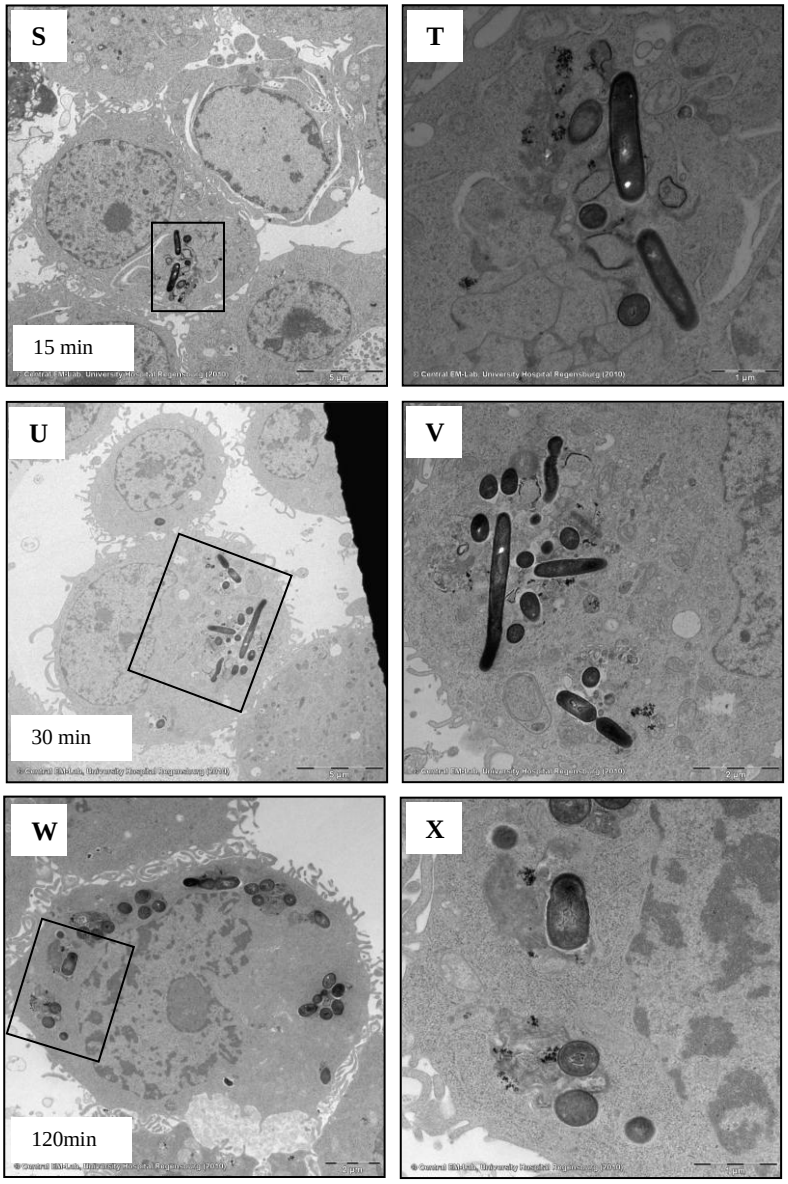

Figure 7.1: TEM of Listeria monocytogenes infected cells
In order to determine constitution of magnetically labelled L.m. and isolated phagosomes, L.m.⊿hly was labelled with 10 µg/ml LB and streptavidin magnetic beads. J774 macrophages were infected for indicated periods of time. ***A)-X)*** *Cells were centrifuged for 10 min 2000 x rpm and the pellet was prepared for electron microscopy with Karnovsky´s fixative. Squares mark the region of magnification.*

7.2. TEM of isolated phagosomes

Isolated phagosomes of unstimulated J774 macrophages

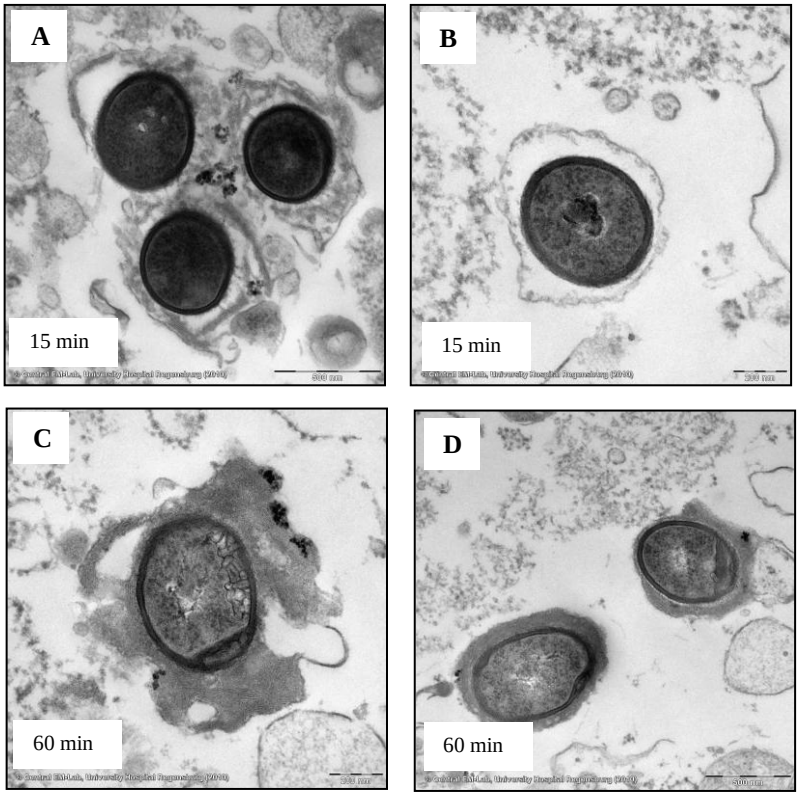

Isolated phagosomes of TNFα stimulated J774 macrophages

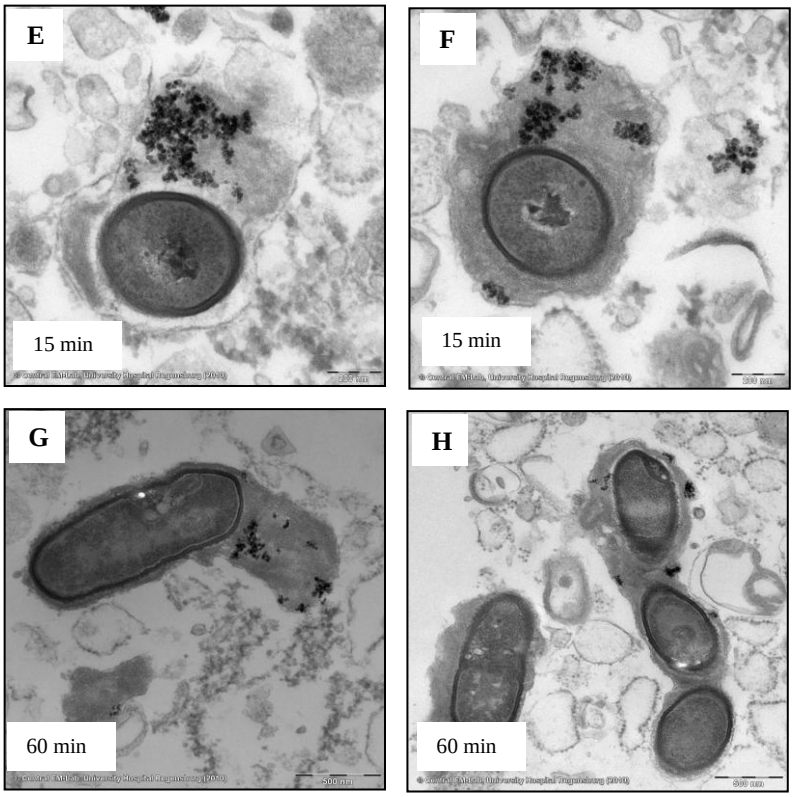

Isolated phagosomes of IFNγ stimulated J774 macrophages

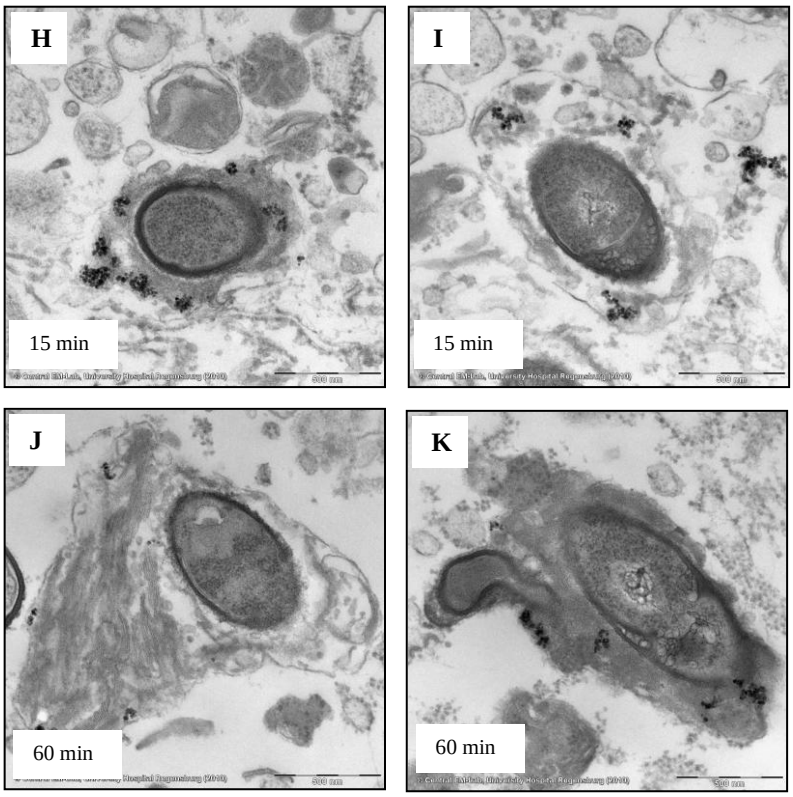

Isolated phagosomes of TNFα+ IFNγ stimulated J774 macrophages

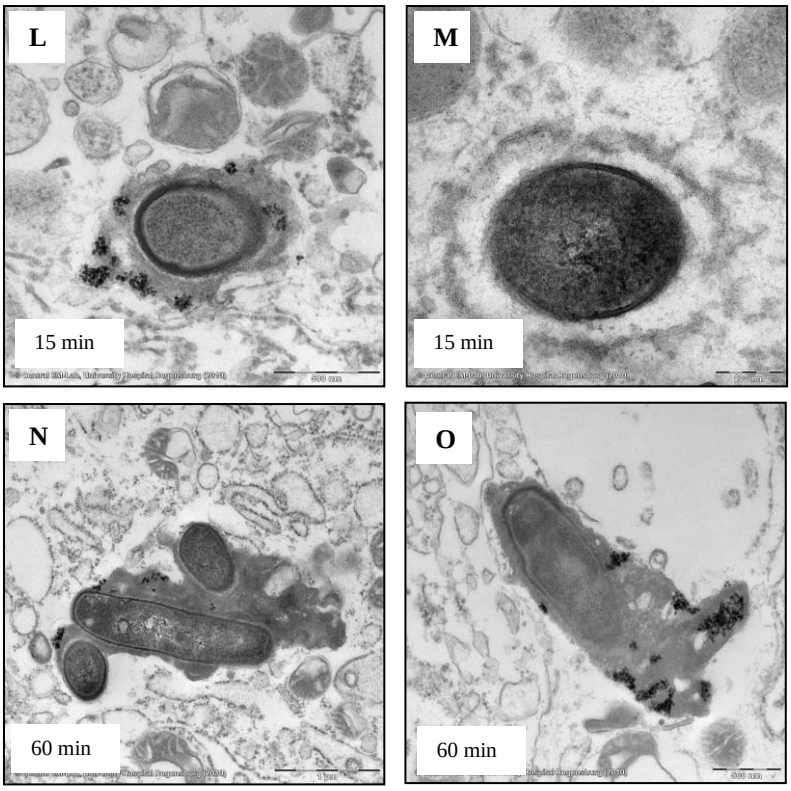

Figure 7.2*: (on previous page) TEM of isolated phagosomes*

In order to determine constitution of magnetically labelled L.m. and isolated phagosomes, L.m.⊿hly was labelled with 10 µg/ml LB and streptavidin magnetic beads. J774 macrophages were infected for indicated periods of time. Infected cells were softly disrupted by sonication and phagosomes isolated in the magnetic chamber as described in 3.3. The magnetic fraction was centrifuged for 15 min with 15000 x g and the pellet was fixated for electron microscopy with Karnovsky´s fixative.

Acknowledgements

An dieser Stelle möchte ich mich bei allen Menschen bedanken, die mich während der Zeit meiner Doktorarbeit begleitet haben.

Meinem Betreuer und Doktorvater **PD Dr. Wulf Schneider** möchte ich herzlich für die Bereitstellung dieses interessanten Themas danken. Die Umsetzung sämtlicher Ideen war stets möglich und die Arbeit wurde in jeder Hinsicht immer unterstützt. Vielen Dank.

Herrn **Dr. Richard Warth** danke ich für die freundliche Bereiterklärung diese Arbeit in der NWF III zu vertreten und als Erstgutachter zu beurteilen.

Ein großer Dank gilt **Maria Kurz**, ohne ihre Unterstützung wären viele Experimente gar nicht möglich und nicht so erfolgreich gewesen. Es ist schön aber zusätzlich auch eine Freundin gewonnen zu haben.

Ohne **Laura Klingseisen** wären wohl viele Stunden im Labor mühsam gewesen. Vielen Dank für das stetige offene Ohr zu jeglichen Problemen, nicht nur hinsichtlich schwieriger Experimente. Danke für die vielen lustigen Kaffeestunden und auch für sämtliche freizeitliche Aktivitäten zusammen.
Hier möchte ich auch **Matthias Hölzl** und **Janina Podolsky** einreihen und mich bei euch dreien bedanken für die schöne Zeit zusammen, die wir nicht nur im Labor verbracht haben.

Für die angenehme Laborathmosphäre möchte ich auch Gertrud Knoll und Elke Perthen danken.

Ein großer Dank geht an **Dr. med. José Ángel Gonzáles-Víctores**, der mir durch die Tücken der englischen Sprache geholfen hat und ohne ihn und seine intensive Hilfe wäre diese Arbeit in englischer Sprache vermutlich nicht so möglich gewesen.

Besonders danke ich auch **Nicholas Putz** für die Korrektur dieser Arbeit und hilfreiche Tipps dazu und für seine langjährige Freundschaft.

Für die angenehme Zeit in Borstel möchte ich **Dr. Norbert Reiling** und seinem Team danken und für die freundliche Aufnahme in seinem Labor.

Herrn **Dr. Thomas Hehlgans** und seinem Team danke ich für die Unterstützung bei den Mausarbeiten.

Nicht zuletzt möchte ich meiner Familie für die moralische Unterstützung und **Michael Wimmer** für die Geduld im Ertragen jeglicher Höhen und Tiefen während dieser Jahre meiner Doktorarbeit danken.